



HAL
open science

Role of tanycytes in Tau clearance and their relevance in Alzheimer's disease

Florent Sauvé

► **To cite this version:**

Florent Sauvé. Role of tanycytes in Tau clearance and their relevance in Alzheimer's disease. *Neurons and Cognition* [q-bio.NC]. Université de Lille, 2022. English. NNT : 2022ULILS038 . tel-04767516

HAL Id: tel-04767516

<https://theses.hal.science/tel-04767516v1>

Submitted on 5 Nov 2024

HAL is a multi-disciplinary open access archive for the deposit and dissemination of scientific research documents, whether they are published or not. The documents may come from teaching and research institutions in France or abroad, or from public or private research centers.

L'archive ouverte pluridisciplinaire **HAL**, est destinée au dépôt et à la diffusion de documents scientifiques de niveau recherche, publiés ou non, émanant des établissements d'enseignement et de recherche français ou étrangers, des laboratoires publics ou privés.

UNIVERSITÉ DE LILLE

École Doctorale Biologie-Santé

THÈSE

Pour l'obtention du grade de

DOCTEUR DE L'UNIVERSITÉ DE LILLE

Spécialité : Neurosciences

Role of tanycytes in Tau clearance and their relevance in
Alzheimer's Disease

Rôle des tanycytes dans la clairance de tau et leur pertinence dans la maladie
d'Alzheimer

Florent Sauvé

Thèse présentée et soutenue à Lille, le 24 octobre 2022

Composition du Jury:

Pr. Florence Pasquier	PU-PH, Centre Mémoire de Ressource et de Recherche, CHRU, Lille	Présidente
Dr. Julie Dam	Chargé de Recherche, Institut Cochin, Inserm U1016, CNRS UMR 8104, Paris	Rapporteur
Dr. Sophie Steculorum	Group leader, Max Planck Institute for Metabolism Research, Cologne	Rapporteur
Pr. Claude-Alain Maurage	PU-PH, Centre de Biologie Pathologie, CHRU, Lille	Examineur
Dr. Philippe Ciofi	Chargé de Recherche, Neurocentre Magendie, INSERM U1215, Bordeaux	Examineur
Dr. Valérie Simonneaux	Directeur de Recherche, Institut des Neurosciences Cellulaires et Intégratives, CNRS UPR 3212, Strasbourg	Examineur
Dr. Virginie Mattot	Chargé de Recherche, Lille Neuroscience & Cognition, INSERM U1172, Lille	Directrice administrative
Dr. Vincent Prévot	Directeur de Recherche, Lille Neuroscience & Cognition, INSERM U1172, Lille	Directeur scientifique

Acknowledgements

As any scientific work is impossible alone, acknowledgements for the people who have directly or indirectly worked with me for the completion of this study are due.

Because this story wouldn't have started without you, I express my deepest gratitude to Dr. Vincent Prévot who directed this work and welcomed me in his laboratory. This study started with one of your ambitious ideas that tancytes would somehow be implicated in aging and Alzheimer's disease. You have guided me along the way but still gave me the freedom to investigate my ideas and lead the project. Even if this story isn't a success yet, I have learned unvaluable lessons from your mentorship and I hope that it will result in a great publication.

Dear Pr. Pasquier and Dr. Ciofi, you have been following the progress of this work since the first year through your participation to my monitoring committees. I am very grateful for your feedbacks on my project and for your participation in my thesis jury.

Dear Dr. Sophie Steculorum and Dr. Julie Dam, I would like to express my gratitude to you for accepting to review and evaluate my work and I'm looking forward to your feedbacks.

Dear Pr. Maurage, I would like to thank you for collaboration in this work. This project wouldn't have been the same without the precious human hypothalamic samples you kindly provided. Also, I would like to thank you for accepting to be part of my thesis jury and I'm looking forward to listening about your views on my work.

Dear Dr. Mattot and Dr. Simonneaux, I would like to thank you for joining my thesis jury and for showing interest in my work.

I gratefully acknowledge the team of Integrative Structural Biology directed by Dr. Isabelle Landrieu and especially Dr. Clément Danis and Dr. Elian Dupre for their collaboration on the production of the fluorescently-labeled tau protein which has been crucial in the development of my project.

I would also like to thank the colleagues who have helped for the completion of this study. Special thanks go to Dr Gaëtan Ternier for his help with the tissue clearing, light-sheet

microscope imaging and all the discussions we had on project and to Julie Dewisme who has considerably helped me technically during her master.

I would like to thank Markus Schwaninger's team for providing the adenoviruses used in this work.

Additionally, I would like to thank the methanol team with which I originally started to work with to finally fly off with my own wings on this Alzheimer's disease project. Monica, Eleonora you have been real moral support along those years and I am deeply grateful for it. Special thanks go to Daniela, even if you're not a methanol member, you've supported me just as much.

I'd like to thank Gaëtan Ternier once more for his support and all the moments we've shared during our Ph.D. in congresses, lab events or parties that have enlightened the up and downs of this 4-year experience.

My gratitude also goes to every member of the laboratory, students, technicians, engineers, principal investigators and secretaries for their contribution in my work and in making the laboratory a comfortable and pleasant workplace.

Lastly, I would like to acknowledge my family and friends for their support during this 4-year period and especially my companion who has been there for me in the high and lows since the beginning of my academic experience.

Finally, I would like to thank the various organizations who have funded this work through different grants. This work was supported by the European Research Council (ERC) Synergy Grant-2019-WATCH No 810331, DistAlz (no. ANR-11-LABEX-0009), EGID (no. ANR-10-LABEX-0046) and I-SITE ULNE (no. ANR-16-IDEX-0004).

Abstract

Alzheimer's disease is characterized by an accumulation of both A β and tau in the brain causing neurodegeneration. Currently described clearance mechanisms for tau involve the brain glymphatic and lymphatic system from which tau can slowly egress to the blood. However, studies have shown that tau can rapidly reach the blood circulation after intracerebroventricular injections, suggesting the existence of a direct CSF to blood transport, but the path taken by tau to reach the circulation within minutes is still unknown. Tau being described as incapable of crossing the blood-brain barrier, a plausible path for tau brain exit is through the blood-CSF barriers (BCSFB). A particular BCSFB is located at the median eminence where hypothalamic tanycytes, whose cell bodies form the floor of the third ventricle and send long processes to the underlying pituitary portal capillary bed, form a bridge between the CSF and the blood. In this work, we show that tanycytes are able to take up and transport tau *in vitro* using tanycyte primary cultures. The production of a fluorescently-labeled tau allowed us to track tau path from the CSF to the blood and to confirm the implication of tanycyte in its transport. Using a novel model of tanycytic shuttle interruption, we demonstrated the major contribution of tanycytes in tau egress from the brain. Lastly, the study of human hypothalamic and median eminence post-mortem tissue showed a sign of tau transport in tanycyte of AD patients and a dramatic alteration of their cytoskeleton which was not observed in another neurodegenerative disease. Altogether, our results demonstrate the role of tanycytes in tau clearance and their implication in the pathophysiology of Alzheimer's disease. Such data raise the questions of tanycytes as actors of the CSF clearance and their potential implications in other neurodegenerative diseases.

Résumé

La maladie d'Alzheimer (MA) est caractérisée par l'accumulation du peptide A β et de la protéine tau dans le cerveau, provoquant une neurodégénérescence. Les mécanismes de clairance de la protéine tau connus impliquent le système glymphatique et lymphatique à partir duquel elle peut lentement s'échapper vers le sang. Cependant, des études ont montré que la protéine tau peut rapidement atteindre la circulation sanguine après des injections intracérébroventriculaires, ce qui suggère l'existence d'un transport direct du LCR au sang, mais le chemin emprunté par celle-ci pour atteindre la circulation en l'espace de quelques minutes est encore inconnu. La protéine tau étant décrite comme incapable de traverser la barrière hémato-encéphalique, une voie plausible pour la sortie de la protéine tau du cerveau est la barrière sang-liquide cérébrospinale (BSLCR). Une BSLCR particulière est située au niveau de l'éminence médiane où les tanocytes hypothalamiques, dont les corps cellulaires tapissent la paroi ventriculaire et envoient de longs processus vers le lit capillaire sous-jacent, forment un pont entre le LCR et le sang. Dans ce travail, nous montrons que les tanocytes sont capables d'absorber et de transporter la protéine tau *in vitro* en utilisant des cultures primaires de tanocytes. La production d'une protéine tau marquée par fluorescence nous a permis de suivre le parcours de la tau du LCR vers le sang et de confirmer l'implication des tanocytes dans son transport. En utilisant un nouveau modèle d'interruption de la navette tanocytaire, nous démontrons la contribution majeure des tanocytes dans l'évacuation de la tau hors du cerveau. Enfin, l'étude de tissus post-mortem d'hypothalamus et d'éminence médiane humains a montré un signe de transport de tau dans les tanocytes des patients atteints de la MA et une altération dramatique de leur cytosquelette qui n'a été observée dans aucune autre maladie neurodégénérative. Dans l'ensemble, nos résultats démontrent le rôle des tanocytes dans la clairance de tau et leur implication dans la pathophysiologie de la MA. De telles données soulèvent la question des tanocytes en tant qu'acteurs de la clairance du LCR et de leurs implications potentielles dans d'autres maladies neurodégénératives.

Short abstract

The accumulation of pathological tau in the brain and cerebrospinal fluid (CSF) and its eventual increase in the blood are hallmarks of Alzheimer's disease (AD). However, the mechanisms of tau clearance from the brain to the periphery are not clear. We show here, using animal and cellular models as well as patient blood samples and post mortem brains, that hypothalamic tanycytes, whose cell bodies line the ventricular wall and send long processes to the underlying pituitary portal capillary bed, take up and transport tau from the CSF and release it into these capillaries, whence it travels to the pituitary and eventually the systemic circulation. In AD and frontotemporal dementia, tanycytic morphology is altered, with a dramatic fragmentation of the secondary cytoskeleton in the former but not the latter. Both the implication of tanycytic degradation in the pathophysiology of a human disease and the evidence for the existence of a brain-to-blood tanycytic shuttle are unprecedented, and raise important questions regarding the role of tanycytes in physiological clearance mechanisms and the development of neurodegenerative disorders.

Résumé court

L'accumulation de la protéine Tau pathologique dans le cerveau et le liquide céphalo-rachidien (LCR) et son augmentation dans le sang sont des caractéristiques de la maladie d'Alzheimer (MA). Cependant la clairance de Tau du cerveau vers la périphérie reste mal décrite. Nous montrons ici, à l'aide de modèles animaux et cellulaires ainsi que d'échantillons de sang et de cerveaux de patients, que les tanocytes hypothalamiques, dont les corps cellulaires bordent la paroi ventriculaire et envoient de longs processus vers le lit capillaire sous-jacent, transportent la protéine tau du LCR et la libèrent dans ces capillaires pour rejoindre la circulation systémique. Dans la MA et la démence frontotemporale, la morphologie des tanocytes est altérée, avec une fragmentation du cytosquelette dans la première. L'implication de la dégradation des tanocytes dans la physiopathologie d'une maladie humaine et la preuve de l'existence d'une navette tanocytaire entre le cerveau et le sang sont sans précédent et soulèvent des questions importantes concernant le rôle des tanocytes dans les mécanismes de clairance et le développement des troubles neurodégénératifs.

Table of content

Acknowledgements	1
Abstract	3
Résumé	4
Short abstract	5
Résumé court	6
Table of content	7
Figures	12
Tables	13
Abbreviations	14
Introduction	19
Alzheimer’s disease, an overview	19
The main cause of dementia.....	19
Sporadic and familial Alzheimer’s Disease	20
Risk factors of Alzheimer’s Disease: from DNA variants to metabolism	20
Cognitive and non-cognitive symptoms of AD	21
Tau protein and amyloid beta peptides in the pathophysiology of AD	22
A β peptides, shifting the balance.....	22
Tau from microtubule binding to prion-like seeding and spreading	24
Tau protein expression, structure and function	24
Post-translational modifications lead to Tau instability	26
Tau protein aggregation.....	27

Is tau toxicity monomers, oligomers or aggregates mediated?	28
Tau as a prion-like protein	29
Extracellular Tau.....	30
Tau and A β act synergically to induce neurodegeneration	32
Diagnosis of Alzheimer’s Disease: mixing neuropsychological and biomarker criteria	33
Neuropsychological evaluation	33
Histopathological staging	34
Braak stages	34
Thal stages.....	35
Fluid biomarkers	37
CSF Tau and amyloid beta concentration	37
Plasmatic A β and tau concentrations	38
Imaging biomarkers.....	39
PET ligands for A β and tau brain burden evaluation	39
Brain glucose hypometabolism.....	40
Brain atrophy by volumetric MRI.....	40
Approaching an accurate natural history of AD.....	41
Disease-modifying therapeutic strategies for Alzheimer’s Disease.....	42
Anti-A β strategies	42
Anti-Tau strategies.....	43
Brain clearance mechanisms help coping with Tau accumulation	44
Cellular degradation systems.....	44
The Ubiquitin-Proteasome System	44
Autophagy	46
The endo-lysosomal pathway.....	46
Extracellular clearance.....	48
Paravascular clearance.....	49
Lymphatic clearance.....	51

Circulatory clearance	52
Blood brain barrier passage	53
Blood-cerebrospinal-fluid barrier passage	54
Tanycytes are mediators of brain and periphery exchanges	56
The circumventricular organs, windows to the brain.....	56
The median eminence, a hotspot for brain/periphery exchanges.....	57
Tanycytes, swiss army knives of the hypothalamus	58
The heterogeneity of tanycytic populations	59
Tanycytic markers, a tool for their visualization and targeting	60
Tanycytes a new stem cell niche?	62
Tanycytes at the blood-cerebrospinal-fluid barrier	63
Tanycytes shuttle blood-borne hormonal cues into the hypothalamus.....	65
Tanycytic regulation of neurosecretion	67
Tanycytes support hypothalamic neuronal populations by sensing and providing nutrients.....	68
Tanycytes in pathology and aging.....	70
The role of tanycyte in metabolic disorders and hormonal imbalance	70
Tanycyte in physiological and pathological aging	71
Are tanycytes new players in brain clearance?	73
Objectives.....	75
Material and Methods	76
Collection and processing of human tissues	76
Immunohistology.....	76
Ilastik segmentation analysis	77
ADNI data extraction and analysis.....	77
Animals	78

Tau-565 and BSA-565 production	79
Tau-565, BSA-565 and Tau-565AG and AAV1/2-Dio2-iCre-A2-GFP delivery	79
Evaluation of AAV1/2-Dio2-iCre-A2-GFP infection efficiency	80
Tau-565 kinetic experiment.....	80
IDISCO tissue clearing	81
Light-sheet microscope imaging	81
3D image processing and analysis.....	81
Human Tau ELISA.....	82
Tanycyte primary culture	82
Primary tanycyte 2N4R Tau and Tau-565 internalization assay	82
Immunocytochemistry	83
Western blot of primary tanycyte extracts.....	83
Primary tanycyte Tau-565 secretion assay	84
Fluorescence microscopy	84
Statistics.....	84
Results.....	86
Tanycytes uptake and secrete exogenous Tau in vitro.....	86
Tanycytes transport Tau protein from CSF to blood in vivo.....	88
Inhibition of tanycytic transport impairs CSF to blood transport of Tau	92
Tau protein CSF to blood transport is altered in AD.....	95
Tanycytes show signs of Tau transport	98

Tanycytes are specifically disorganized and degraded in AD	100
Discussion	108
Tanycyte’s contribution in tau clearance bigger picture	108
Tanycytes, a two-way conduit between CSF and blood	109
The chicken or the egg, is tanycytic alteration a cause or a consequence of Tau pathology?	109
Mechanisms of tanycytes degradation	110
Tanycytic alterations may be a cause of the metabolic and hormonal increased risks for AD onset	111
Peripheral tau: a mere symbol of clearance or a real contributor to AD	112
New opportunities for tanycyte’s role in AD	113
Tanycytes in other neurodegenerative diseases.....	115
Conclusion	116
Bibliography	117

Figures

Figure 1: The amyloidogenic and non-amyloidogenic pathways.	23
Figure 2: Tau isoforms result from alternative splicing.	25
Figure 3: Physiological and pathological phosphorylation sites of tau and their specific antibodies.....	26
Figure 4: The prion-like hypothesis of Tau spreading.	30
Figure 5: Mechanisms of secretion and uptake of extracellular Tau.....	31
Figure 6: Braak staging of neurofibrillary changes in AD.....	35
Figure 7: Thal staging of amyloid depositions in AD.	36
Figure 8: Temporal evolution of biomarker changes in Alzheimer’s Disease.....	41
Figure 9: Degradation of proteins by the ubiquitin-proteasome system.	45
Figure 10: Degradation of tau by autophagy and autophagy-independent pathways. .	47
Figure 11: The paravascular clearance pathways of the brain.....	49
Figure 12: The lymphatic system of the mice and human brain.	51
Figure 13: The anatomy of the arachnoid villi.	52
Figure 14: The blood-brain barrier anatomy and function.....	54
Figure 15: The anatomy of the brain-cerebrospinal fluid barrier.	55
Figure 16: The circumventricular organs of the mouse and human brain.	57
Figure 17: The median eminence is at the interface of the hypothalamus-pituitary system	58
Figure 18: Tanycyte’s classification.	60
Figure 19: The tanycytic tight junction barrier is under metabolic control.	64
Figure 20: The molecular mechanisms of the tanycytic shuttle.	66
Figure 21: Primary rat tanycytes uptake and secrete tau <i>in vitro</i>	87
Figure 22: Kinetic of Tau-565 distribution in the wild-type mice.....	89
Figure 23: Tanycytes transport tau from CSF to blood in male and female mice.....	91

Figure 24: Inhibition of tanyocyte's transcytosis blunts tau efflux from brain to blood.	93
Figure 25 : Plasma-to-CSF Tau ratio is lower in AD patients.	96
Figure 26: Tanycytes of AD patients contain Tau-positive vesicles.	99
Figure 27: Tanycytes in AD patients are degraded and disorganized	101
Figure 28: The cytoskeletal degradation is limited to tanycytes and impairs their interaction with the vasculature.	104
Figure 29: Tanycytic degradation occurs throughout the median eminence in AD but not in FTD.	106

Tables

Table 1: Antibodies	85
Table 2: Patients' information.	98

Abbreviations

A β : Amyloid beta

AD: Alzheimer's Disease

ADNI: Alzheimer's Disease Neuroimaging Initiative

AICD: APP intracellular domain

AP: Area postrema

OVLT: Organum vasculosum of the lamina terminalis

APOE ϵ 3: Apolipoprotein E epsilon 4

APOE ϵ 4 : Apolipoprotein E epsilon 3

APP: Amyloid precursor peptide

AQP4: Aquaporin 4

ATP: Adenosine tri-phosphate

BBB: Blood-brain barrier

BCSFB: Blood-Cerebrospinal fluid barrier

BLBP: Brain lipid-binding protein

BoNT/B: Botulinum neurotoxin serotype B

BrdU: Bromo-desoxy-uridine

BSA: Bovine serum albumin

BSA-565: Atto-565 coupled bovine serum albumin

CBD: Corticobasal degeneration

CMA: Chaperone-mediated autophagy

ESCRT: Endosomal sorting complex required for transport

CP: Choroid plexus

CSF: Cerebrospinal fluid

CTF α : C-terminal fragment alpha

CTF β : C-terminal fragment beta

CVO: Circumventricular organs
DAPI: 4'-6-diamidino-2-phenylindol
DARPP-32: Dopamine and cAMP-regulated phosphoprotein
DIO: Diet-induced obesity
Dio2: Deiodinase 2
Dio3: Deiodinase 3
DMH: Dorsomedial hypothalamic nuclei
DNA: Deoxyribonucleic acid
DUBs: Deubiquitinating enzyme
e-MI: Endosomal microautophagy
EEA1: Early Endosome Antigen 1
EGFP: Enhanced green fluorescent protein
EMA: European Medicines Agency
ERK: Extracellular signal-regulated kinase
FAD: Familial Alzheimer's Disease
FDA: Food and Drug Administration
FDG: Fluoro-deoxyglucose
FGF2: Fibroblast growth factor 2
FGF21: Fibroblast growth factor 21
FSH: Follicle stimulation hormone
FTD: Fronto-temporal Dementia
GAPDH: Glyceraldehyde-3-phosphate dehydrogenase
GFAP: Glial fibrillary acid protein
GFP: Green fluorescent protein
GK: Glucokinase
GLAST: Glutamate Aspartate transporter
GnRH: Gonadotropin releasing hormone
GPCR: G protein-coupled receptor

GPR50: G protein-coupled receptor 50

GWAS: Genome wide association study

HDL: High density lipoprotein

HPA: Hypothalamic-pituitary-adrenal axis

HPG: Hypothalamic-pituitary-gonadal axis

HPT: Hypothalamic-pituitary-thyroid axis

HRP: Horseradish peroxidase

HSC70: Heat shock cognate 71 kDa protein

iBot: Botulinum neurotoxin serotype B expressing mouse line

ICS: Incubation solution

IDISCO: immunolabeling-enabled three-dimensional imaging of solvent cleared organs

IGF1: Insulin-like growth factor 1

IPAD: Intramural periarterial drainage

ISF: Interstitial fluid

IWG: International working group

K_{ATP}: ATP-dependent potassium channel

LH: Luteinizing hormone

LRP1: Low density lipoprotein receptor-related protein 1

MAPT: Microtubule-associated protein tau

MCI: Mild cognitive impairment

ME: Median eminence

MRI: Magnetic resonance imaging

mRNA: messenger ribonucleic acid

MVB: Microvesicular bodies

NFT: Neurofibrillary tangles

NIA-AA: National Institute on Aging – Alzheimer's Association

NMDA: N-methyl-D-aspartate

NPY: Neuropeptide Y

NSC: Neural stem cell

O-GlcNAcylation: O-GlcNAc-glycosylation

PBS: Phosphate buffer saline

PET: Positron emission tomography

PFA: paraformaldehyde

PG: Pineal gland

PGE2: Prostaglandin E2

PiD: Pick's disease

PLVAP: Plasmalemmal vesicle associated protein

POMC: Pro-opiomelanocortin

PPII: Pyroglutamyl peptidase II

PSP: Progressive supranuclear palsy

PTM: Post-translational modification

PV1: Plasmalemmal vesicle associated protein-1

RIPA: Radioimmunoprecipitation Assay

RNA: Ribonucleic acid

S.D.: Standard deviation

sAPP α : soluble APP alpha

sAPP β : soluble APP beta

SCO: subcommissural organ

Sema7A: Semaphorin 7A

SFO: Subfornical organ

SIMOA: Single molecule array

SNARE: Soluble N-ethylmaleimide sensitive factor attachment protein receptor

T3: Tri-iodothyronin

T4: Thyroxin

Tas1r2/3: Taste receptor type 1 member 2/3

Tau-565: Atto-565 coupled Tau protein

TBI: Traumatic brain injury

TBS: Tris buffer saline

TDP-43: TAR DNA-binding protein 43

TGF- α : Transforming growth factor alpha

TGF- β 1: Transforming growth factor beta 1

TRH: Thyrotropin-releasing hormone

TRHR1: Thyrotropin-releasing hormone receptor 1

TSH: Thyroid stimulating hormone

UPS: Ubiquitin-proteasome system

VAMP1/2/3: Vesicle-associated membrane protein

VEGF-A: Vascular endothelial growth factor A

Wt: wild type

ZO1: Zona occludens 1

Introduction

Alzheimer's disease, an overview

Alzheimer's Disease (AD) is a neurodegenerative disease biologically characterized by β -amyloid ($A\beta$)-containing extracellular senile plaques and microtubule associated tau protein (tau)-containing intracellular neurofibrillary tangles (NFTs). Clinically, AD patients present with memory impairments and cognitive decline leading to behavioral, speech and motor impairments. AD is characterized by a long asymptomatic preclinical phase making definite clinical AD diagnosis and research difficult. Once in the symptomatic phase, patients exhibit progressive cognitive impairments leading to the development of dementia and limiting their abilities to maintain their independence.

The main cause of dementia

Dementia is a syndrome characterized by a pathological deterioration of cognitive functions. It affects around 50 million people in the world and costs over a trillion dollars annually. Dementia is an age-related condition but a study on centenarians shows that is not necessarily an outcome of aging ¹. Among the variety of its causes, Alzheimer's Disease is estimated to account for 60 to 70% of cases. Due to extended life expectancy, the prevalence of all-cause dementia is expected to double, reaching 131,5 million worldwide cases by 2050 ². Dementia represents a significant societal and economic burden as patients progressively lose their independence and rely on caregivers. AD being the first cause of dementia, research efforts were deployed to identify the causes of the AD onset finding both genetic and environmental factors contributing to its development.

Sporadic and familial Alzheimer's Disease

AD can be genetically divided into familial cases with Mendelian inheritance or sporadic cases with no familial aggregation. Autosomal dominant familial AD (FAD) is estimated to represent less than 1% of patients with mutations in the amyloid precursor protein gene (APP) and presenilin genes leading to APP misprocessing and deposition of A β peptides into senile plaques³. FAD patients are usually presenting with earlier disease onset, around 30 to 40 years-old, compared to sporadic cases, after 50 years-old. For the rest of AD cases, a combination of genetic polymorphisms and environmental risk factors participates in the onset of the disease.

Risk factors of Alzheimer's Disease: from DNA variants to metabolism

Beyond autosomal dominant mutations described in familial AD, twin studies in sporadic late-onset AD showed a heritability factor for AD⁴. Several DNA variants have been associated with increased risk of AD development. Among AD risk variants, the most common is the apolipoprotein ϵ 4 (APOE ϵ 4) allele increasing the risk for dementia by 4 times in heterozygotes and by 15 times in homozygotes compared with APOE ϵ 3 allele carriers⁵. This increased risk can partly be explained by APOE ϵ 4 competition with A β for brain clearance mechanisms⁶. However, APOE ϵ 4 alleles alone do not explain the heritability observed in AD cohorts. Interestingly, tau-linked variants also exist such as an ancestral inversion on chromosome 17q21, including the microtubule-associated tau protein (*MAPT*) gene, generated different tau haplotypes (H1 and H2). Tau H1 haplotype has been reported to be a risk factor for AD, linking tau with AD onset⁷⁻⁹. To identify the DNA variants explaining the remaining fraction of AD heritability Genome wide association studies (GWAS) have been set up. They have shown since 2007¹⁰⁻¹⁴, the association of more than 70 loci with AD. Functional annotation of these risk-loci have enabled the identification of new pathways playing a role in AD such as the modulation of immune response, endocytosis or lipid metabolism. In addition

to genetic risk factors, environmental risk factors for AD have been identified. Metabolic disorders occurring at midlife or late-life, including diabetes mellitus, hypertension, obesity and low high-density lipoprotein (HDL) cholesterol, have been shown to increase risk of later-life dementia from 1,5 to 1,8-fold¹⁵. While most genetic risk factors have been linked with AD pathological processes, the influence of these modifiable environmental risk factors on AD pathogenesis remains unclear.

Interestingly, metabolic and hormonal dysfunction appear not only as risk factors of the development of AD but can also arise from its development. Indeed, longitudinal studies suggest that metabolic disturbances such as weight loss can precede the cognitive declaration of AD¹⁶.

Cognitive and non-cognitive symptoms of AD

Cognitive deficits are the most notable symptoms of AD and are at the basis of AD diagnosis. The development of memory impairment is the most common cognitive impairment observed in AD patients and can be accompanied by defects in other cognitive domains including aphasia, an inability to comprehend or formulate language, apraxia, an inability to perform learned movements on command, agnosia, an inability to recognize or comprehend the meaning of objects, and disturbance of executive functioning, difficulties to plan, organize, sequence or abstract thoughts or information. Longitudinal studies on cognitive decline, cerebrospinal fluid (CSF) and neuroimaging biomarkers have unraveled a significant preclinical phase of disease preceding the onset of cognitive impairment by 10 to 20 years¹⁷. AD patients can also exhibit significant non-cognitive impairments which may even occur before the initial cognitive deficits. AD patients can present metabolic and/or hormonal deficits such as weight loss, sleep-wake disorders and neuroendocrine alterations attributable to hypothalamic dysfunction^{16,18-20}. Notably, AD patients experience disruptions in several hypothalamic-pituitary axis namely the hypothalamic-pituitary-adrenal (HPA) axis, with reports of increased basal cortisol levels and overall insensitivity to glucocorticoid feedback, the

hypothalamic-pituitary-thyroid (HPT) axis, with studies showing either hypothyroidic or hyperthyroidic states, and the hypothalamic-pituitary-gonadal (HPG) axis, consisting of lower levels of sex steroids associated with poorer cognitive performance^{21–23}. These observations suggest an alteration in hypothalamic functions that could be related to either the death of hypothalamic neurons or its inability to sense peripheral cues which are essential to its regulatory functions.

Cognitive and non-cognitive symptoms are the consequences of the progressive neurodegeneration occurring in the course of AD. Decades of research have led to the identification of the progressive accumulation and aggregation of tau and A β and of their direct involvement in the pathogenesis of AD.

Tau protein and amyloid beta peptides in the pathophysiology of AD

The pathology of AD is characterized by the accumulation and aggregation of A β peptides in extracellular senile plaques that progressively spread throughout the brain on one hand and tau hyperphosphorylation, accumulation and intracellular aggregation into neurofibrillary tangles occurring in a specific spatiotemporal pattern on the other. These two histopathological hallmarks are key for the post-mortem diagnosis and staging of AD. Since the identification of A β and tau as the components of senile plaques and neurofibrillary tangles in the 80s, significant efforts have been deployed to characterize the mechanisms involved in their aggregation^{24–28}.

A β peptides, shifting the balance

A β peptides derive from the sequential cleavage of APP, a transmembrane protein enriched in neurons, by β -secretase and γ -secretase and coined the amyloidogenic pathway^{29–35} (Figure 1). A β generation occurs in all cells but is produced in high amount by neurons during synaptic

activity. A β is released in the extracellular compartment where it aggregates in a concentration dependent-manner³⁶. Due to a stepwise processing by γ -secretases A β sequence varies resulting in the production of A β 39-43 with two major species being A β 40, the most abundant, and A β 42³⁷. The slightly longer form, A β 42, is more prone to aggregation and is the principal specie deposited in the brain of AD patients. Studies have shown a neurotoxic effect of A β 42 through its binding with neuronal synaptic receptors and the induction of pathological changes in dendritic spines and synaptic efficiency^{38,39}.

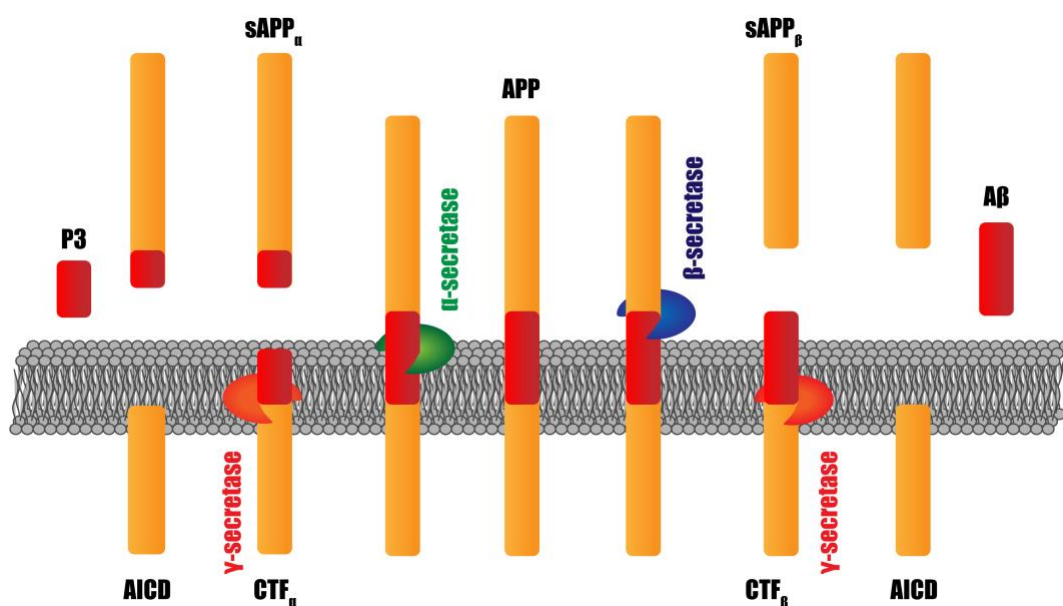


Figure 1: The amyloidogenic and non-amyloidogenic pathways.

The amyloidogenic pathway is the process of A β biogenesis: APP is cleaved by β -secretase, producing soluble APP fragments β (sAPP $_{\beta}$) and C-terminal fragment β (CTF $_{\beta}$), and CTF $_{\beta}$ is then cleaved by the γ -secretase, generating APP intracellular domain (AICD) and A β . The non-amyloidogenic pathway prevent the generation of A β , as APP is firstly cleaved by α -secretase within A β domain, generating soluble APP fragments α (sAPP $_{\alpha}$) and C-terminal fragment α (CTF $_{\alpha}$), CTF $_{\alpha}$ is then processed by γ -secretase, producing non-toxic P3 and AICD fragments.

The amyloidogenic pathway is counterbalanced by the non-amyloidogenic pathway during which APP is also sequentially cleaved. In this case, a α -secretase first cleaves APP inside the A β sequence and is followed a second cleavage performed by the γ -secretase also

involved in the amyloidogenic pathway. This difference in the first cleavage site prevents the formation of A β peptides. In the context of AD, a shift in A β production balance occurs with an increased production of longer A β forms, especially A β 42. This shift is caused in familial AD by the different mutations found in APP and presenilin 1 and 2, forming the catalytic subunit of the β -secretase⁴⁰. In sporadic AD, multiple risk genes are involved in A β homeostasis, either in its production or clearance, such as APOE ϵ 4 the main risk gene of sporadic AD negatively influencing A β 42 clearance⁴¹.

Tau from microtubule binding to prion-like seeding and spreading

Tau protein expression, structure and function

Tau protein was discovered in 1975 in a study on microtubule assembly⁴². It is encoded by the *MAPT* gene which comprises 16 exons and is localized on chromosome 17q21. In the adult brain, tau exists in six isoforms due to alternate splicing of its exon 2,3 and 10^{43,44}. Tau isoform nomenclature is based on the presence of either three or four microtubule binding domains, 3R or 4R, and of either 1, 2 or no N-terminal insertion, 1N, 2N or 0N (Figure 2)⁴⁵. The splicing of tau is developmentally regulated as only the shortest tau isoform is expressed in the fetal brain while all six isoforms are expressed in the adult brain. Also, 3R/4R tau ratio is roughly equivalent but 0N, 1N, and 2N tau relative proportions are different (around 37%, 54% and 9% respectively)⁴⁶. The splicing of tau seems to be important for the development of pathological conditions and especially the splicing of the exon 10. Indeed, tauopathies – neurodegenerative diseases characterized by the accumulation and aggregation of tau proteins – can be classified by into three groups depending on the preponderant tau isoforms involved. For example, progressive supranuclear palsy (PSP) and corticobasal degeneration (CBD) are characterized by aggregates formed with 4R isoforms and classified as 4R tauopathy, Pick's disease (PiD) is a 3R tauopathy as its aggregates are composed of a majority of 3R isoform and AD is a 3/4R tauopathy since both 3R/4R isoforms are found in the PHF. Since these disease differs

in lesioned brain areas and symptoms, it suggests the existence of different pathological processes according to the tau isoforms involved⁴⁷. Although tau is found to be aggregated in tauopathies, physiological tau is a natively unfolded protein and has little propensity to self-aggregate⁴⁸. Despite this unfolded nature, tau appears to preferentially adopt a paper-clip like structure where the N-terminal, C-terminal and the repeat domains are in proximity⁴⁹.

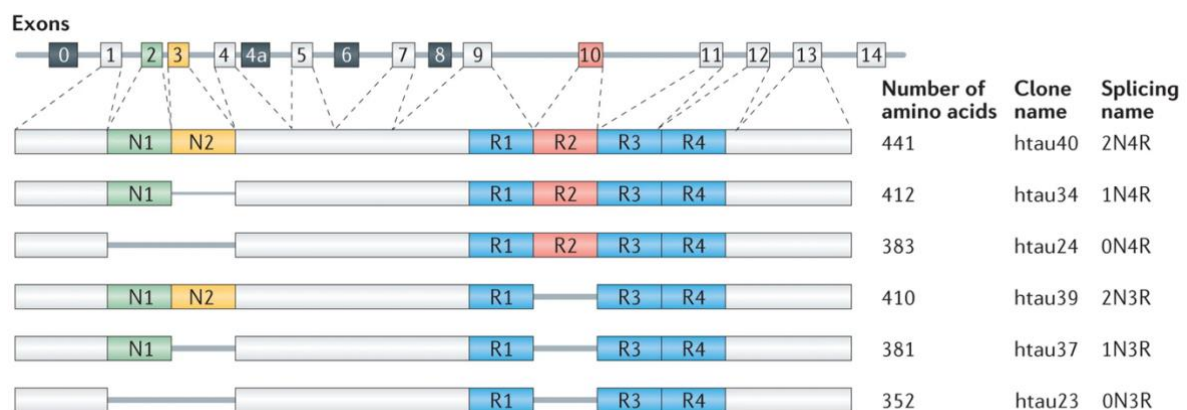


Figure 2: Tau isoforms result from alternative splicing.

The MAPT gene contains 16 exons and generates 6 tau protein isoforms by alternative splicing of exon 2, 3 and 10. The isoforms differ from each other based on the number of N-terminal repeats (N0, N1, N2) and microtubule-binding domain repeats (R3 or R4). All six isoforms are expressed in the adult brain but only the shortest isoform is expressed in the fetal brain. Illustration from Wang et al, 2016⁵⁰.

Tau expression is mainly cerebral even if some peripheral organs such as the heart or the kidney show tau expression⁵¹. In the brain, tau is mainly expressed in neurons even if low expression levels can also be found in oligodendrocytes and astrocytes^{52,53}. In neurons, tau is mainly distributed in the axons where it stabilizes the microtubule but a variety of other functions and subcellular localization of tau have been identified in the past decade⁵⁴. Beside stabilizing the microtubules, axonal tau can compete with kinesin and dynein microtubule motors directly influencing the anterograde and retrograde transport of cargoes along the axon *in vitro*^{55,56}. Tau has also been shown to be located at the dendrites where its function are still unclear⁵⁷ and in the nucleus where it exerts a role in RNA and DNA protection⁵⁸⁻⁶⁰. Tau being

involved in many cellular processes its functions need to be regulated. The main regulator of a protein function is post-translational modification (PTM) and tau has been described to undergo several types of PTM.

Post-translational modifications lead to Tau instability

In the context of AD, tau proteins undergo massive post-translational modifications. The general role of post-translational modifications is to regulate a protein’s functional diversity by altering its electrostatic and/or structural properties. Tau is described to be subjected to a wide variety of PTMs including phosphorylation, acetylation, methylation, O-GlcNAcylation. Among those PTMs, phosphorylation has generated a lot of interest especially since abnormal phosphorylation at specific residues have been found in AD brains and were suggested to be involved in tau aggregation process (Figure 3) ^{26,61,62}. Therefore, a lot of effort have been put in the production of phospho-specific tau antibodies for the detection of pathological tau species for research and diagnostic.

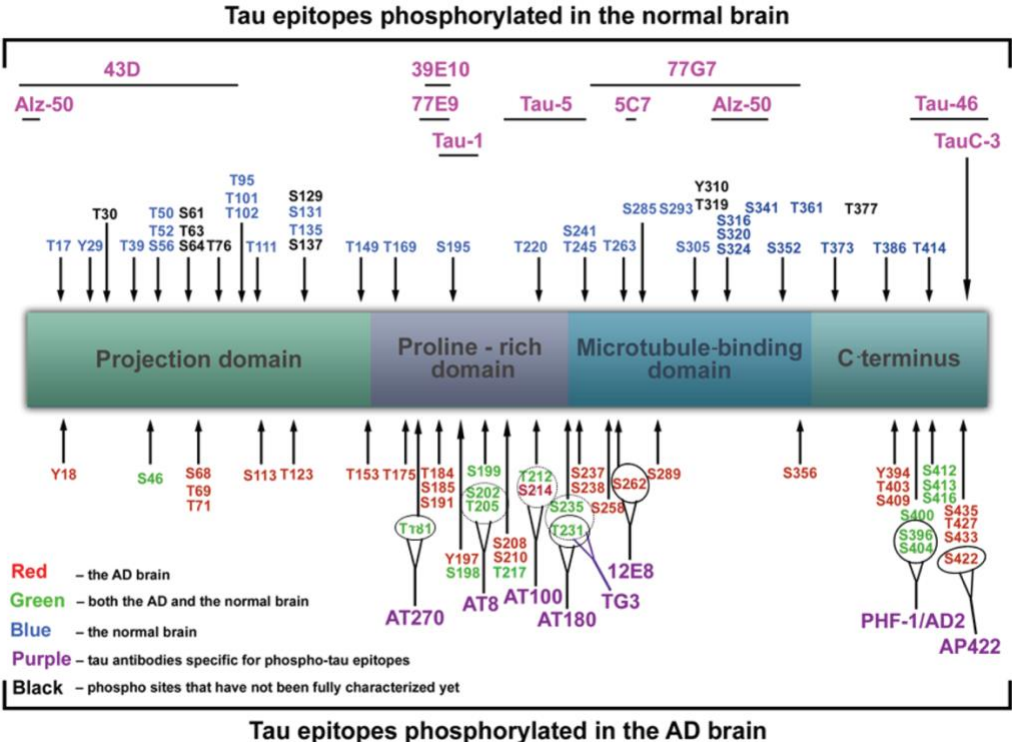


Figure 3: Physiological and pathological phosphorylation sites of tau and their specific antibodies.

Tau has more than 80 putative phosphorylation sites among which some are specific to the AD brain (red), to the normal brain (blue) or found both in AD and normal brain but in varying proportion (Green). The differential phosphorylation of tau in AD has been used to detect pathological species of Tau in research and diagnostic. To do so, phospho-specific antibodies (purple) have been generated and are extensively used in the field of AD biomarker and histopathology. Illustration from Simic et al, 2016⁶³.

Despite different reports suggesting the role of phosphorylation in Tau aggregation remains controversial since polyanionic factors induce Tau aggregation *in vitro* regardless of its phosphorylation state⁶⁴ and hypothermia-induced Tau hyperphosphorylation in hibernating animals isn't associated with Tau aggregation^{65,66}. However, tau phosphorylation is collectively accepted as a regulator of its physiological functions. For example, phosphorylation inside the microtubule-binding domain and/or proline-rich domain negatively impacts its ability to interact with microtubules for example^{67,68}. Therefore, Tau aberrant phosphorylation in AD interferes with its normal function and is described to induce the detachment of Tau from the microtubules, to promote its delocalization to the somatodendritic compartment and to alter its intracellular degradation⁶⁹⁻⁷². Overall, abnormal Tau phosphorylation is associated with a loss of physiological Tau functions, its delocalization and accumulation.

Other PTMs such as acetylation or truncation have emerged as relevant Tau modifications both to its physiological and pathological functions. Tau acetylation has been found in AD brains and shown to be critical for Tau turnover and cytotoxicity *in vitro* and *in vivo*^{73,74}. Truncation by different proteases has been demonstrated to generate aggregation-prone Tau fragments in cells and rodents⁷⁵⁻⁷⁷. PTMs are thus drifting tau away from its physiological role and promote its accumulation and aggregation in the context of AD.

Tau protein aggregation

In AD, tau assembles into filaments through its microtubule-binding domain repeats while the remaining N-terminal and C-terminal parts form the "fuzzy coat"^{78,79}. Tau aggregation forms either straight filaments or paired-helical filaments, the latter being the predominant component of neurofibrillary tangles⁸⁰. The oligomerization of tau requires two hexapeptides

motifs in the microtubule-binding domain region named PHF6 and PHF6*^{81,82}. Despite being a key event in AD, tau does not spontaneously aggregate and the trigger of its aggregation *in vivo* has not been identified yet^{83,84}. Several factors influencing tau aggregation were identified *in vitro*. As discussed previously, PTMs such as phosphorylation on specific residues and enzymatic cleavage promote tau aggregation. Tau concentration appears to also be a key factor by inducing conformational changes promoting Tau self-assembly⁸⁵. Polyanionic factors, including heparin, are known to seed tau aggregation and are extensively used for *in vitro* generation of tau aggregates^{86,64,87,88}.

Despite these *in vitro* data, the *in vivo* trigger of tau aggregation remains a mystery. The aggregation of tau has long been postulated to be the toxic form of Tau, the culprit of tau-induced neurodegeneration, yet this view is challenged by recent findings arguing that Tau oligomers or even monomers might be the guilty ones.

Is tau toxicity monomers, oligomers or aggregates mediated?

Tau aggregation into NFTs has long been considered as the endpoint of tau pathology in AD as it revealed the extent of Tau-induced neurodegeneration in post-mortem tissues of AD patients. However, studies on regulatable tauopathy mouse lines have suggested that NFT formation is not the cause of synapse loss, neurodegeneration and subsequent cognitive impairments. Indeed, switching off tau expression in a tau P301L mouse line (rTg4510) or in a transgenic mice expressing the repeated domain of tau with the Δ K280 mutation (both mutations promoting the appearance of tau pathology) improved the cognitive performance of the mice even though NFTs were still present^{89,90}. These studies have created a new school of thought proposing tau soluble species as the mediators of neurodegeneration. Some have even suggested that tau aggregation would possibly represent a protective process allowing the sequestration of toxic monomers and oligomers of tau⁹¹. Supporting this view, studies have found that soluble tau (monomeric and/or oligomeric) to be cytotoxic, partly by inducing mitochondrial damage⁹²⁻⁹⁵.

Despite these promising data, research on soluble tau species is still in its beginning and suffers from the lack of standardized methods for Tau oligomers production and for its detection in human and rodents brain tissues. Regardless of these technical limitations, several groups went further in the study of soluble tau species and have ignited the idea of tau spreading from diseased neurons to healthy ones, supporting a critical role for soluble tau monomers and oligomers in the pathophysiology of AD.

Tau as a prion-like protein

Interestingly, tau protein loss of microtubule-binding function is accompanied by a toxic gain-of-function consisting of the ability of tau oligomers to co-aggregate with normal tau protein in a prion-like manner (Figure 4). Early work by Braak & Braak, not only set the basis of tau staging but gave birth to the hypothesis of Tau spreading from the entorhinal cortex to the rest of the brain through its connectivity⁹⁶. This hypothesis was further supported by the discovery that pathological Tau species are taken up by neurons and are able to recruit native tau *in vitro*^{97–100}. Moreover, multiple studies have proven this phenomenon to be also true *in vivo* using both transgenic and injection mouse models^{101–106}. Interestingly, Tau seeding activity can be found in AD brain regions before the onset of tau aggregation reinforcing the argument of a transport and seeding of tau to other brain regions preceding the appearance of NFTs¹⁰⁷.

The emerging hypothesis behind tau spreading is its synaptic transfer from neuron to neuron. Indeed, clinical data show that tau spreads amongst anatomically connected brain areas in patients with AD^{108–111}. The aforementioned mouse models are also pointing towards the same direction since tau spreads in these models from the original tau expressing or tau injected brain area to distant but connected brain regions. Yet tau spreading mechanisms are still a debate, extracellular tau seeds can be found away from primary lesioned areas and even in the ventricular system, either in free forms or encapsulated in exosomes which could also participate in tau spreading^{112,113}. Therefore, the extracellular tau species are gaining interest

and research is focused on determining which of them have seeding capacities, how they are secreted to the extracellular space and how they are taken up.

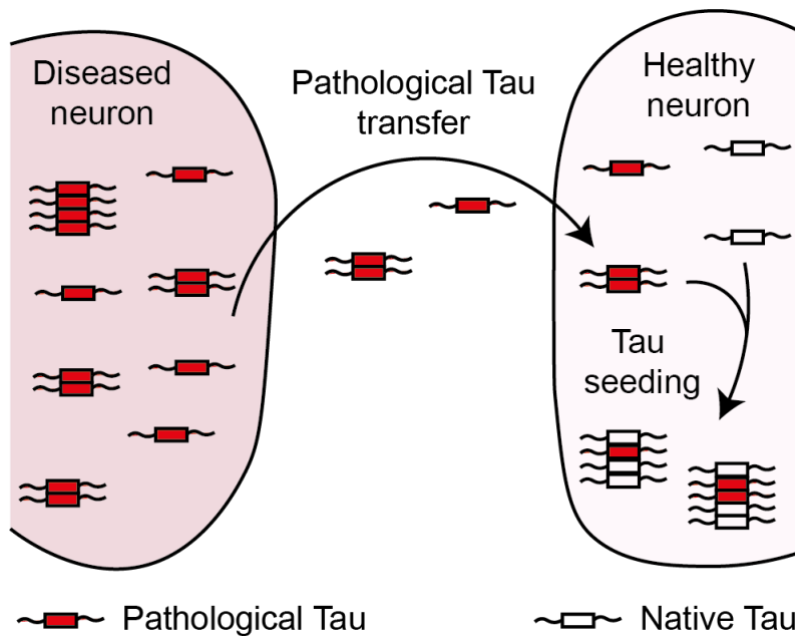


Figure 4: The prion-like hypothesis of Tau spreading.

Neurons bearing pathological tau species can secrete it in the extracellular space and transfer it to neighboring cells. Once inside another neuron the pathological tau species recruit native tau isoforms and seed their aggregation similarly to what is observed with the prion protein in Creutzfeldt-Jakob disease.

Extracellular Tau

Tau was originally considered as an intracellular protein which presence in the extracellular space was associated with its release during neuronal death. Yet, several studies showing evidences of Tau secretion by living cells *in vitro* and *in vivo* have challenged this conventional view. Although tau lacks a signal sequence for secretion, several groups have reported its secretion in mouse neuronal primary cultures as well as induced pluripotent stem cell-derived human cortical neurons^{114,115}. Tau is secreted by unconventional secretion pathways such as direct translocation across the plasma membrane, membranous organelles-based unconventional secretion and microvesicle shedding at the plasma membrane¹¹⁶⁻¹²². Also, tau can be secreted at the endpoint of degradative pathways resulting in the release of full lengths Tau and Tau fragments¹²³.

Interestingly, studies on tau secretion have shown that a variety of tau species are found in the extracellular space. Full length, C-terminally-truncated or phosphorylated tau are found in extracellular mediums of neuronal primary culture and are similar to the tau species

found in AD patients CSF further supporting the role of neuronal tau secretion in its presence in the CSF ^{124,117}.

Tau internalization is as unconventional as its secretion. Indeed, no specific membrane receptors are known for Tau but it interacts with several membrane-bound proteins. Tau binding to the muscarinic receptors, heparan sulfate proteoglycans and LDL receptor related protein 1 (LRP1) and subsequent internalization by endocytosis are, to date, the three known Tau cellular uptake mechanisms ^{125–128}. Finally, membrane encapsulated Tau is believed to be internalized by cells thanks to the fusion of the vesicles containing Tau with the plasma membrane. Ultimately, tau secretion and uptake by a variety of modalities explain its ability to spread from the primary lesioned area to the rest of the brain.

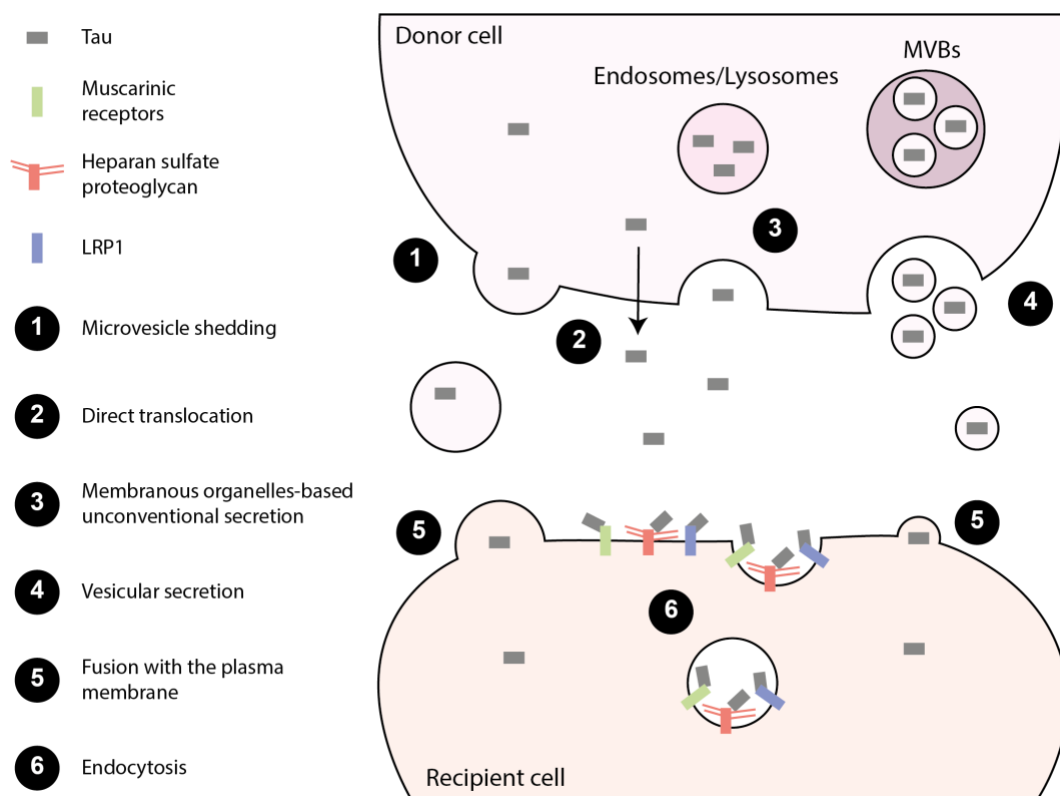


Figure 5: Mechanisms of secretion and uptake of extracellular Tau.

Tau secretion can occur *via* different mechanisms. Tau can be encapsulated in ectosomes during membrane microvesicle shedding (1). It can be released in free form through a direct translocation across the membrane (2) but also after the exocytosis of late endosomes and lysosomes resulting from

degradation pathways, a process also known as membranous organelles-based unconventional secretion (3). Lastly, Tau can be secreted in exosomes contained in multivesicular bodies (MVBs) (4). Once in the extracellular space, tau-containing vesicles can be uptaken by recipient cells by fusion with the plasma membrane (5) and free tau species can interact with several membrane-bound proteins and undergo endocytosis (6).

Tau and A β act synergically to induce neurodegeneration

The relative importance of both proteins in AD pathogenesis is a source of debate^{129–131}. Familial AD cases are pointing toward a major role of A β as a trigger of AD since mutations are only found in genes related to A β pathology. However, while A β pathology progression poorly correlate with the evolution of cognitive decline in AD, tau pathology spreading from medial temporal cortex to the neocortex is associated with the onset of cognitive deficits¹³². An increasing body of evidence supports the role of tau and A β interaction as a keystone of AD pathogenesis. In a first attempt to recapitulate A β and tau role in AD, the amyloid beta cascade hypothesis has been formulated putting A β as the causative agent of AD¹³³. From a linear hypothesis of A β being the sole culprit of AD, the current hypothesis has evolved to integrate Tau as an important actor of AD neurodegenerative process.

Significant advances in the comprehension of pathological mechanisms underlying AD onset and progression have come from preclinical studies. However, their transfer to the clinical setting remains the ultimate challenge and is particularly difficult. A reason for this complicated preclinical to clinical transfer has been the difficulty to diagnose AD patients accurately during their lifetime. Indeed, definite AD diagnosis have relied on post-mortem diagnosis for a long time but tremendous efforts deployed in finding fluid and imaging biomarkers of AD are able to break down this transfer barrier.

Diagnosis of Alzheimer's Disease: mixing neuropsychological and biomarker criteria

Diagnosis of AD represents a major challenge for AD research and clinical practice. The first guidelines for AD, published in 1984, were set on two points: diagnosis of AD could only be “probable” until AD pathology was confirmed post-mortem and it could only be assigned when patients presented significant functional disability and met the criterion of dementia¹³⁴. Increasing knowledge on AD, especially on tau and amyloid beta pathology, and significant technological advances have allowed the development of tau and amyloid beta measurements in different biological material or through imaging techniques as relevant biomarkers for AD, helping to set new criteria for AD diagnosis. More recently, two new sets of criteria have been proposed for AD, one by the International Working Group (IWG) for New Research Criteria for the Diagnosis of Alzheimer's Disease and the other by the National Institute on Aging-Alzheimer's Association (NIA-AA), which integrate clinical symptoms and biomarkers of AD^{135–138}. Both sets of criteria differs from the original criteria by identifying several temporal stages of AD before dementia onset and relying on specific biomarkers such as: CSF A β , CSF total or phosphorylated tau, amyloid positron emission tomography (PET), atrophy on magnetic resonance imaging (MRI) and brain glucose hypometabolism using Fluorodeoxyglucose (FDG) PET. Three main stages of AD arise from these criteria: the asymptomatic or preclinical phase with presence of AD biomarkers and absence of cognitive deficits, the prodromal phase with presence of biomarkers and mild cognitive impairments (MCI) and the symptomatic or clinical phase with presence of biomarkers and dementia.

Neuropsychological evaluation

The clinical diagnosis process of AD usually begins with a determination of the presence and severity of cognitive impairments in the context of patient's, family or healthcare professional concerns about cognitive impairments in the patient. Cognitive decline *per se* isn't

specific of AD since any neurodegenerative, cerebrovascular disease or depression can lead to cognitive impairments. However, extensive research on AD cognitive symptoms have identified impairments of specific cognitive functions. Episodic memory deficits are frequently the first cognitive symptom in AD patients, preceding the important cognitive and behavioral changes appearing with the dementia state^{139–142}. Several others cognitive functions are altered during the course of AD pathology such as progressive visuospatial, executive functions or aphasia but are variable in appearance and severity amongst patients (reviewed elsewhere¹⁴³). This diversity has resulted in the proposition of AD subclassification into typical AD and atypical AD variants depending on the impaired cognitive functions¹³⁵. Unfortunately, other neurodegenerative diseases are also associated with impairments in the same cognitive fields and their differentiation from AD is challenging.

The first complementary diagnostic tool has been the development of histopathological staging techniques for AD. Tau and amyloid pathology staging were and remain gold-standard diagnostic tools for AD as they allow the discrimination of AD amongst other confounding neurodegenerative diseases.

Histopathological staging

Braak stages

In Alzheimer's Disease, Tau pathology is staged following the Braak staging scheme. In a 1991 report, Braak & Braak examined 83 post-mortem brains from control and AD patients for senile plaques and neurofibrillary changes (Figure 6)¹⁴⁴. While they could not find any specific pattern of distribution for A β -containing senile plaques, they identified a spatiotemporal evolution in the distribution of neurofibrillary tangles and neuropil threads (axonal tau-positive inclusions). Six Braak stages were characterized:

- The transentorhinal stages I and II correspond to the presence of these neurofibrillary changes in transentorhinal cortex in increasing density.

- The limbic stages III and IV are associated with the progression of the lesions from the transentorhinal cortex to the limbic system and especially to the first sector of the Ammon's horn of the hippocampus.
- The isocortical stages V and VI are marked by the spreading of the lesions to all isocortical association areas.

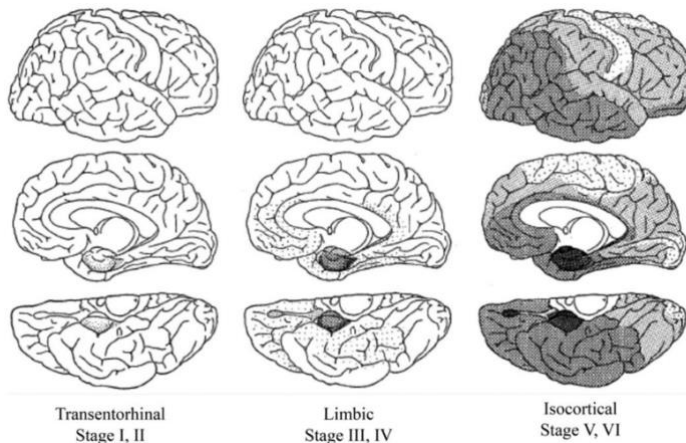


Figure 6: Braak staging of neurofibrillary changes in AD.

Braak staging comprises 6 stages grouped in 3 steps. The first step of tau pathology is the affliction of the transentorhinal cortex (stages I and II) then the deposition spreads to the limbic system (stages III and IV) and finally throughout the isocortex (stages V and VI). From stage I to stage IV patients

usually display no or mild cognitive impairments while stages V to VI are often found in patients with a full-blown dementia state. Illustration from Braak & Braak, 1991¹⁴⁴.

Clinically, Braak stages progression is correlated with the extent of cognitive impairment measured with the clinical dementia rating scale. However, while before stage IV, Braak staging doesn't allow the distinction between cases with or without mild cognitive impairment, cases with Braak stages superior to IV are consistently associated with cognitive impairments¹⁴⁵.

Thal stages

A decade after Braak staging, Thal analyzed 47 post-mortem control and AD brains for A β depositions and successfully deciphered a spatiotemporal evolution of senile plaques distribution (Figure 7)¹⁴⁶. The Thal staging is subdivided in 5 phases:

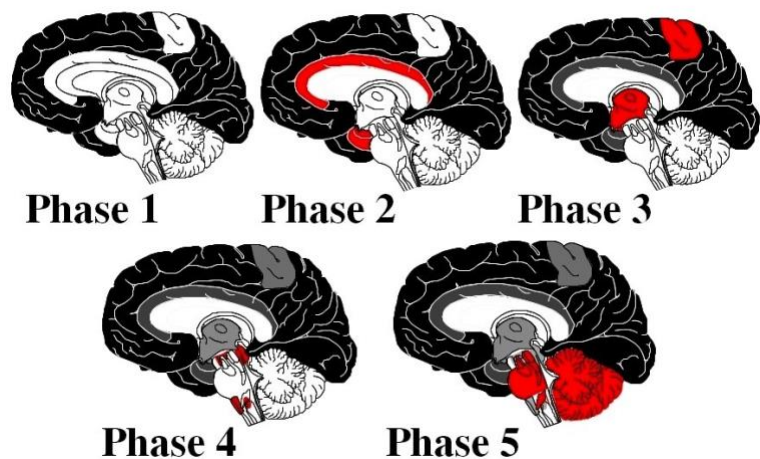
- In phase 1, A β is found exclusively in the neocortex.

- In phase 2, allocortical brain regions (hippocampus and olfactory bulb) are involved.
- Phase 3 is characterized by the involvement of the diencephalic nuclei, striatum and cholinergic nuclei of the forebrain.
- Phase 4 is marked by the deposition of A β in several brainstem nuclei.
- Phase 5 is associated with the cerebellar A β deposition.

Intriguingly, Thal staging in contrary to Braak staging does not correlate well with cognitive impairments¹⁴⁷ suggesting that the progression of A β deposition isn't a good predictor of cognitive decline.

Figure 7: Thal staging of amyloid depositions in AD.

The Thal staging is divided into 5 phases. In the first phase only sparse and small groups of diffuse neocortical plaques are present. The evolution to phase 2 is associated with the progression of the lesions to the allocortical areas. Phase 3 is characterized by a striatal and diencephalic involvement.



Phase 4 corresponds to the spreading of A β deposition in several brainstem nuclei and phase 5 is marked by a cerebellar A β deposition.

Despite being an efficient diagnosis method, histopathological staging tools are obviously incompatible with clinical trials or research during the patient's life. Therefore, fluid and imaging biomarkers were developed to answer the need of an accurate AD diagnosis during the patient's life.

Fluid biomarkers

CSF Tau and amyloid beta concentration

First proof of A β secretion to the cerebrospinal fluid paved the way for quantitative immunoassays for A β in CSF¹⁴⁸. Following this discovery, enzyme-linked immunosorbent assays (ELISA) for A β 42 peptides were developed and showed lower CSF A β 42 in AD patients compared to cognitively normal elderly¹⁴⁹. This counterintuitive result of a decreased A β 42 content in the context of increased A β 42 production due to AD was later explained by studies associating low CSF A β 42 with higher counts of senile plaques, implying the sequestration of A β 42 into senile plaques^{150,151}. Finally, A β 42/A β 40 ratio has been shown to be more performant by using A β 40 concentrations as a proxy for total A β production¹⁵².

Soon after the discovery of A β in CSF, tau was showed to be detectable in CSF samples from AD patients by western blot and ELISA^{153–155}. Since the first studies, hundreds have replicated these results and ascertained CSF tau as a biomarker of AD. However, CSF tau measured by total tau ELISA assays, recognizing all tau protein isoforms irrespective of post-translational modification states, have been shown to increase not only in AD but also in other neurodegenerative diseases. Therefore, it has been suggested to be a proxy of neurodegeneration rather than a specific AD biomarker^{156–159}. Since tau is post-translationally modified in the context of AD, especially phosphorylated at disease-specific residues, ELISAs detecting phosphorylated tau protein were developed and tested in the hope of finding specific tau phosphorylation associated with AD. The concentration of several CSF tau phospho-epitopes were proven to be specifically increased in AD, including p-Tau181, p-Tau199 and p-Tau231, and equally performant compared to nondemented controls^{160–164}. Lastly, studies have highlighted a correlation between CSF tau levels and tangles as well as neuritic plaques, corresponding to tau positive degenerating neurites around senile plaques, counts^{151,165}. Overall, CSF A β and tau represents sensitive and accurate biomarkers of AD in the earliest

stages of the disease but they have a significant drawback, they require an invasive lumbar puncture.

Plasmatic A β and tau concentrations

Blood biomarkers represent a less invasive and thus promising alternative. However, tau blood dosage has been challenging due to its low very plasmatic concentrations. The emergence of new techniques, such as single molecule array (SIMOA), has allowed the development of ultrasensitive immunoassays directed against A β and tau. Both A β and Tau plasmatic levels were shown to be significantly altered in AD patients compared to control individuals. As for CSF A β , plasmatic A β 42/A β 40 ratio decreases in AD patients as observed in several cohorts^{166–169}. One study has even shown that plasmatic A β 42/A β 40 identifies individuals with abnormal CSF A β or A β PET status with high accuracy and is associated with clinical progression to MCI or dementia¹⁷⁰. Thus, plasmatic A β 42/A β 40 ratio seems promising for patients prescreening in a clinical context to identify patients with probable AD before lumbar punctures or PET scan, but its ability to distinguish between AD and non-AD dementia is still unknown. Total tau plasmatic concentration is increased in AD patients but its overlap with control individuals does not support it as an AD biomarker^{171–173}. Interestingly, when analyzing post-translationally modified plasma tau, studies have found promising results. Plasmatic concentrations of tau phosphorylated at different sites, pTau181/217/231, are markedly increase in AD patients compared to control individual, individuals with cognitive impairments and non-AD dementia^{174–180}. Additionally, truncated tau species have been also described to be increased in plasma and CSF of AD patients^{181,182}. Overall, plasma biomarkers for AD are expanding and showing promising abilities to specifically identify patients with AD. Fluid tau and A β biomarkers are exquisite tools for AD screening but their limits come from their incapacity to assess the extent of the lesions or the progression of the disease.

Imaging biomarkers

PET ligands for A β and tau brain burden evaluation

Due to the invasive nature of CSF biomarkers and the inability of both CSF and blood biomarkers to accurately determine disease progression and severity, PET ligands have been developed to map and quantify A β and tau pathology in the living brain of patients. Several ligands have been used for A β brain PET imaging in the past 15 years among which three have been approved by the US Food and Drug Administration (FDA) and the European Medicines Agency (EMA) for imaging in AD patients. Being available to researchers in the field for quite some time, amyloid PET has been widely used allowing extensive standardization and validation. It has been shown to match neuropathological examination allowing longitudinal assessment of A β burden and representing a key method for the evaluation of disease-modifying drugs clinical trials^{183–185}. Considering tau PET imaging, its use and development are still in their beginning. To date, tau PET ligands show significant retention in AD patients compared to control individuals in brain regions matching AD histopathological stages^{132,186–190}. Despite its novelty, promising are arising from its use in clinical research. Expanding on already described tau lesions progression, a patient-centered longitudinal study suggested new spreading patterns in AD patients, starting from different “tau epicenters” and spreading to strongly connected brain regions¹¹¹. Yet their novelty has its drawbacks, tau PET ligands have weaknesses: significant off-targets retentions are observed in some patients and they lack extensive clinical validation and standardization of quantification methods, and should be interpreted with caution. PET ligands are nevertheless advantageous biomarkers in longitudinal studies by enabling a precise staging of A β and tau pathology throughout AD patients’ life.

Accumulation of A β and tau in the brain triggers neuronal dysfunction and death which in turn induce a diminution of brain glucose uptake and brain atrophy, both of which can be visualized through brain imaging techniques.

Brain glucose hypometabolism

Significant brain hypometabolism, likely reflecting synaptic dysfunctions, cell loss and metabolic dysfunction is consistently observed in several brain regions of AD patients^{191–194}. FDG PET is used as a proxy of brain glucose metabolism, FDG retention being a mirror of cellular glucose uptake. Studies have also found that FDG regional retention patterns are disease-specific and can classify with a high accuracy AD cases from non-AD dementia and control patients¹⁹⁵. Still, FDG PET alone can be misleading, especially in asymptomatic cases, since brain hypometabolism may develop for other reasons than AD^{196–198}. This is why most studies use FDG, A β and/or tau PET to overcome this limitation and improve early differential diagnosis of AD by preventing the misdiagnosis of A β and tau negative patients. When the neurodegeneration is more advanced and neuronal death consequent, classical brain MRI can be used to visualize the structural changes of the brain.

Brain atrophy by volumetric MRI

AD is characterized by progressive neurodegeneration inevitably leading to brain atrophy. Structural imaging based on MRI has shown a close correlation of whole brain, entorhinal cortex, hippocampus and temporal lobe atrophy with cognitive impairment^{199–202}. Interestingly, MRI atrophy measurements were proven to be more sensitive to changes in cognitive performance than CSF A β and tau or amyloid PET²⁰². However, structural changes succeed the changes in CSF A β and tau or amyloid PET in early pathological stages. Therefore, brain atrophy appears as a potent marker for indirect assessment of neurodegeneration and cognitive decline occurring late in the pathology.

All biomarkers having their own limitations, the combination of several of them allow to drastically improve the accuracy of AD diagnosis. Moreover, the compilation of all the biomarkers changes have allowed to approach a more accurate timeline of pathological events in AD.

Approaching an accurate natural history of AD

The integration of the fluid biomarkers, imaging biomarkers and neuropsychological symptoms of AD in a single model not only allows a more accurate and sensitive diagnosis of AD but also a clearer picture of pathological course of events in a patient-centered manner (Figure 8).

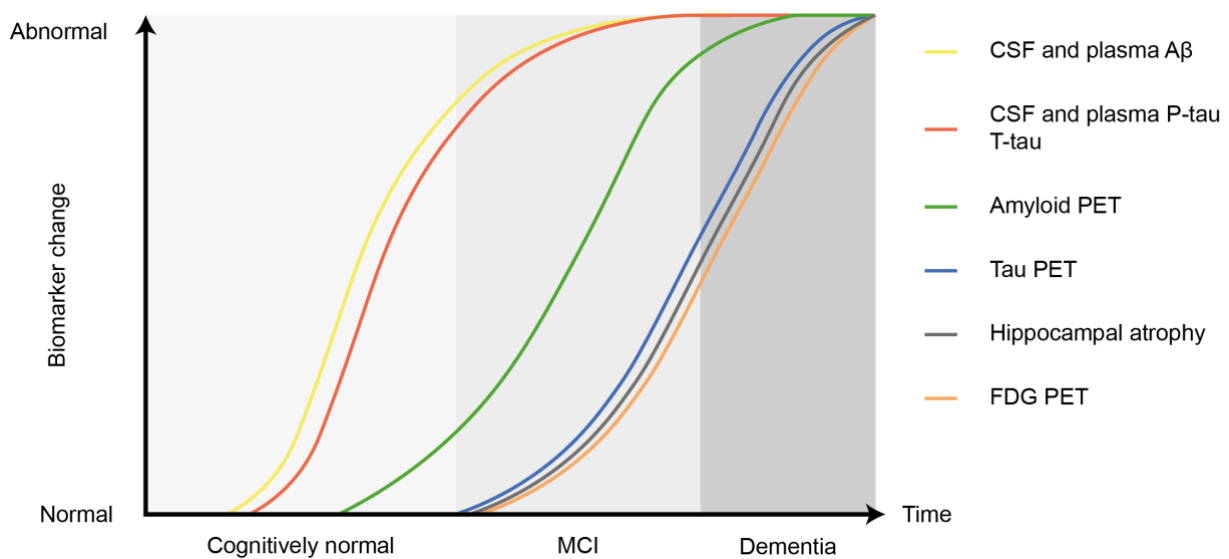


Figure 8: Temporal evolution of biomarker changes in Alzheimer's Disease.

Fluid biomarkers are the first detectable changes with decrease in A β 42/ A β 40 ratio in CSF and plasma shortly followed by an increase in T-tau and p-Tau in CSF and plasma. These biomarkers indicate the underlying progression of Tau and A β pathology in the brain of the patients. Then, the amyloid brain burden becomes visible in amyloid PET. With the appearance of cognitive impairments, Tau PET signal becomes positive and the first signals of neurodegeneration appear with the detection of hippocampal atrophy and decreased FDG PET signal. These biomarkers of neurodegeneration gradually increased with the worsening of cognitive deficits until reaching a plateau when dementia sets in. Illustration adapted from Zetterberg & Bendlin, 2020²⁰³.

Chronologically, CSF A β and tau are the first detectable changes followed by plasma A β and tau both reflecting the first steps of A β and tau pathology. A β and tau PET ligands retention changes come second, reflecting the progression and spreading of A β and tau. In between the changes of A β and tau PET retention and the first cognitive impairments, FDG-

PET and brain atrophy on MRI are observed. Once in the prodromal stage, cognitive and imaging changes incrementally increase to reach the dementia state. From the neuropathological and biomarkers point of view, A β and tau accumulation and aggregation in the brain appears as triggers of AD neurodegenerative process. Therefore, disease-modifying therapeutics strategies were designed to prevent A β and tau accumulation and subsequently stop or slow down the development of cognitive decline in AD.

Disease-modifying therapeutic strategies for Alzheimer's Disease

Historically, AD patients have been treated with cholinesterase inhibitors (donepezil, rivastigmine, galantamine) or NMDA receptor antagonist (memantine). Some of these treatments are still approved for demented patients in the United States and Europe but have shown to provide modest benefits delaying symptoms progression of several months. Moreover, they remain symptomatic treatments since they have no effect on the biological processes involved in AD. The amyloid cascade putting A β as the major cause of AD, significant efforts were deployed to develop strategies preventing A β production or promoting its clearance from the brain.

Anti-A β strategies

In the aim to reduce A β brain burden, pharmacological strategies reducing A β production were the first line of molecules developed by pharmaceutical companies and public research. A plethora of compounds with different modes of action (β -secretase inhibitors, α -secretase activators, A β degrading enzyme activators, A β brain clearance modulators) were promising in preclinical studies but failed to demonstrate benefits in clinical trials. Additionally, most passive-immunotherapy strategies of first generation, based on the injection of anti-A β

antibodies, have met the same fate as pharmacological A β production modulators (reviewed elsewhere²⁰⁴). Despite the failures of the first attempts, some A β antibodies showed greater efficiency. One of them, Aducanumab, has passed clinical Phase III and was controversially approved by the FDA for a phase IV randomized, controlled clinical trial^{205–207}.

During the development of A β passive immunotherapies and in regard to their multiple failures in clinical trials and to the increasing body of evidence implicating tau as an important driver of neurodegeneration, strategies targeting tau were designed.

Anti-Tau strategies

As for A β , disease-modifying strategies targeting tau aim at preventing or slowing pathological tau production, accumulation and aggregation. A variety of methods have been proposed including anti-aggregation agents, antisense therapies but the most promising and developed strategies are passive and active immunotherapy. Injections of tau therapeutic antibodies targeting different tau species (monomers, aggregates, phosphorylated at specific residues) have been proven effective on both tau pathology and cognition in preclinical studies^{208–210}. However, only a few are currently being investigated in various phases of clinical trial and none have reached phase III yet. Tau active immunotherapy, or tau vaccines, are also explored and have shown promises in preclinical studies both ameliorating tau pathology and cognition^{211–213}. Albeit showing great potential in early clinical phases, anti-tau immunotherapies are in their beginning and anti-A β immunotherapy multiple failures force us to wait until late phases of clinical trials before stating their future use as AD treatments.

A significant trend in potential AD treatments is the clearance of either tau and A β from the brain using immune responses or exogenous compounds. Nonetheless, studies have shown that the brain is intrinsically able to clear both proteins either by degradation or excretion into the blood circulation. Therefore, the identification tau and A β clearance mechanisms would

provide new therapeutical avenues. While significant effort has been invested into elucidating A β degradation and clearance, tau degradation and clearance remain partially unexplored.

Brain clearance mechanisms help coping with Tau accumulation

Brain waste removal comprises different overlapping clearance systems. Proteins can be cleared from the intracellular compartment or from the extracellular compartment, including the interstitial fluid (ISF) surrounding brain cells and the cerebrospinal fluid surrounding the brain. Depending on the nature of the protein, it can be removed by enzymatic degradation, undergo cellular uptake, be transferred from ISF to CSF or excreted into the blood or lymph. While A β clearance have been extensively documented, tau protein clearance mechanisms remain poorly understood.

Cellular degradation systems

Degradation clearance involves enzymatic digestion of proteins by brain cells. Protein degradation can occur both in the extracellular compartment, involving secretion of proteases by different brain cells such as astrocytes or microglia, and in the intracellular compartment, implicating either intracellular proteins or requiring the uptake of proteins from the ISF by neurons and glial cells. Intracellular degradation mainly relies on the endo-lysosomal pathway for protein internalization and on the ubiquitin-proteasome or autophagy pathway for protein degradation.

The Ubiquitin-Proteasome System

The Ubiquitin-Proteasome System (UPS) is common to all eukaryotic cells and allows the selective degradation of intracellular proteins. UPS involves the ubiquitination of proteins, their conjugation to a chain of ubiquitin peptides, targeting them to the 26S proteasome, a

macromolecular protease. Ubiquitination requires a set of three enzymes families E1, E2 and E3 which respectively catalyze the activation of ubiquitin, the recruitment of the targeted protein and the ligation of ubiquitin to the targeted protein. Finally, the 26S proteasome composed of two multisubunits - the 20S core and 19S regulatory core - degrades ubiquitinated proteins after their docking to the 19S regulatory core (Figure 9). Ubiquitination is proposed to promote Tau aggregation into insoluble Tau aggregates and prevent the accumulation of toxic tau and seeding competent Tau soluble monomers and oligomers. Ubiquitination of several tau residues have been found in paired helical filaments of AD patients brains suggesting that in the course of PHF formation Tau protein is targeted to the proteasome but isn't successfully degraded²¹⁴⁻²¹⁷. Interestingly, a study isolating oligomeric Tau from patients at different Braak stages highlighted the fact that ubiquitination occurs with the formation of PHFs but not in early aggregation stages of Tau²¹⁸. Moreover, several reports of proteasome impairment in AD confirming the failure of UPS in degrading Tau in this context²¹⁹.

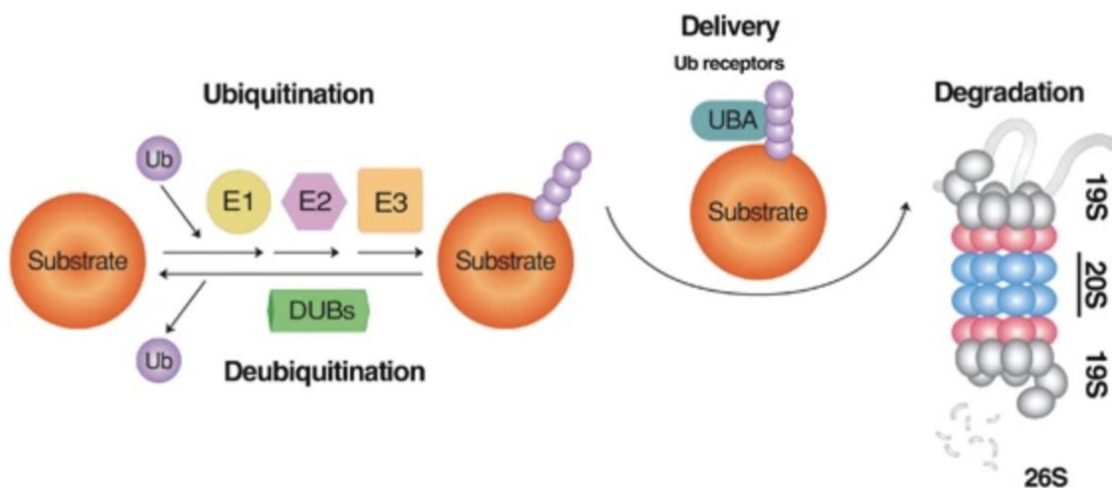


Figure 9: Degradation of proteins by the ubiquitin-proteasome system.

Misfolded protein can be targeted to the UPS for degradation. This selective degradation systems, proteins are targeted for degradation through the addition of a ubiquitin chain. First, ubiquitin is primed by the E1 and transferred to E2. At the same time, proteins destined for UPS degradation are recognized by chaperones and associated to E3, ubiquitin ligases, in order to covalently bind the ubiquitin chain to the protein. This ubiquitination is reversible and catalyzed by the deubiquinating enzymes (DUBs).

Ubiquitinated proteins are then degraded by the 26S proteasome. Illustration by Ciechanover & Kwon, 2015²²⁰.

Autophagy

The autophagy pathway allows the degradation of intracellular protein through the formation of an autophagosome. Three types of autophagy have been described: the chaperone-mediated autophagy, involving the targeting of protein waste by chaperones and the translocation of the cargo to the lysosomes for degradation, the microautophagy: a direct engulfment of intracellular material by lysosomes, and the macroautophagy: requiring the formation of an autophagosome to engulf intracellular components. The induction of macroautophagy occurs at the phagophore assembly site and consists in the nucleation of an isolation membrane called phagophore, destined to engulf the protein waste. After elongation and engulfment of the cargo, the newly formed vesicle is called the autophagosome. Lastly, autophagosomes fuse with the lysosome allowing the degradation of their cargos.

In AD patient's brain, tau is found in lysosomes and co-localized with autophagic markers²²¹. Chaperone-mediated autophagy, microautophagy and macroautophagy have been implicated in tau intracellular clearance (Figure 10, A-C)²²²⁻²²⁴. The first two are involved in the degradation of soluble tau species via their interaction with chaperones such as HSC70²²⁴. The latter can lead to the degradation of Tau aggregates²²². Despite the efficiency of autophagy to degrade tau monomers and oligomers in physiological conditions, tau resists autophagic degradation due to a decline in autophagic activity observed in AD²²⁵.

The endo-lysosomal pathway

The endo-lysosomal pathway is involved in the uptake of extracellular and membrane proteins for degradation, secretion or recycling purposes. Endocytosis, the process of extracellular and membrane protein internalization, occurs by a variety of mechanisms depending on the cargo size. Large cargos, such as cell debris, are taken up by either phagocytosis or micropinocytosis. Small cargos, such as extracellular proteins, can be

internalized either in a clathrin-dependent and independent manner. In the former, clathrin, a coat protein, and a myriad of other coating and regulatory proteins assemble at the endocytic site to form a membrane invagination and engulf the cargo into a vesicle requiring the pinching of the plasma membrane by dynamin. In the latter, a clathrin coat isn't required and can occur either with other coating proteins such as caveolins or without any. The resulting intracellular vesicle is coined the endosome. Depending on the cargo nature, the endosome will be sorted and matured.

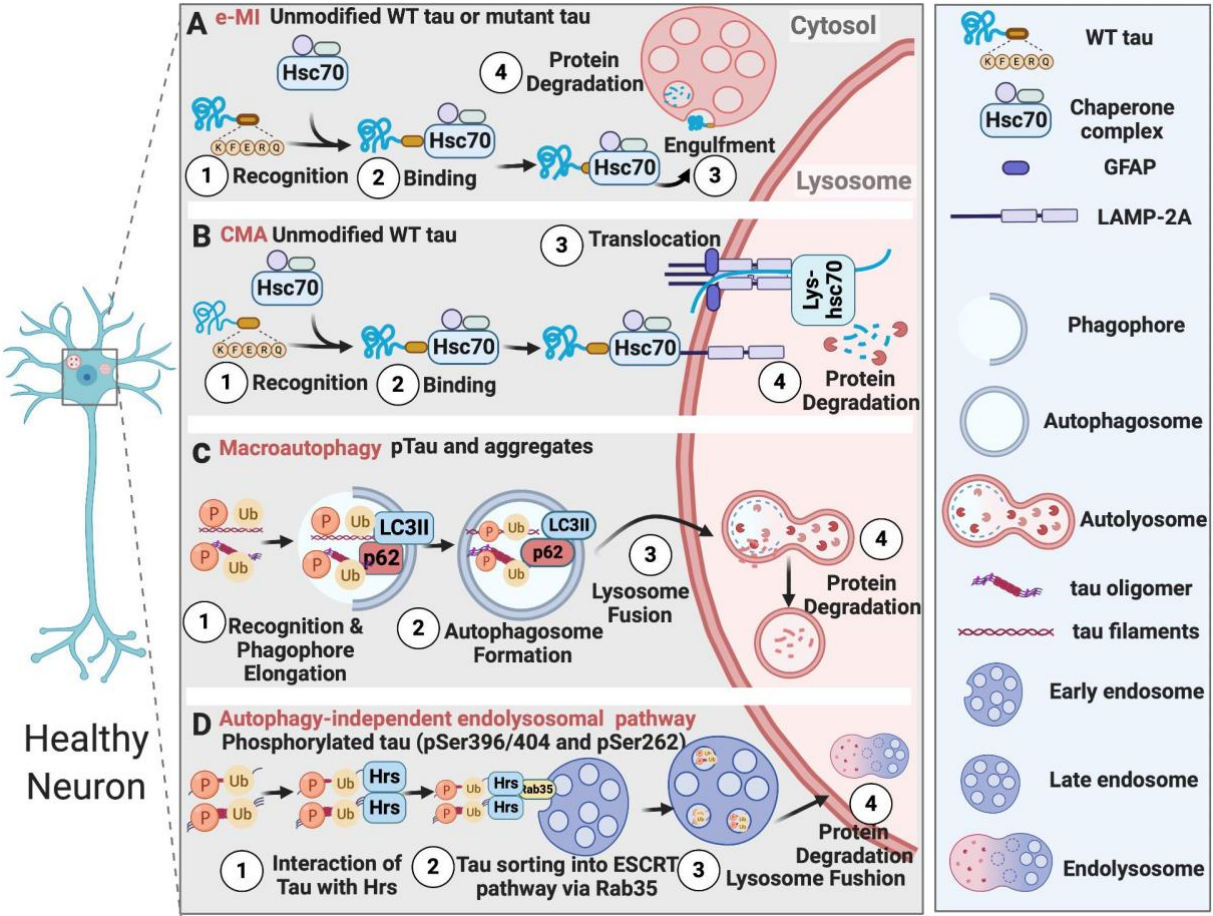


Figure 10: Degradation of tau by autophagy and autophagy-independent pathways.

A & B. Endosomal microautophagy (e-MI) and chaperone-mediated autophagy (CMA) degradation of tau rely on the detection of a peptidic motif (KFERQ) by molecular chaperones such as Hsc70. While e-MI results in the engulfment of tau in MVBs and can result in its degradation or secretion to the extracellular space, CMA involves the translocation of Hsc70-bound tau to the lysosomes through its interaction with LAMP-2A. C. Macroautophagy allows the degradation of tau aggregates (oligomers and filaments). D. The endolysosomal pathway is able to degrade tau monomers and oligomers by their

sorting and transport to the MVBs involving ESCRT proteins. As for e-MI, the endolysosomal pathway can result in both degradation and secretion of tau.

The early endosome, directly arising from the endocytosis event, can be matured into either late endosome, containing proteins fated to degradation, or recycling endosome, containing proteins fated to regain the plasma membrane or extracellular space. While recycling endosomes are transported to the plasma membrane for fusion, the late endosomes undergo acidification and fusion with lysosomes for protein degradation. During the maturation process of late endosomes, endosome membrane invagination can occur, generating exosomes, and result in the formation of multivesicular bodies. Ultimately, the endo-lysosomal pathway leads to the transcytosis, transport across the cell, or the degradation of the cargo. The endo-lysosomal pathway has been implicated in Tau degradation by neurons and also required for astrocytic and neuronal uptake and degradation of Tau^{226–228}. Cytosolic free Tau can also be encapsulated in MVBs through its recruitment by endosomal sorting complex required for transport (ESCRT) protein (Figure 10, D)²²⁶. On the other hand, Tau is able to bypass the endo-lysosomal degradative pathway and take advantage of it for its secretion and seeding. Indeed, studies have found that neuronal tau secretion involves its liberation from endosomes or lysosomes^{227,229–231}. Ultimately a substantial amount of tau species ends up in the extracellular space where other clearance mechanisms take place.

Extracellular clearance

When it comes to secreted proteins or proteins escaping the intracellular clearance systems to end up in the extracellular space, extracellular clearance mechanisms take over to ensure the elimination of waste from the brain. The extracellular fluid of the brain, the ISF, is subjected to a regulated circulation called the perivascular clearance, which relies on the glymphatic system and the perivascular drainage system to push solutes into the CSF. From the CSF, protein wastes can exit to the brain lymphatic circulation or the blood circulation

through a diverse set of pathways: lymphatic clearance, circulatory clearance and passage through the blood-brain barrier (BBB).

Paravascular clearance

Unlike all other organs, the brain is devoid of internal lymphatic vessels that remain restricted to the meninges. Traditionally, the transport of solutes from ISF to CSF was thought to only involve passive diffusion. Based on the injection of fluorescent or radioactive tracers, a set of studies challenged this dogma and showed a mechanism by which solutes from the ISF transfer to the CSF through the arterial basement membrane, coined Intramural Peri-Arterial Drainage (IPAD) and the egress of solutes from ISF to CSF through a perivascular space (Figure 11). The latter has been described to be dependent on glial aquaporin-4 (AQP4) expression, generating a hydrostatic pressure driving the perivascular ISF flow, and was therefore coined the glymphatic system²³².

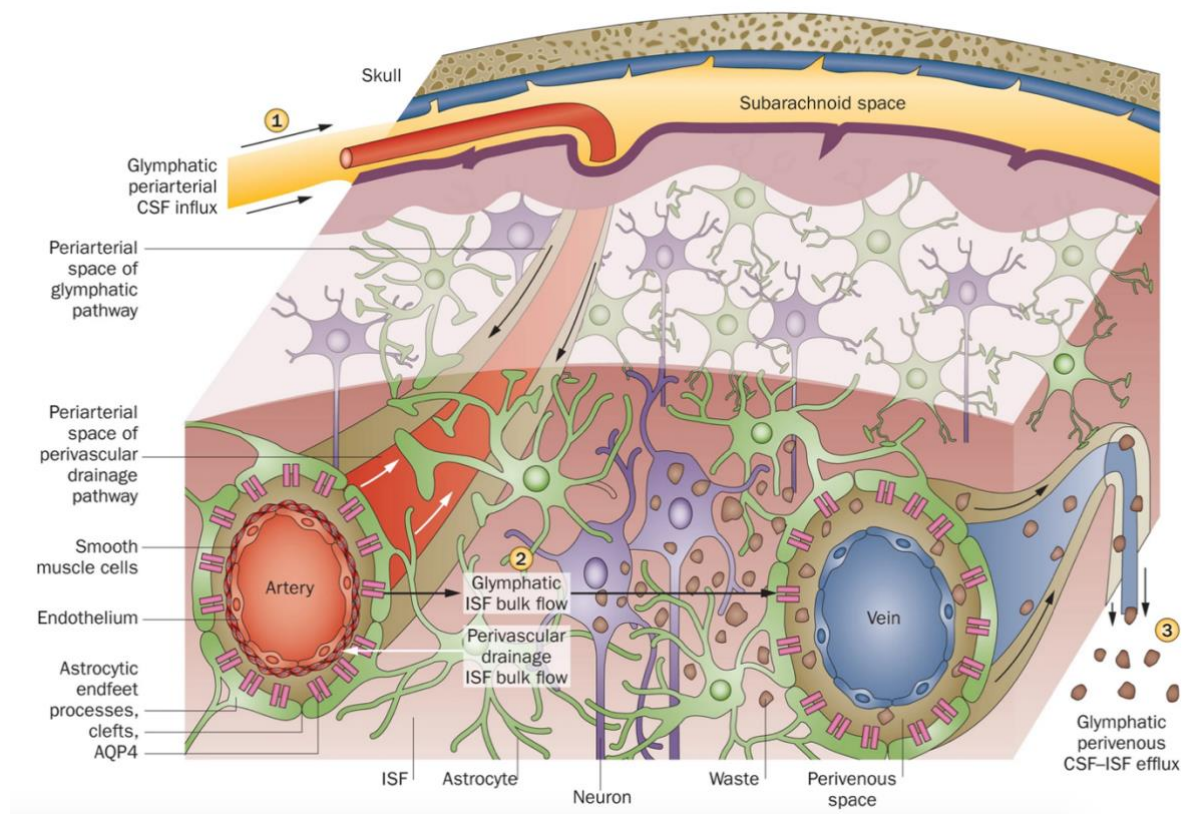


Figure 11: The paravascular clearance pathways of the brain.

The intramural periarterial drainage (white arrows) moves soluble waste through the capillary basement membrane towards the subarachnoid space in opposite direction of the blood flow and periarterial CSF influx. On the other hand, the glymphatic pathway (black arrow) creates a flow of solutes from the periarterial space to the perivenous space passing through the brain parenchyma. It comprises a CSF influx from the subarachnoid space to the periarterial space (1) from which water flows into the parenchyma through astrocytic AQP4 channels. This phenomenon creates a ISF bulk flow towards the perivenous space (2) draining soluble wastes on its way. Lastly, the ISF is drained along the deep-draining vein, mixes with and recirculate with the CSF and is eventually absorbed into the lymphatic system. Illustration from Tarasoff-Conway et al, 2015²³³.

In brief, the transport of water through AQP4 channels generates a flow from the parenchyma to the perivascular space that drains ISF solutes in its way. Once in the perivascular space, the solutes are flushed towards the subarachnoid space and reach the CSF. Both IPAD and glymphatic pathway generate an ISF-to-CSF active flow of solutes subjected to regulation. For example, IPAD efficiency has been shown to be dependent on cerebral arteriole vasomotion ²³⁴ and the glymphatic pathway clearance changes according to the sleep-wake cycle ²³⁵, arterial pulsatility ²³⁶, intracranial pressure ²³⁷ and regional glial AQP4 expression ²³⁸. After reaching the CSF, solutes such as protein wastes, have been shown to be transferred to the lymph and blood.

Tau clearance by the glymphatic system was first discovered in 2014 ²³⁹, in the context of traumatic brain injuries, and more recently validated in the context of AD ^{240,241}. Deregulation of glial AQP4 expression has been shown to occur both in traumatic brain injury (TBI) and AD mouse models disrupting the glymphatic clearance system and promoting the accumulation of Tau^{239,242}.

The glymphatic system has been shown to be efficient in draining tau out of the ISF to the CSF. From there tau could follow three classically described paths to exit the brain: the lymphatic clearance, the circulatory clearance or the blood-brain barrier passage.

Lymphatic clearance

The existence of an authentic brain lymphatic vasculature has recently been discovered in the meninges of rodents, non-human primates and humans (Figure 12) ^{243–245}. These lymphatic vessels were shown to be able to absorb CSF-derived macromolecules and drain them to the deep cervical lymph nodes. However, while numerous studies have confirmed the brain lymphatic absorption of CSF molecules, the exact mechanism(s) resulting in the transfer of solutes from the CSF to the lymphatic vessels remain elusive. The main mechanism contributing to CSF to lymph transfer is believed to be CSF egress following the cranial nerves, the so-called perineural pathway^{246,247}. Currently, only one study has reported the involvement of lymphatic vessels in Tau clearance. It showed a delayed Tau clearance following intrahippocampal injections of fluorescently-labeled tau in a transgenic mouse line lacking brain lymphatic vessels²⁴⁸. If tau efflux to the blood is still present in mice lacking brain lymphatic vessels, then other pathways for tau clearance have to exist. Several authors suggest that Tau can directly pass from brain to blood but the mechanism involved in this phenomenon are still poorly described.

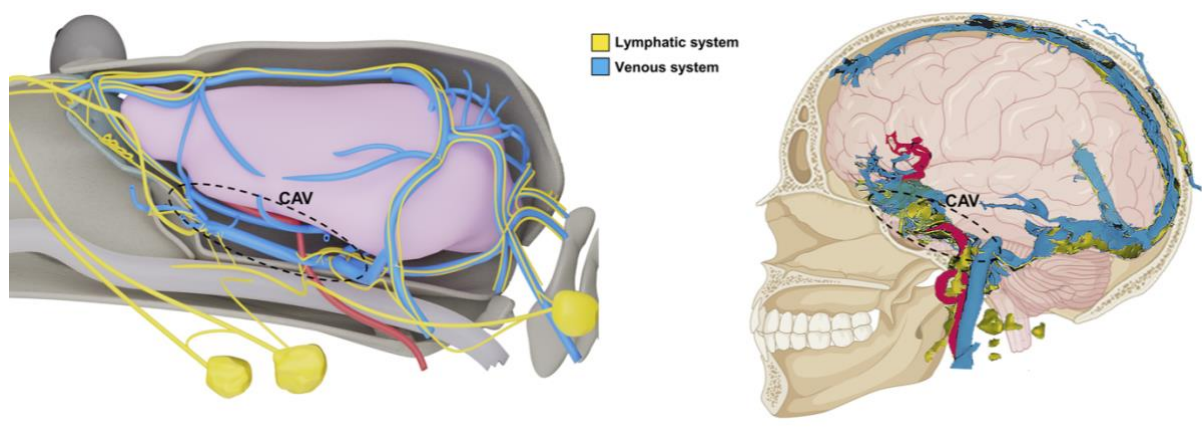


Figure 12: The lymphatic system of the mice and human brain.

Schematic of the mice (left) and human (right) lymphatic (yellow) and venous (blue) system. CAV: cavernous system. Illustration from Jacob et al, 2022.

Circulatory clearance

The circulatory clearance is believed to be a default CSF clearance mechanism. It consists in the passage of CSF molecules to blood circulation through arachnoid villi or granulations following CSF circulation from the choroid plexus to the subarachnoid space. Arachnoid villi are unidirectional valves located at venous sinuses and allow the passage of CSF to brain venous circulation. Research on arachnoid villi CSF clearance dates back to the early 1950s and has stopped since the late 1990s. While their existence makes no doubt, their relative importance in CSF clearance hasn't been assessed *in vivo* in regards of the other systems currently studied and the mechanism of CSF flow through the arachnoid villi didn't reach consensus. Moreover, arachnoid villi clearance has so far only been assessed with exogenous dyes such as Evan's Blue, India ink or Microfil up-to-date raising doubts on its relevance for endogenous molecules. Even if the arachnoid villi are frequently suggested as a Tau clearance pathway, no studies have directly demonstrated this fact yet.

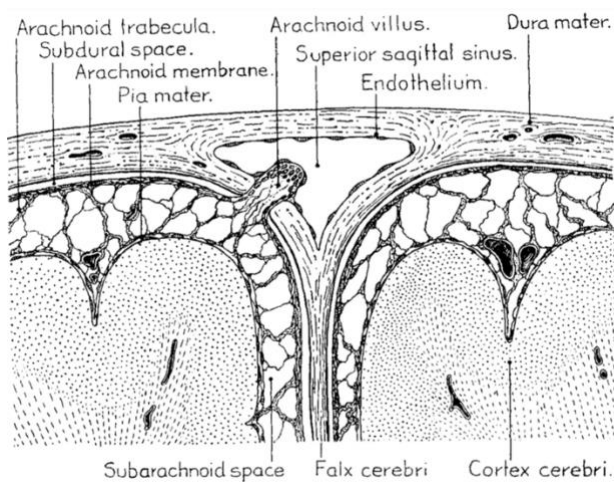


Figure 13: The anatomy of the arachnoid villi.

Original drawing of the arachnoid anatomy by Lewis Weed, 1923²⁴⁹. The arachnoid villi are located in the vicinity of the superior sagittal sinus. They project through the dura into the lumen of the superior sagittal sinus. The cap of the villus is covered by endothelial cells and represent an area of CSF to venous blood exchange. However, the nature of the CSF outflow from the villus to the superior sagittal sinus is still controversial.

Therefore, tau is left with the option of blood-brain barrier passage representing the one of the most selective brain to blood transfer modality.

Blood brain barrier passage

The blood-brain barrier term refers to the unique ability of brain blood vessels to tightly regulate the exchanges of ions, molecules and cells between the blood and the brain. This physiological barrier allowing the control of blood and brain exchanges is formed by the interaction of endothelial cells forming the wall of the blood vessels with different vascular, glial and immune cells. The organization of tight junctions in between each endothelial cells prevents the paracellular diffusion of factors from brain to blood and blood to brain and, depending on the zone, pericytes, astrocytes and smooth muscle cells maintain the integrity of the BBB and participate to blood/brain exchanges. The passage of molecules through the BBB is highly specific, with the exception of gases and small lipophilic molecules which crosses freely, and requires the expression of transporters, receptors, efflux pumps, ion channels and regulatory proteins by the endothelial cells (Figure 14). Several articles have demonstrated the ability of Tau to exit the CNS and reach the blood circulation. In the first studies, radiolabeled Tau injection in the lateral ventricle or in the cisterna magna were performed and showed a rapid appearance of Tau in blood and in peripheral organs^{250,251}. When injected in the brain parenchyma, Tau is detectable in the blood at 2 hours post-injection and peaks at 24 hours post-injection²⁴⁸. Such data implies that Tau readily crosses the BBB during its clearance process. Yet, the pathway taken by Tau to cross the BBB is still unclear. The consensus in the literature is that, unlike A β , Tau isn't transported by endothelial cells. So, to rapidly reach the blood circulation Tau would thus be left with one last possible pathway: crossing through the blood-cerebrospinal fluid barrier (BCSFB) located at the choroid plexus or the circumventricular organs.

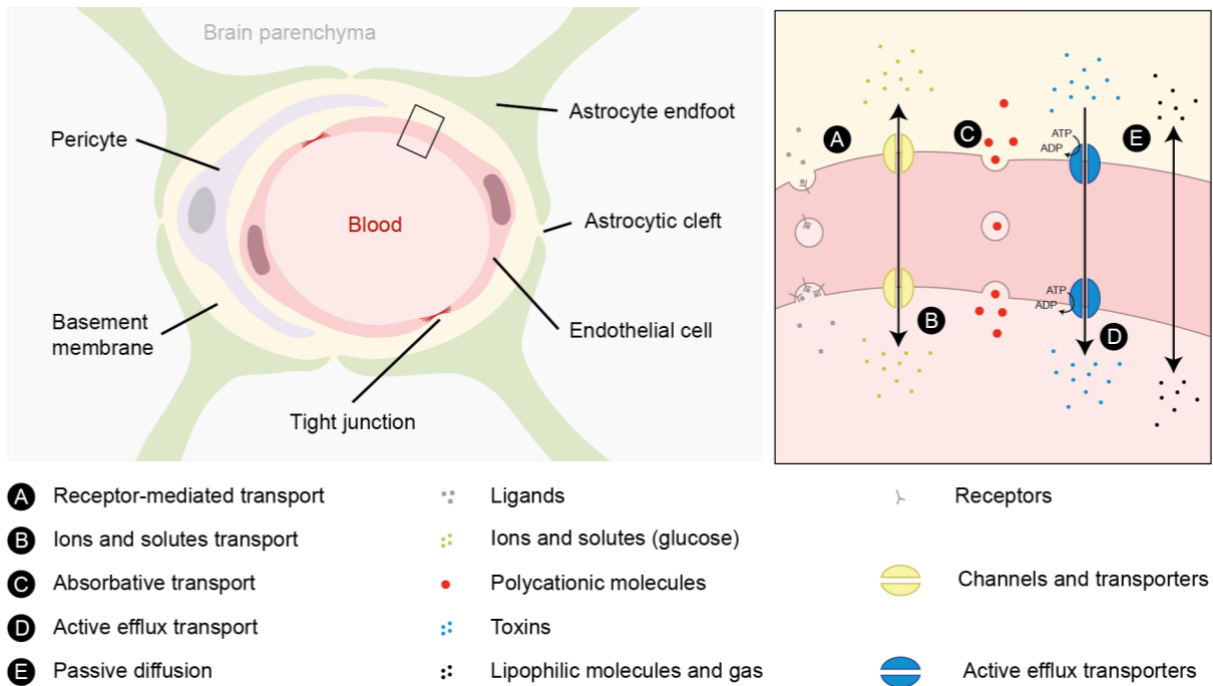


Figure 14: The blood-brain barrier anatomy and function.

The brain capillary network is formed by a monolayer of endothelial cells which paracellular space is sealed by tight junctions. These tight junctions act as a physical barrier preventing the paracellular diffusion of molecules. The capillaries are unsheathed by pericytes and astrocytic end-feet collaborating with the endothelial cells for the maintenance of the BBB integrity and the regulation of blood/brain exchanges. The basement membrane, the extracellular matrix secreted by endothelial cells, also participates in preserving the BBB regulation. This cellular and molecular organization allows a strict regulation of brain accessibility to blood-borne molecules. Most blood factors have to be transported across the brain endothelium by various modes: receptor-mediated transport (A), transport of ions and solutes through channels or transporters (B), absorptive transport (C), active efflux transport through ATP dependent transporters (D). Gas and lipophilic molecules are exceptions to this rule since most of them can diffuse freely across the endothelium (E). Adapted from Neumaier et al, 2021 and Knox et al, 2022.

Blood-cerebrospinal-fluid barrier passage

Despite the BBB regulating the majority of blood/brain exchanges, particular brain regions lacking the BBB exist: the choroid plexus (CP), the CSF production site, and the circumventricular organs (CVOs), small regions lining the third and fourth ventricles implicated in the communication between the brain and peripheral organs (Figure 15). In these regions, the vasculature is fenestrated and permeable allowing the diffusion of blood-borne molecules.

Thus, the barrier function is exerted by different cell types, the cuboidal cells in the CP and the tanycytes or tanycyte-like cells in the CVOs, expressing tight junction proteins^{252–254}. CP most common function is the secretion of CSF but it is also a region of CSF/blood exchanges with the CP cuboidal cells being able to actively transport selected molecules by transcytosis such $A\beta$ or antibodies^{255,256}.

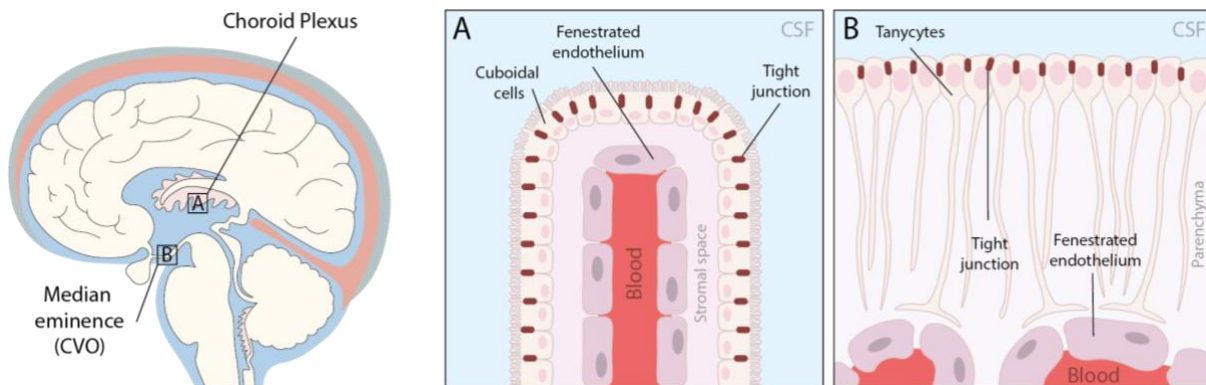


Figure 15: The anatomy of the brain-cerebrospinal fluid barrier.

In particular brain regions such as the choroid plexus or the circumventricular organs (CVO) an interface between the cerebrospinal fluid (CSF) and the blood exist. These regions lack the traditional blood-brain barrier as they have a fenestrated endothelium allowing the diffusion of blood-borne factors. However, specialized ependymal cells, the cuboidal cells in the choroid plexus and the tanycyte or tanycyte-like cells in the circumventricular organs, harbor intercellular tight junctions preventing the spillage of blood molecules into the CSF.

CVOs are extensively studied in the context of hormonal and metabolic homeostasis as they are the gateways for peripheral organ's hormones to access the brain and for neurohormones to reach the periphery²⁵⁷. The tanycytes or tanycyte-like cells, forming the barrier between the CSF and the blood in these regions are known to actively transport molecules from blood to CSF and studies using exogenous tracer suggest that they are also capable of CSF to blood transfer^{253,258,259}. In the context of AD, CP has already been studied for $A\beta$ clearance but Tau hasn't been demonstrated to take the same path. The hypothesis of a passage of $A\beta$ and Tau through the CVOs has never been tested yet and may represent a new clearance pathway for these pathological proteins.

This hypothesis becomes even more interesting knowing that most of the previously mentioned clearance mechanisms have been proven to be deficient in the context of AD. Intracellular tau clearance mechanisms, such as autophagy or the UPS, as well as extracellular clearance mechanisms, including the glymphatic system, were shown to be defective in AD patient's brains and/or mouse models^{225,233,240,260}. Thus, tau transport through the CVOs would represent the last standing tau efflux mechanism in the context of AD.

Tanycytes are mediators of brain and periphery exchanges

The circumventricular organs, windows to the brain

The CVOs comprise the median eminence (ME), the neurohypophysis, the subfornical organ (SFO), the pineal gland (PG), the area postrema (AP) and the organum vasculosum of the lamina terminalis (OVLT) and debatably the subcommissural organ (SCO) (Figure 16). These brain regions are in proximity with the ventricles and characterized by a fenestrated endothelium allowing blood/brain exchanges. The SCO being a CVO is controversial since its endothelium is deprived of fenestration and stands out as an exception. CVOs are critical for brain/periphery communication as they allow the sensing of peripheral cues by specific neuronal populations and the secretion of neurohormones in the blood circulation. They are considered as windows to the brain. Depending on their function CVOs have been classically divided into two types:

- Sensory CVOs comprising the AP, OVLT, SCO and SFO. They are implicated in the sensing of peripheral cues by the neurons projecting directly in their parenchyma.
- Secretory CVOs including the ME, PG and neurohypophysis. In those regions, neurohormones are directly secreted into their blood circulation.

Despite being devoid of the classical BBB, a physical barrier between the blood and the CSF exists in the CVOs. The barrier property of CVOs is relocated from the endothelium to the

ependymal cells in contact with the CSF thanks to the expression of tight junction proteins. Among all CVOs, one has been subjected to extensive attention due to its major role in the regulation of metabolism and hormonal axis: the median eminence.

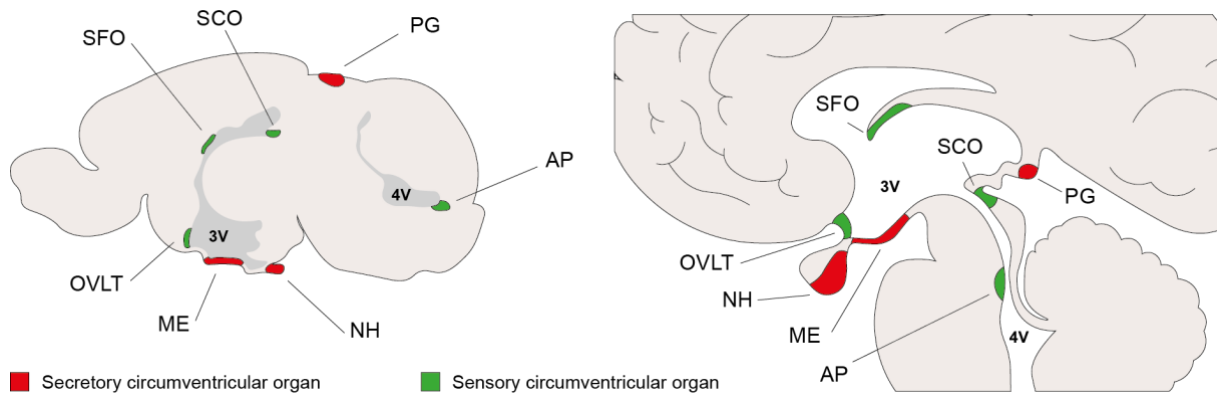


Figure 16: The circumventricular organs of the mouse and human brain.

At the interface between the cerebrospinal fluid and the blood, the circumventricular organs (CVOs) are crucial for the neuroendocrine systems relying on peripheral signals to regulate physiological functions. The endothelium of these brain structure is fenestrated allowing the diffusion of blood signal for neuroendocrine neurons to perceive and the secretion of neurohormones towards the general circulation. Depending on their predominant function, the CVOs are classified into secretory CVOs and sensory CVOs. However, recent evidences would suggest that CVOs, like the median eminence, can exert both functions equally. CVOs are located in the vicinity of the third and fourth ventricle (3V, 4V). Abbreviations: AP: area postrema, ME: median eminence, NH: neurohypophysis, OVL: organum vasculosum of the lamina terminalis, PG: pineal gland, SCO: subcommissural organ, SFO: subfornical organ.

The median eminence, a hotspot for brain/periphery exchanges

The median eminence extends from the mammillary bodies to the optic chiasm, forms the ventral limitation of the third ventricle and is located at the base of the hypothalamus, the master regulator of a myriad of physiological function. It is a key interface between the hypothalamic neuronal populations involved in the regulation of reproduction, lactation, stress, growth, and the pituitary. As all CVOs, the median eminence possesses a fenestrated vasculature composed of a capillary bed located in its external zone and capillary loops reaching the internal zone. ME dense vasculature allows the rapid diffusion of blood-borne

molecules into its parenchyma and the secretion of neurohormones to the pituitary portal circulation (Figure 17).

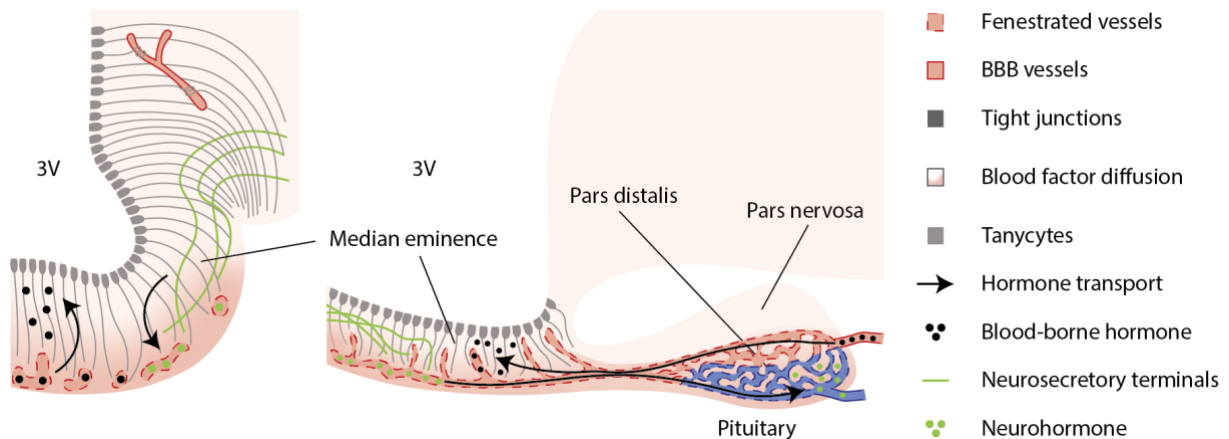


Figure 17: The median eminence is at the interface of the hypothalamus-pituitary system

Schematic of a coronal (left panel) and sagittal (right panel) view of the median eminence. The median eminence is at the interface of the hypothalamus and the pituitary. Blood-borne hormones coming from the general circulation pass through the pituitary portal circulation to reach the median eminence (black arrows). Neurosecretory neurons of the hypothalamus project directly into the parenchyma of the median eminence allowing neurohormones to directly access the pituitary portal circulation in order to reach their target cells in the pars distalis of the adenohypophysis.

This duality of function makes the ME a hotspot for brain and blood communication with information from the periphery crossing path with information from the brain. However, even if peripheral hormones diffuse freely into the ME parenchyma, they are not able to diffuse further into the hypothalamus and are precluded to diffuse into the CSF. Similarly, CSF factors can't diffuse freely into the median eminence explaining why hypothalamic neurons project inside the ME parenchyma and secrete neurohormones directly into the ME vasculature. This strict regulation of exchanges, at the center of brain and blood communication, is due to the relocation of the barrier function to the ependymal cells of the ME, the tanycytes.

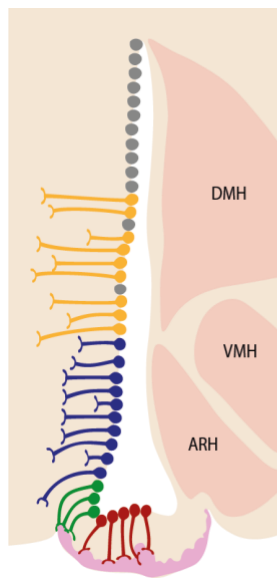
Tanycytes, swiss army knives of the hypothalamus

The heterogeneity of tanycytic populations

The discovery of cells, resembling radial glial cells, with cell bodies residing in the third ventricular wall and extending long process toward the pial surface of the ME dates back to the early 20th century with drawings from Ramon y Cajal²⁶¹. In 1954, Horstmann coined these peculiar ependymal cells after the Greek for “stretched cells”, tanycytes²⁶². Tanycytes are specialized ependymal cells lining ventral third ventricle. Their cell body forms the ventral third ventricular wall and their long processes extends into the hypothalamus and the ME. Tanycytes are traditionally classified into different populations according to their dorsoventral localization, the direction of their processes and their histological characteristics (Figure 18)²⁶³:

- Alpha tanycytes (α -tanycytes) are the most dorsal tanycytes. They are located in the third ventricular wall facing the arcuate, ventromedial and dorsomedial hypothalamic nuclei. They extend their processes into the hypothalamus and contact capillaries possessing the traditional BBB. They are subdivided into α 1-tanycytes and α 2-tanycytes, with α 1-tanycytes being the most dorsal.
- Beta tanycytes (β -tanycytes) are the ones forming the floor of the third ventricle. They project cellular extensions through the ME to contact the fenestrated endothelium with their “end-feet”. They are also subdivided into β 1-tanycytes and β 2-tanycytes, with β 1-tanycytes being located dorsolaterally, in the corner of the ME.

This traditional classification is challenged by the growing literature on tanycytes describing their transcriptome, embryonic origins, cell-cell interactions and expression of tight junction proteins, possibly leading to the description of new subpopulations or/and a change in their classification²⁶⁴. Being a such heterogenous cell type and lying at the crossroad of diverse physiological functions, tanycytes harbor a variety of functions among which are their barrier and shuttle function, the regulation of neurosecretion, their metabolic support and stem cell niche function for hypothalamic neurons²⁶⁴. These development in the field of tanycyte were supported by the identification of tanycyte markers allowing their immunohistological observation and the design of tanycyte-specific genetic approaches.



- Ependymal cells
- α1-tanycytes
- α2-tanycytes
- β1-tanycytes
- β2-tanycytes
- Fenestrated endothelium
- Hypothalamic nuclei

Figure 18: Tanycyte's classification.

From dorsal to ventral third ventricle, tanycytes are classified as α 1-tanycytes facing the dorsomedial hypothalamic nucleus (DMH), α 2-tanycytes projecting into the arcuate nucleus (ARH) and the ventromedial hypothalamic nucleus (VMH), β 1-tanycytes at the frontier between the arcuate nucleus and the median eminence and β 2-tanycytes projecting in the median eminence external zone and contacting the fenestrated endothelium. Adapted from Akmayev et al, 1973 ²⁶³.

Tanycytic markers, a tool for their visualization and targeting

Cellular markers are essential to cell-specific research, they provide a way to identify the cells of interest and to enable their targeting via promoter driven genetic manipulations. The first tanycytic markers were identified through immunohistological approaches with the discovery of tanycyte-specific expression of several protein in the hypothalamus. The first two tanycyte-specific markers identified were vimentin, an intermediate filament protein, and dopamine- and cAMP-activated phosphoprotein of molecular weight 32kDa (DARPP-32)²⁶⁵⁻²⁶⁸. While DARPP-32 immunohistochemistry has been abandoned by most since the late 1990s, vimentin has been extensively used in the field for tanycyte-specific immunostainings. However, vimentin is not a truly specific tanycytic marker as it is expressed by endothelial and ependymal cells especially in human tissues and in rodents to a lesser degree. But since vimentin stains tanycytes from the cell bodies to the end-feet, tanycytic vimentin expression is easily distinguishable from its ependymal and endothelial expression on immunostaining. Vimentin staining remains the gold-standard for tanycyte visualization in mouse and human tissue.

The growing interest in tanycyte research led to the discovery of new tanycyte-marker. Expression of thyroid hormone maturing enzyme, deiodinase 2 (Dio2) and deiodinase 3 (Dio3), was observed in tanycytes across species and linked to seasonal changes in hamsters^{269,270}. Taking advantage of Dio2 tanycyte-specific expression, Müller-Fielitz and collaborators successfully used Dio2 promoter driven viral vectors to only target tanycytes after an intracerebroventricular stereotaxic viral injection²⁷¹. Tanycytes were also shown to be specifically enriched in a variety of classical stem-cell marker such as Sox2, brain lipid binding protein (BLBP), glutamate/aspartate transporter (GLAST), nestin or Rax in several species including humans, which led to the hypothesis of tanycytes being part of a stem-cell niche in the hypothalamus^{272,272-275}. Moreover, this expression of GLAST, nestin and Rax prompted the use of GLAST-Cre, nestin-cre and Rax-Cre recombinase mouse model to study tanycyte's functions²⁷⁶⁻²⁷⁸. However, while GLAST and Rax expression are restricted to tanycytes in the median eminence and hypothalamus, other cell types are expressing them in the brain or peripheral organs limiting the use of these models. Another interesting protein is the G-coupled protein receptor 50 (GPR50), an orphan G-protein coupled protein receptor (GPCR) sharing high homology with the melatonin receptor, which was shown to be enriched in tanycytes and dorsomedial hypothalamic nucleus (DMH) neurons in rodents and humans²⁷⁹.

With the development of new techniques such as single-cell transcriptomics new markers for tanycytes are arising. The same year two publications, one using single-cell RNA sequencing and the other Drop-seq on hypothalamic dissection have generated an explosion in potential tanycyte marker^{280,281}. Both studies have provided a long list of tanycyte-marker and tanycyte subpopulations markers. These data represent a significant advance in tanycyte research allowing a prediction of protein expression and biological pathway presence from which researchers can build hypothesis and discover new tanycytic functions. Yet, transcriptomics data have caveats, the first one being that mRNA expression is not always associated with protein expression or activity depending on the biological pathways in question²⁸². Nowadays, only a handful of markers discovered through high throughput sequencing technologies have been fully validated and further research is required to identify

new markers suitable for tanycyte targeting and/or identification as well as their role in tanycytic functions.

Tanycytes a new stem cell niche?

Compiling data support the view of a hypothalamic neural stem-cell niche in which tanycytes are able to generate new glial and neuronal cells. Due to the radial glia origin of tanycytes, this stem-cell property was long suspected but never proven. Advances in tanycyte research allowed the development of tanycytic fate tracing and targeting, spurring tanycyte stem cell research.

As previously discussed, tanycytes have been proven to express a long list of neural stem-cell (NSC) related proteins. But to be considered NSCs, tanycytes need to meet their functional properties which are the ability to proliferate, self-renew and differentiate into other cell types. Several studies have shown that tanycytes are able to proliferate *in vivo*, notably through the observation of BrdU incorporation denoting cell cycle entry and cell proliferation^{273,276,283}. Tanycytes are also capable of self-renewal and differentiation into other glial and neuronal cell types. Indeed, lineage-tracing mouse models have shown that tanycytes not only produce new tanycytes but also astrocytes and neurons in the mediobasal hypothalamus^{274,276,283,277}. The regulation of tanycyte's stem cell properties is mostly unknown but two growth factors have been shown to impact their proliferative capacities *in vivo*: Fibroblast growth factor 2 (FGF2) and insulin-like growth factor 1 (IGF1)^{273,284,276}.

The role of tanycyte proliferation and differentiation is still vague. Studies have found that hypothalamic neurogenesis is important in the regulation of energy homeostasis but since tanycytes aren't the only NSC in the hypothalamus and the methods used are not specific to tanycyte, their exact role is still hard to rule out.

Tanycytes at the blood-cerebrospinal-fluid barrier

As previously mentioned, the brain is protected and maintained stable thanks to the blood-brain barrier, formed by the brain neurovascular unit, tightly regulating the entry of substances into the brain. In the ME, as in all CVOs but the SCO, the endothelium is fenestrated and characterized by the expression of the plasmalemmal vesicle-associated protein (PLVAP or PV1)²⁸⁵. The BBB function is thus relocated to the ependymal cells, the tanycytes. Tanycytes express several tight junction proteins (e.g., zona occludens 1 (ZO1), occludins and claudins) between their cell bodies assembling tight junctions and forming an impermeable wall for both blood-borne and CSF-borne molecules²⁵³. The injection of dyes into the blood circulation or into the ventricular system clearly illustrates this view. Peripherally injected dyes are precluded to the brain blood vessels and the ME parenchyma while centrally injected dyes do not reach the ME^{253,286}. Interestingly this barrier has been shown to respond to the metabolic status of the individual. Upon fasting, the vasculature of the ME becomes even more permeable and fenestrated vessels appears in the arcuate nucleus²⁸⁷. In response, α -tanycytes reorganize their tight junction proteins to prevent blood-borne molecule from leaking out of the arcuate nucleus and into the CSF. This phenomenon is reversed after refeeding via a vascular endothelial growth factor A (VEGF-A)-dependent mechanism (Figure 19). Preventing the free diffusion of blood-borne molecule out of the ME is essential to maintain a controlled brain environment, but raises the question of how peripheral hormones reach hypothalamic neurons out of their diffusion limit.

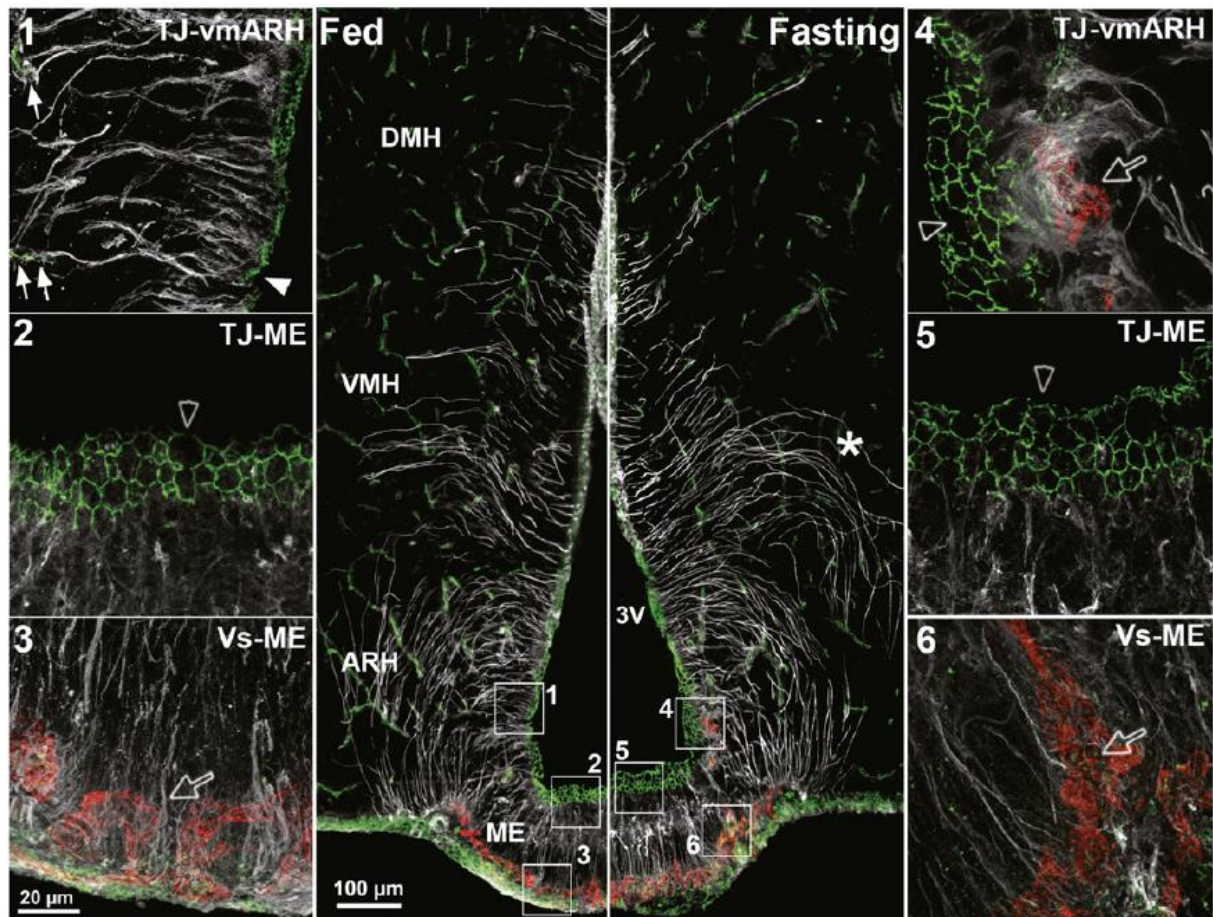


Figure 19: The tanycytic tight junction barrier is under metabolic control.

Immunofluorescence for vimentin (white), ZO1 (green) and PLVAP (red). In fed animals (left, 1, 2, 3), the β -tanycytes, contacting the median eminence's fenestrated vessels, display a honeycomb pattern of ZO1 (2, hollow arrow heads) when α -tanycytes, contacting the hypothalamic BBB vessels, have a disorganized ZO1 expression pattern (1, white arrow head) and the fenestrated endothelium of the median eminence is restricted to the external zone (3, hollow arrow). Under fasting conditions (right, 4, 5, 6), fenestrated vessels are present in the arcuate nucleus (4, hollow arrows) and α -tanycytes shift to a honeycomb ZO1 pattern (4, hollow arrow head), β -tanycytes keep their ZO1 honeycomb expression pattern (5, hollow arrow head) and fenestrated vessels loops reaching the internal zone of the median eminence are present (6, hollow arrow). These changes promote the diffusion of blood-borne molecules to the arcuate nucleus. Illustration from Prevot et al, 2018²⁶⁴ adapted from Langlet et al, 2013²⁸⁷.

Tanycytes shuttle blood-borne hormonal cues into the hypothalamus

To maintain a stable metabolic state, a fine balance between energy intake and energy expenditure needs to be at equilibrium. This concept is called energy homeostasis and revolves around an intricate regulatory system involving peripheral signals and their integration by the brain. One key player of energy homeostasis is leptin, an orexigenic hormone produced by the adipocytes. Leptin is an adiposity signal, as it is produced proportionally to the fat mass, which reduces food intake and increases energy expenditure through its central action on hypothalamic neurons. In brief, when the fat mass increases, leptin plasmatic concentration raises leading to a decrease in food intake, an increase in energy expenditure and finally to a decrease in body weight reestablishing the energy balance or homeostasis. Leptin acts on peripheral organs, regulating lipolysis or glucose metabolism for example, but more importantly on the brain and especially on the arcuate nucleus of the hypothalamus where leptin sensitive neurons regulating food intake and glucose homeostasis are located. Considering the peripheral origin of leptin, one can wonder how it reaches the arcuate nucleus to trigger its action.

Tanycytes have long been described to actively transport blood-borne substances to the CSF ^{288,259,289}. The ME being permeable to blood-borne molecule and adjacent to the arcuate nucleus, the tanycytes represent ideal candidates for leptin transport from blood to brain. This hypothesis was shown to be true by Balland and collaborators in 2014, who demonstrated that tanycytes were the first leptin responsive cells in the brain and that they were transporting leptin from the ME to the CSF in an extracellular signal-regulated kinase (ERK) pathway dependent manner²⁵⁸. Once in the CSF, leptin is able to reach the hypothalamus and more distant areas. Expanding on this seminal discovery, Duquenne and collaborators further demonstrated the tanycytic expression of the leptin receptor and the requirement of a leptin receptor/epithelial growth factor receptor complex for the tanycytic shuttling of leptin²⁹⁰. To date, other peripheral hormones have been shown to be transported by tanycytes through receptor dependent transcytosis among which ghrelin, insulin, hepatic FGF21, GLP1, and GLP1 analogs ²⁹¹⁻²⁹⁵. In the study demonstrating the transport of GLP1 by

tanycytes, Imbernon and collaborators described a new model for the study of tanycytic transcytosis. This model consists in the selective expression of the botulinum toxin light chain serotype B (BoNT/B), inhibiting SNARE-dependent exocytosis, in tanycytes by inducing a tanycyte-specific cre recombinase expression in a BoNT/B-EGFP^{loxP}-STOP-^{loxP} mice model^{294,296}. Upon recombination of the stop codon preceding the BoNT/B gene, tanycytes expressed the toxin inhibiting their ability to transport molecules through transcytosis. This body of evidence demonstrates the ability of tanycyte to shuttle blood-borne hormones to the hypothalamus and allow their integration by specific hypothalamic neuronal populations.

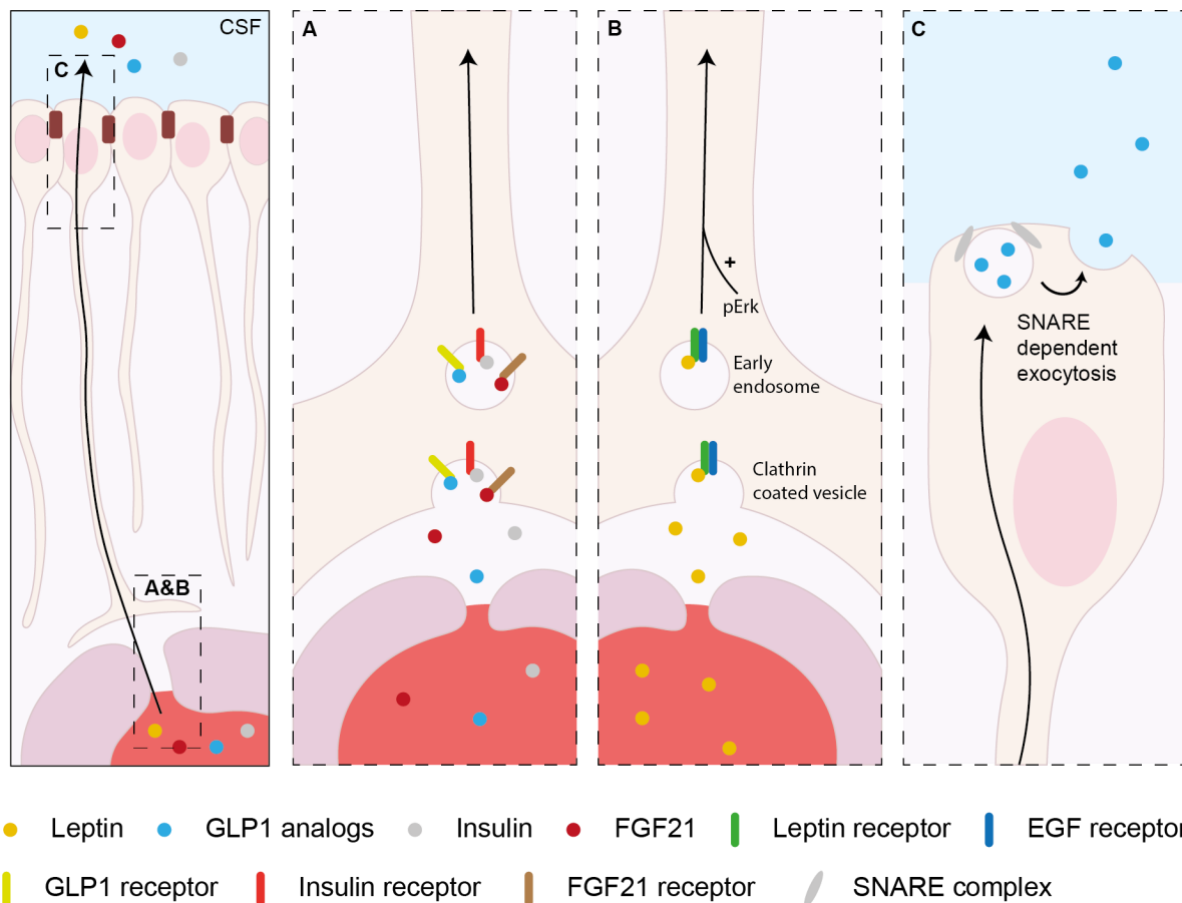


Figure 20: The molecular mechanisms of the tanycytic shuttle.

Tanycytes have been implicated in the transport of hormones from the blood to the brain. This transport requires the expression of the hormone's receptors and potential co-receptor such as the heterodimer complex of leptin receptor and EGF receptor for the transport of leptin (A & B). After leptin binding, the receptor is internalized through clathrin-mediated endocytosis and sorted into early endosomes. The

transport and release of leptin by tanycytes is regulated by the ERK pathway (B). Finally, SNARE-dependent exocytosis appears to be the exocytosis mode used by tanycytes for secretion (C).

Furthermore, these studies unraveled several molecular mechanisms underlying the tanycytic shuttle (Figure 20). It can be speculated that these newly identified pathways are applicable to any molecule susceptible to be transported by tanycytes, and to the hormones already identified to be transported but for which the pathways of uptake and secretion weren't studied. Additionally, tanycytes not only control the entry of hormones to the hypothalamus but they were also shown to modulate the secretion of neurohormones into the hypophyseal portal circulation of the ME, regulating the exit of hormones from the hypothalamus.

Tanycytic regulation of neurosecretion

The ME is the privileged exit route for neurohormones of the hypothalamic-pituitary axis. Indeed, neurosecretory hypothalamic neurons project directly into the ME and in proximity with ME fenestrated capillaries allowing their circulation towards the pituitary. Several studies have highlighted the role of tanycytes in the regulation of this process, with two hypothalamic-pituitary axes particularly well described: the hypothalamic-pituitary-gonadal (HPG) axis and the hypothalamic-pituitary-thyroid (HPT) axis. By unsheathing neurosecretory terminals, tanycytes are regulating their access to the pituitary portal circulation and their secretory activity. The master regulators of the HPG axis are the gonadotropin-releasing hormone (GnRH) neurons, regulating luteinizing hormone (LH) and follicle-stimulating hormone (FSH) production by the pituitary (reviewed elsewhere²⁹⁷). In the context of the HPG axis, a plasticity in the tanycytic coverage of axon terminals has been demonstrated. According to the estrous cycle stage, tanycyte end feet morphology is changing in adult females controlling the access of GnRH terminals to the fenestrated capillaries. In diestrus, when estrogens levels are low, tanycytes end-feet tightly encompass GnRH terminals preventing their contact with ME capillaries. Inversely, in proestrus, tanycytes' end-feet retract allowing the GnRH terminals to discharge into the ME capillaries leading to the stimulation of LH and

FSH secretion by the pituitary during the preovulatory surge. This phenomenon has been described to involve transforming growth factor-alpha (TGF- α), prostaglandin E2 (PGE2), and endothelial nitric oxide for the retraction of tanycytic end-feet and transforming growth factor-beta 1 (TGF- β 1) and semaphorin 7A (Sema7A) for tanycytic end-feet outgrowth^{298–300}.

The HPT axis is regulated by the thyrotropin releasing hormone (TRH) neurons, regulating the pituitary secretion of thyroid-stimulating hormone (TSH) directly acting on L-thyroxine (T4) production by the thyroid. T4, the inactive thyroid hormone, is then locally converted by different deiodinases (Dio1, 2 and 3) into T3, the active thyroid hormone (reviewed elsewhere³⁰¹). Similar to GnRH terminals, TRH terminals are surrounded by tanycytes end-feet³⁰². However, the nature of tanycytes/TRH neurons interaction is different. Tanycytes are able to directly influence TRH neurons secretion by several mechanisms: an increased expression of a TRH degrading enzyme, the pyroglutamyl peptidase II (PPII), in response to TRH binding on TRHR1 receptor on tanycytes and a reciprocal regulation microcircuit involving TRH secretion inhibition by tanycytic endocannabinoid and the induction of endocannabinoid release by TRH-neuron glutamate secretion^{271,303}. Therefore, tanycytes are closely interacting in with TRH neurons through different modalities adding another layer to the HPT axis.

The interaction of tanycytes with hypothalamic neuronal populations is not limited to neuroendocrine systems. Several reports have also highlighted the ability of tanycytes to sense and provide metabolites in order to finely tune the activity of hypothalamic neurons implicated in the control of energy homeostasis.

Tanycytes support hypothalamic neuronal populations by sensing and providing nutrients

As mentioned above, tanycytes are at the interface of blood and CSF and are able to respond to changes in metabolic state suggesting a possible role as metabolic sensors. Interestingly, tanycytes express glucose transporter 2, the glucokinase (GK) and ATP-

sensitive potassium (K_{ATP}) channels shown to be involved in β -pancreatic cells glucose sensing^{304–306}. A study has shown that tanycytes are indeed capable of sensing glucose since application of glucose on acute brain slices results in intracellular calcium waves in tanycytes leading to the secretion of ATP towards the extracellular space³⁰⁷. This ATP secretion has been shown to tune the activity of neuropeptide Y (NPY) and proopiomelanocortin (POMC) neurons, regulators of food intake in the arcuate nucleus. More specifically, it was shown that the induction intracellular calcium waves in tanycytes triggered by ATP binding to purinergic receptors results in the induction of hyperphagia³⁰⁸. Moreover, ATP release has a paracrine effect, which could represent a possible amplifying mechanism by propagating the calcium waves to the neighboring tanycytes³⁰⁹. Lastly, tanycyte also express sweet-taste receptors (Tas1r2 and Tas1r3) through which they are capable of sensing glucose and artificial sweeteners inducing the same intracellular calcium response³¹⁰. This set of reports support a role for glucose-induced tanycyte ATP release in the regulation of food.

In addition, tanycytes were shown to be able to tune POMC neurons activity in response to peripheral glucose levels. A recent study of the laboratory has demonstrated that tanycyte are supplying POMC neurons with lactate to fuel their neuronal activity³¹². Indeed, it showed that lactate is produced by tanycytes in response to increased peripheral glucose levels and shuttled through monocarboxylase transporter 1 and 4 to POMC neurons. Subsequently, POMC neurons perceive this raise in lactate concentration and increase their firing rate to balance the metabolism. Thus, tanycytes allow the integration of changes in glucose homeostasis by POMC through a modulation of the arcuate nucleus lactate concentrations.

Tanycytes are able to sense hormonal and metabolic changes and respond to adapt their function or influence the function of nearby neurons. They are also capable of shuttling a variety of molecules from the blood to the brain for the proper functioning of metabolic and hormonal systems. Overall, the versatility of tanycytic functions and their peculiar localization at the interface between the brain and the periphery prompt the question of their implications

in diseases characterized by metabolic and hormonal disturbances, such as obesity or type 2 diabetes, but also in the metabolic and hormonal changes occurring during the course of aging.

Tanycytes in pathology and aging

The role of tanycyte in metabolic disorders and hormonal imbalance

Tanycytes are influencing a variety of neuroendocrine systems involved in the regulation of metabolic and hormonal status. Their involvement in metabolic and hormonal diseases and the impact of these diseases on tanycyte function are legitimate questions. While clinical data on tanycyte's implications in human diseases are lacking, an increasing corpus of reports suggest that tanycytes could have a role and be altered in the context of metabolic and hormonal diseases in humans.

Studies on diet-induced obesity (DIO) mouse models have shown that the impairment of tanycytic leptin transport is the first event of central leptin resistance. When injected peripherally injected leptin reaches the mediobasal hypothalamus in 45 minutes in wild-type mice, denoted by Stat3 phosphorylation, DIO do not exhibit any changes in Stat3 phosphorylation at the same time window²⁵⁸. Deleting leptin receptor expression from tanycytes prevent leptin from reaching the mediobasal hypothalamus phenocopying the DIO model and indicating that an alteration in tanycyte leptin transcytosis occur in these mice²⁹⁰. Interestingly, leptin plasmatic concentration is positively correlated with leptin CSF concentration in control patients but this correlation is lost in obese patient suggesting that there is a disruption of leptin transport to the brain could occur in the development of obesity³¹³. Tanycytes might thus be implicated in the development of obesity in humans. Recent studies showing tanycyte-mediated insulin transport to the hypothalamus also suggest a role of tanycytes in obesity-associated insulin resistance²⁹². The deletion of the insulin receptor in tanycytes has been shown to prevent insulin access to the mediobasal hypothalamus and trigger a systemic insulin resistance. Similarly to leptin, control patients have correlated

plasmatic and CSF insulin concentrations but this correlation is lost in obese patients suggesting that tanycytes could be implicated in insulin transport in humans and participate in obesity-associated insulin resistance^{314,315}. Therefore, since both leptin and insulin transport are disrupted in obesity, tanycytes – known transporters of both hormones – might be altered during the development of the pathology in patients. In DIO mice, tanycytes were shown to undergo ultrastructural changes with alterations of projections patterns, loss of intercellular junctions, and accumulation of lipid droplets and vesicular organelles³¹⁶. Finally, tanycytes appear to have a role in the pathogenesis of obesity and might represent new therapeutic targets for the treatment of these conditions.

Interestingly, the process of aging is accompanied by the occurrence of metabolic and hormonal disfunctions³¹⁷. Therefore, tanycytes might also be altered during course of aging and perhaps have a role in aging-associated metabolic and hormonal changes.

Tanycyte in physiological and pathological aging

Only a few studies have documented the effects of aging on tanycytes and reported age-related protein expression changes and morphological changes. A first study on tanycyte in the context of aging reported a loss of intercellular connections between β -tanycytes suggesting an alteration of the tanycytic tight junction barrier³¹⁸. Others later found that tanycytes of 2 years-old old rats showed a decreased DARPP-32 expression accompanied by an increase in glial acidic fibrillary protein (GFAP) expression compared to 3 months-old rats. They also observed a loss of tanycytic processes which may represent a age-related loss of tanycyte or changes in their projection patterns³¹⁹. Also, tanycyte projection are altered in old female rats with changes in the orientation of the projection and abnormal perivascular contacts^{320,321}. Thus, aging appears to disrupt the structure of the tanycytic network in rodents. The age-related loss of tanycyte processes have also been reported in humans. In a histological study of the median eminence from subjects aged from 5 months-old to 100 years-old, Koopman and collaborators suggested that tanycytes processes density decrease with

aging³²². However, caution must be taken with this formulation. Indeed, the tanycytic process density is significantly higher in the infant/pre-pubertal period compared to the adult and elderly period but the adult and elderly period do not vary significantly. Thus, even if age was a factor influencing the density of tanycytic projections, it was shown to only impact the transition from infant/pre-pubertal age to adult age. Lastly, a study addresses the compelling hypothesis of hypothalamic stem cell's role in systemic aging³²³. Although they do not mention tanycytes in their report, they found that the expression of stem-cell markers Bmi1 and Sox2 decrease in the cells forming third ventricular wall and in the mediobasal hypothalamus. They showed that ablation of these cells significantly reduces the animals' lifespan. Strikingly, the graft of hypothalamic NSC in old animals was able to expand their lifespan, emphasizing on the direct control of hypothalamic NSC on systemic aging. This study concludes on the role of hypothalamic neural stem-cells, which tanycytes are part of, on the control of aging speed³²³.

Tanycyte involvement in pathological aging, characterized by the occurrence of age-related disease such as AD, is unknown. Only one group have indirectly tackled this question by their description of A β fragments brain distribution following stereotaxic intracerebroventricular injections³²⁴. After 1 hour, the injected A β was found in the internal zone of the median eminence and in the external zone up to 3 weeks post-injection. They proposed the involvement of tanycytes in the transport of A β fragments from the CSF to the median eminence parenchyma and a role for tanycyte in A β clearance – although they did not directly evaluate this eventuality. Moreover, A β fragments are already known to cross the BBB by endothelial cell transport and the BCSFB at the choroid plexus. Lastly, the kinetic of such transport, with the presence of A β fragments 3 weeks after injection, would suggest that they remain sequestered in the ME and do not reach the portal blood circulation. In the context of AD, studies on tau protein intracerebroventricular injections have never documented its presence in the median eminence.

The study of tanycytes in the context of physiological and pathological aging is promising as age-related diseases are often accompanied by neuroendocrine disorders,

metabolic disturbances and disruptions of the communication between the brain and the periphery. Moreover, neurodegenerative diseases, such as AD, are characterized by the accumulation of pathological proteins in the brain and the mechanisms allowing their evacuation are still poorly described. Seminal work pointing toward a role of tanycyte in brain to blood transport they represent a potentially new clearance mechanism for those proteins.

Are tanycytes new players in brain clearance?

As discussed above, tanycyte have been proven to be efficient blood-to-brain transporters for a variety of endogenous and exogenous molecules. In addition, several studies on their capacity to transport molecules have also suggested that they possibly transfer CSF-borne molecules to the blood. Indeed, several articles using horseradish peroxidase (HRP) intracerebroventricular injections resulted in the incorporation of HRP in tanycytes and revealed the presence of HRP from the cell bodies to the end-feet contacting the ME vessels as well as in the vessels themselves^{259,288,289}. However, those results were contested and another study claimed that this phenomenon was depending on a paracellular transport and not on transcytosis³²⁵. Later on, several groups confirmed using different tracers and immunohistochemical techniques that tanycytes are in fact capable of absorbing CSF factors and to secrete them in the portal circulation of the ME^{326–328}. Not only β -tanycytes but also α -tanycytes were shown to uptake molecules from the CSF and transport it along their long processes³²⁸. These results are supported by ultrastructural studies identifying a tanycytic enrichment in intracellular vesicles and the identification of several key proteins involved in endocytotic process such as caveolin-1, clathrin and several Rab proteins, regulators of vesicle sorting and transport, at the level of their cell bodies implying an adaption of tanycyte to extensive endocytosis and vesicular transport³²⁷. The physiological role of this tanycytic transport is yet undetermined but the authors of the aforementioned articles have speculated its involvement in hypothalamic regulation of metabolic and hormonal systems or considered it as a mechanism of support for hypothalamic neurons in which tanycytes provide CSF-borne

growth factor and bioactive molecules to the hypothalamic nuclei. To date, only an involvement of tanycytes in A β fragments clearance has been proposed but was not directly evaluated by the authors³²⁴. Further studies using physiologically-relevant molecules are required to identify the exact role of CSF factors uptake by tanycytes. Interestingly, the hypothesis of tanycytes being a CSF clearance system has never been directly investigated. Yet, they possess all the characteristics required to exert this function.

Objectives

Alzheimer's disease is characterized by an accumulation of both A β and tau in the brain causing neurodegeneration. Several clearance mechanisms for tau have been described, involving the brain glymphatic and lymphatic system, from which tau can slowly egress to the blood. However, studies have shown that tau can rapidly reach the blood circulation after intracerebroventricular injections suggesting the existence of a direct CSF to blood transport but the path taken by tau to reach the circulation within minutes is still unknown.

Tanycytes being at the CSF/blood interface and capable of transcytosis, they represent ideal candidates for tau CSF to blood efflux. Therefore, we set three objectives to our work: (1) investigate tanycytic tau transport *in vitro*, (2) confirm tanycytic tau transport *in vivo* and determine its contribution to the overall CSF to blood tau efflux and (3) investigate possible tanycyte-related pathological changes in AD patient's post-mortem brain tissues.

To fulfill these objectives, we designed a set of *in vitro*, *in vivo* and human post-mortem experiments. We investigated the capacity of tanycytes to perform tau transcytosis and dissected its underlying mechanism in a tanycyte primary culture model. To expand on the *in vitro* data, we performed stereotaxic fluorescent tau injections in the lateral ventricle and analyzed the kinetics of its brain distribution and its presence in pituitary and blood. To figure out the contribution of tanycytes to tau CSF to blood efflux, we took advantage of the BoNT/B tanycyte-specific expression mouse model, in which tanycytic exocytosis is abolished. Lastly, to put our observation of a tanycytic tau clearance *in vitro* and *in vivo* into perspective, we studied the hypothalamus and median eminence of control and AD patients to identify signs of tau transport in tanycyte and their possible morphological alterations.

Material and Methods

Collection and processing of human tissues

Tissues were obtained in accordance with French laws (Good Practice Concerning the Conservation, Transformation and Transportation of Human Tissue to be Used Therapeutically, published on December 29, 1998). Permission to use human tissues was obtained from the French Agency for Biomedical Research (Agence de la Biomedecine, Saint-Denis la Plaine, France, protocol no. PFS16-002) and the Lille Neurobiobank.

Adult human brain tissue blocks containing the hypothalamus and median eminence were dissected using the following anatomical landmarks: the mammillary bodies for the posterior limit, the optical chiasma for the anterior limit, the width of the mamillary bodies for the lateral limits and the anterior commissure for dorsal limit. The dissected blocks were fixed by immersion in 4% paraformaldehyde in PBS, pH 7.4 at 4°C for 1 week. The tissues were cryoprotected in 30% sucrose/PBS at 4°C until the fragment sunk, embedded in Tissue-Tek OCT compound (Sakura Finetek), frozen in dry ice and stored at -80°C until sectioning. Fragments were cut either in coronal or sagittal sections of 20 µm.

Immunohistology

For human hypothalamus immunolabeling, a citrate-buffer antigen retrieval step, 10mM Citrate in TBS pH 6 for 30 min at 70°C, was performed on 20µm sections. For mice brain immunolabeling, no antigen retrieval step was performed. After 3 washes of 5 minutes with TBS, sections were blocked in incubation solution (ICS: 10% normal donkey serum, 3mg/ml BSA in TBS-Triton 0.3% pH 7,4) for 1 hour. Blocking was followed with primary antibody incubation (Table 1) in ICS for 24h at 4°C for mice tissues and 48h at 4°C for human tissues. Primary antibodies were then rinsed out, before incubation in fluorophore-coupled secondary antibodies for 1h in ICS at room temperature. Secondary antibodies were washed and sections

counterstained with DAPI (D9542, Sigma). Finally, human tissue sections were treated with Autofluorescence Eliminator Reagent (2610, Merck Millipore) to quench lipofuscin aggregates autofluorescence before mounting using Mowiol.

Ilastik segmentation analysis

Ilastik toolkit ³²⁹ was used for tancytic processes and fragments segmentation analysis. We used the pixel classification followed by object classification pipelines to segment vimentin signal and classify vimentin positive objects into two classes: the “process” class including long and slim vimentin positive tancytic processes and the “fragment” group including short and circular vimentin positive tancytic fragments. To this end, high magnification z-stack confocal acquisitions (x63, 80 stacks, 0,25 μ m z-step) of vimentin immunolabeled hypothalami were acquired for all patients and transformed into maximum intensity projections. First, a set pictures of control and AD patients (5 patients per group, 1 section per patient, 3 images per section) was used to train a pixel classification and an object classification algorithm based on user’s inputs. Then, a second set of control and AD patients’ acquisitions (5 patients per group, 5 sections per patient, 2-3 pictures per sections) were analyzed using the trained pipelines. Finally, the data was extracted and compiled as mean per patients and mean per groups. The relative coverage of processes and fragments was computed as the percentage of processes area or fragments area over the total immunoreactive area, being the sum of processes area and fragments area.

ADNI data extraction and analysis

Data for control and AD patients were extracted from patients included in the ADNI1 cohort and for which CSF and plasma Tau concentrations at baseline were available (from ADNIMERGE, version: 2013-04-29 for baseline CSF Tau and BLENNOWPLASMATAU, version: 2015-08-04, for baseline plasma Tau). Plasma tau was analyzed by the Single

Molecule array (Simoa) technique and the Human total tau assay that uses a combination of monoclonal antibodies that give a measure of total tau levels. CSF Tau was measured using the Research Use Only (RUO) INNOBIA AlzBio3 immunoassay (Fujirebio). The ADNI was launched in 2003 as a public-private partnership, led by Principal Investigator Michael W. Weiner, MD. The primary goal of ADNI has been to test whether serial magnetic resonance imaging (MRI), positron emission tomography (PET), other biological markers, and clinical and neuropsychological assessment can be combined to measure the progression of mild cognitive impairment (MCI) and early Alzheimer's disease (AD). A total of 105 control patients and 95 AD patients were found in the database. From CSF and plasma Tau concentration, CSF to plasma Tau ratio was calculated for each patient. Patients identified as outliers for CSF, plasma or CSF to plasma Tau by the ROUT method ($Q=0,1\%$) were excluded resulting in the inclusion of 96 control and 88 AD patients for final analysis. To stratify patients into two groups of age (younger and older group) the median age of the cohort (75,8 years-old) was used (younger, $n= 49$ and 42 ; older, $n= 47$ and 46 ; for control and AD patients respectively).

Animals

All C57Bl/6J adult male mice were housed under specific pathogen-free conditions in a temperature-controlled room (21–22 °C) with a 12-h light/dark cycle and 40% humidity, and ad libitum access to food and water. All experiments were performed on 2 to 4 months old mice. B6.FVB-Tg(CAG-boNT/B,-EGFP)U75-56Fwp/J (iBot) mice (JAX:#018056) were purchased from *Jackson Laboratories*. All experiments and procedures involved in this study were approved by the Ethics Committee of the Universities of Lille, in accordance with European Union norms for animal experimentation.

Tau-565 and BSA-565 production

2N4R recombinant human Tau protein was produced as previously described³³⁰. Tau protein and purified bovine serum albumin (BSA, A7030, Sigma Aldrich) were labeled with Atto-565-NHS-ester (72464, Sigma Aldrich) using a 4-fold molar excess of Atto-565-NHS-ester at 4°C for 4 hours. After labelling, 15 mM of Tris was added to quench the reaction and the proteins were centrifugated in Zeba desalting columns (87767, ThermoFisher Scientific) to remove any unreacted fluorophores. To ensure protein coupling, a mass spectrometry analysis of the conjugated Tau protein (Tau-565) was performed using a Shimadzu AXIMA Assurance Linear MALDI-TOF Mass Spectrometer showing the coupling of a maximum of 5 Atto-565 label per protein. Finally, average label incorporation was determined by measuring fluorescence and protein concentration ($A_{\max} \times \text{MW of protein} / [\text{protein}] \times \epsilon_{\text{dye}}$). Tau-565 and BSA-565 label incorporation was respectively estimated at around 2 moles and 3 moles/mole of proteins.

Tau-565, BSA-565 and Tau-565AG and AAV1/2-Dio2-iCre-A2-GFP delivery

AAV1/2-Dio2-iCre-A2-GFP ($1,25 \cdot 10^9$ genomic particles per μL) was produced as detailed previously²⁷¹. Tau-565 was produced as detailed above and adjusted to a $1 \mu\text{g} \cdot \mu\text{L}^{-1}$ concentration before injection. Both AAV1/2-Dio2-iCre-A2-GFP and Tau-565 were stereotaxically infused into the lateral ventricle ($1 \mu\text{L}$ over 5 minutes, anteroposterior: -0,3mm, lateral: $\pm 1\text{mm}$, dorsoventral: -2,5mm) of wild-type (wt) or transgenic iBot isofluorane-anesthetized mice. For dual injections, wt and iBot mice were injected with AAV1/2-Dio2-iCre-A2-GFP three weeks before Tau-565 injections.

Evaluation of AAV1/2-Dio2-iCre-A2-GFP infection efficiency

Three weeks after LV AAV1/2-Dio2-iCre-A2-GFP infusion in iBot mice, animals were sacrificed, their brain collected and post-fixed by 4% paraformaldehyde (PFA) in PBS immersion overnight. Brains were cryoprotected in 30% sucrose overnight, embedded in TissueTek OCT (Sakura) and frozen. Coronal sections (40 μ m) were cut and processed for immunofluorescence using chicken anti-vimentin (1:1,000; PCK-594P, BioLegend) and rabbit anti-GFP (1:5,000; A-11122, Invitrogen) primary antibodies revealed with donkey anti-chicken Alexa Fluor 647 (1:1,000; 703-545-155; Jackson Immuno Research) and donkey anti-rabbit Alexa Fluor 488 (1:1000; A-21206, ThermoFisher Scientific). Sections were counterstained with DAPI and mounted using mowiol. Five representative ME slides per mice were analyzed and tanycytes were divided into two groups (ventral for tanycytes projecting to the ME and dorsal for tanycytes projecting in the hypothalamic nuclei). Vimentin⁺/GFP⁺ and vimentin⁺/GFP⁻ cell number was reported to vimentin⁺ cells bordering the third ventricle.

Tau-565 kinetic experiment

For experiments assessing Tau-565 clearance from brain to blood, anesthetized wt mice were stereotaxically injected with 1 μ L of Tau-565 over 5 minutes in the lateral ventricle. Immediately after the 5-minutes injection or after 15, 30 minutes, 1- and 2-hours post-injection brains, pituitaries and blood of the mice were collected (n=5 per group, except for the 30 minutes group n=3). The brains were immersion fixed overnight at 4°C in 4% PFA. The pituitaries were immediately frozen in dry-ice and serum prepared from blood by centrifugation (2,000g, 15 min at 4°C). A group of animals were used to establish Tau clearance to the blood using tail-blood sampling. Blood was sampled from the tail at the end of the injection of Tau-565 and after 15, 30 minutes, 1- and 2-hours post-injection and serum prepared by centrifugation (10,000g for

15minutes) allowing the assessment of the whole kinetic in the same mice. At 2-hours post-injection, the brain was collected and fixed overnight at 4°C in 4% PFA.

IDISCO tissue clearing

Immersion fixed brains were processed using an adapted version of the iDISCO+ protocol described previously³³¹. Briefly, samples were dehydrated with ethanol gradient (20%, 40%, 60%, 80%, 100%, 1 hour each) and delipidated in 66% dichloromethane / 33 % ethanol overnight. Ethanol was washed out of the samples by 100% dichloromethane incubation for 1h. Finally, the samples were cleared by immersion in dibenzylether for at least 2 hours in rotation. After transparency was achieved, a fresh solution of dibenzylether was used for storage, and the samples were kept protected from light at room temperature until imaging.

Light-sheet microscope imaging

Imaging of cleared tissues was performed in dibenzylether on the Ultramicroscope 1 (Lavision BioTec, available at the BioImaging Center of Lille) and using MI PLAN 12x/0.53 with 2x zoom objective. Sequences were acquired with InspectorPro Software. The following parameters were used: z-step was set to 2 µm, laser width and numerical aperture were kept to the maximum.

3D image processing and analysis

Tiff sequences resulting from light-sheet acquisitions were converted to the Imaris file format using Imaris FileConverter. Finally, Imaris 9.1-9.5 (Bitplane) was used for visualization and 3D processing of the datasets. Figures were prepared in Photoshop (Adobe) and videos were edited with Shotcut (<https://shotcut.org/>).

Human Tau ELISA

For human Tau ELISA, pituitary protein extract was prepared by mechanical tissue dissociation in 1x RIPA buffer (20-188, Millipore) using tube potters and sonication. For primary tanycyte Tau-565 secretion experiment, cell medium was collected and immediately frozen in dry-ice. Tau-565 concentrations in pituitary extracts, serum and cell medium were measured using Tau (Total) Human ELISA Kit (KHB0042, ThermoFisher Scientific) according to manufacturer instructions except for 1:10 pituitary extract ($0,2\mu\text{g}\cdot\mu\text{L}^{-1}$), serum and cell medium dilution.

Tanycyte primary culture

Tanycyte were isolated from the median eminence (ME) of the hypothalamus of 10-days-old rats and cultured as described previously³³². Briefly, after decapitation and removal of the brain, MEs were dissected and dissociated using a $40\mu\text{m}$ nylon mesh. Dissociated cells were culture in DMEM without pyruvate, high glucose (D5796-500ML, Sigma) supplemented with 10% donor bovine serum (16030074, Gibco), 1% L-Glutamine (25030-024, Gibco) and 1% Penicilin/streptomycin (15140-122, Gibco). Culture medium was changed after the 10th day *in vitro* and twice per week afterwards. On reaching confluence, tanycytes were trypsinized and plated in plastic culture plate for internalization and secretion assays, on poly-L-lysine coated glass coverslips for immunocytochemistry or on poly-L-lysine Ibidi glass bottom μ -Slide 8 well (80827, Ibidi) for live imaging and immunocytochemistry.

Primary tanycyte 2N4R Tau and Tau-565 internalization assay

Primary tanycytes were treated with either recombinant 2N4R human Tau (25 nM, 30 minutes) or Tau-565 (25 nM, 15 to 30 minutes) and Tau internalization was analyzed using western blot, immunocytochemistry and live imaging.

Immunocytochemistry

For immunocytochemistry, Ibidi slides or coverslip seeded primary tanycytes, untreated and Tau-565 treated (25nM, 30 minutes), were washed three times with PBS and fixed in 4% PFA for 15 minutes at 4°C. After fixation, cells were washed with PBS and stored at 4°C in PBS 0,1% azide. Coverslips of both untreated and Tau-565 tanycytes were incubated with primary antibodies (see Table 1) overnight in ICS at 4°C. The coverslips were washed three times in PBS prior to secondary antibody incubation in ICS for 1 hour at room temperature. Excess of secondary antibody was washed three times with PBS and cells were counterstained using DAPI before mounting in Mowiol.

Western blot of primary tanycyte extracts

For western blot, confluent 6 well plates were treated with recombinant 2N4R human Tau (25nM, 30 minutes). After treatment, cells were washed five times with PBS and immediately frozen in dry ice. Proteins extracts were prepared by scraping the cells in 1x RIPA buffer (20-188, Millipore) and homogenization by sonication. For each lane, 10µg of proteins in Laemlli buffer (1610747, Bio-Rad) was loaded in a 10% acrylamide gel. Migration was performed for 1h at 120V and followed by protein transfer onto a 0,45 µm nitrocellulose membrane for 1h at 100V. Immunolabeling of the membrane was performed using Tau5 mouse anti-Tau primary antibody (1:2,000, 606-320, ThermoFisher Scientific) or rabbit anti-GAPDH (1:5,000, G9545, Millipore) overnight in 5% milk TBS-Tween 0,05% at 4°C. Primary antibody was then washed three times with TBS-Tween 0,05% and incubated with HRP-coupled rabbit anti-mouse (P026002-2, Agilent) or HRP-coupled goat anti-rabbit (P044801-2, Agilent) secondary antibody for 1 hour at room temperature. Secondary antibodies in excess were washed three times with TBS-Tween 0,05% and membranes were incubated in SuperSignal™ West Dura

Extended Duration Substrate (34076, Thermo Scientific). Chemiluminescent signal was detected using an Amersham ImageQuant 800 system (Cytiva).

Primary tanycyte Tau-565 secretion assay

For tanycyte Tau-565 secretion assay, tanycytes were treated with Tau-565 (25nM, 30 minutes), washed five times with hot PBS and incubated with fresh Tau-565 free culture medium for 5, 15, 30 and 60 minutes. After the different secretion time points, the medium was recovered and immediately frozen in dry ice. Tau concentration in the medium was measured by ELISA as described above.

Fluorescence microscopy

Microphotograph acquisitions were performed on a Zeiss AxioObserver Z1 confocal microscope associated with a spinning disk head (Yokogawa CSU-X1) and a camera (sCMOS Photometrics Prime 95B), using PLAN-APOCHROMAT 10x/0.45, 20x/0.8 and 63x/1.4, objectives under Zen 2.3 (Zeiss) software control.

Statistics

Results are given as mean \pm standard deviation (S.D.). Data were excluded after ROUT method for outliers' identification (Q=0,1%) for human data or when an objective experimental failure was observed for cell and animal experimentation. Studies were not randomized and investigators were not blind to treatment group. To test whether data followed a Gaussian distribution, a normality test was performed (Kolmogorov-Smirnov and Shapiro-Wilk tests). The statistical tests used for each figure are described in the legends. Data analysis was performed using GraphPad Prism Software v8.1.1 (GraphPad). The threshold for significance was $P < 0.05$.

Table 1: Antibodies

Antigen	Manufacturer	Reference / Clone	Dilution
Vimentin	BioLegend	PCK-594P	1/500 to 1/1000
Caveolin-1	Cell Signalling	D46G3	1/500
Tau pSer396/404	Gift from Peter Davies	PHF1	1/200
GFAP	Dako	Z0334	1/500
GPR50	Servier	pAb7 ²⁷⁹	1/200
CD31	BD Pharmingen	550274	1/200
Clathrin	Abcam	Ab2731	1/400
EEA1	Cell Signalling	C45B10	1/500
LRP1	Abcam	Ab92544	1/500

Results

Tanycytes uptake and secrete exogenous Tau *in vitro*

In order to determine whether Tau could be transported by tanycytes, we first examined its uptake by rat tanycytes in primary culture. To be able to track Tau internalization, we conjugated 2N4R Tau to a fluorescent tag (Tau-565), resulting in a mix of Tau molecules carrying 1 to 5 fluorophore tags (Figure 21A). Spectral analysis of the resulting Tau-565 revealed an excitation maximum at 565 nm and emission maximum at 590 nm (Figure 21B). These parameters were later used for the microscopic observations. The incubation of primary rat tanycytes with Tau-565 for 30 minutes led to the visualization of intracellular Tau-positive vesicles, as shown by both Tau-565 fluorescence and immunolabeling using the Tau5 antibody (Figure 21C). Since clathrin-mediated endocytosis has already been implicated in tanycyte leptin uptake in early endosomes, we stained Tau-565 incubated primary tanycytes for clathrin and EEA1, an early endosome marker. After 30 minutes of incubation, Tau-565 was found in clathrin and EEA1 positive vesicle suggesting that the endocytosis mechanism involved in tau uptake is similar to leptin's one (Figure 21D). LDL receptor related protein 1 (LRP1) have recently been demonstrated as mediator of tau internalization¹²⁸. Staining for LRP1 on Tau-565 incubated primary tanycyte show that tanycyte express LRP1 and that Tau-565 positive vesicles are also LRP1 positive supporting a role for LRP1 in tau uptake by tanycytes *in vitro* (Figure 21D). Western blotting of untreated rat tanycytes revealed no detectable Tau protein, but a 30-minute treatment with an unconjugated human recombinant 2N4R Tau isoform led to a positive signal on the blots (Figure 21E), suggesting that Tau conjugation has no effect on its uptake. To verify whether internalized Tau was being exocytosed by tanycytes, we incubated rat primary tanycytes with Tau-565 for 30 minutes, and used an ELISA specific to human tau to measure its levels in fresh medium and cell lysate at various time points.

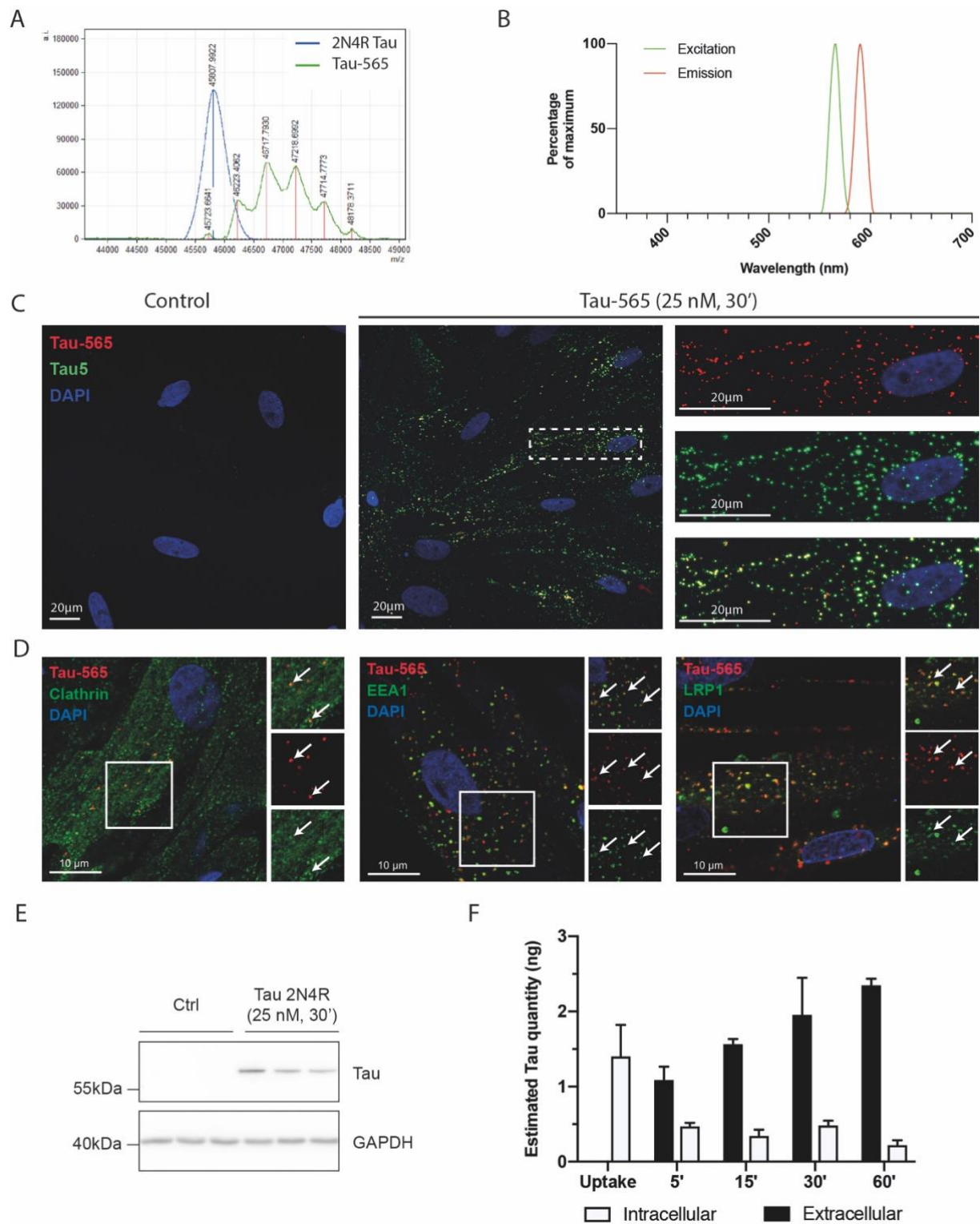


Figure 21: Primary rat tanycytes uptake and secrete tau *in vitro*.

A. Mass spectrometry plot of unconjugated recombinant 2N4R Tau and Atto-565-conjugated recombinant 2N4R Tau (Tau-565). Tau-565 peaks (noted by a red line) represent different Atto-565 conjugated 2N4R Tau species having up to 5 fluorophores per protein. B. Excitation (green) and emission (red) spectra of Tau-565 respectively reaching their maximum at 565nm and 590nm. C. Photomicrograph of cultured rat primary tanycytes treated or not with Tau-565 (red) and immunolabeled

for Tau (Tau5 antibody, green). D. Photomicrograph of cultured rat primary tanycytes treated with Tau-565 (red) and immunolabeled for clathrin (green, left panel), EEA1 (green, middle panel) and LRP1 (green, right panel). E. Western blot for Tau protein in protein extracts of primary tanycyte cultures, untreated and treated with recombinant human 2N4R Tau, using the Tau5 antibody. F. Estimated tau intracellular (white bars) and extracellular (black bars) quantities based on ELISA cell medium and cell lysates dosage in uptake condition (30 minutes after incubation) and after 5, 15, 30 and 60 minutes of secretion.

Primary tanycytes showed a rapid release of tau that increased over time accompanied by a decrease in intracellular tau content, supporting the view that Tau uptake by tanycytes is the first step in its tanycytic clearance (Figure 21F).

Tanycytes transport Tau protein from CSF to blood in vivo

Since tanycytes appear to both take up and release Tau *in vitro*, we next investigated the time course and destination of this Tau cleared from the CSF *in vivo*, using wild-type mice. We performed ICV injections of Tau-565 into the lateral ventricle, followed by immunohistofluorescence and ELISA measurement of Tau in the pituitary, to which the portal capillaries of the ME lead, and in the general circulation. In the brain, Tau was observed at the luminal surface of the ventricular wall at all time points (Figure 22). However, while this labeling remained faint and restricted to the lumen in other areas bordering the ventricles, tanycytes of the ME were strongly positive for Tau-565 as soon as the end of the 5 minutes-long injection (Figure 22), corroborating our observations in rat tanycytes *in vitro*.

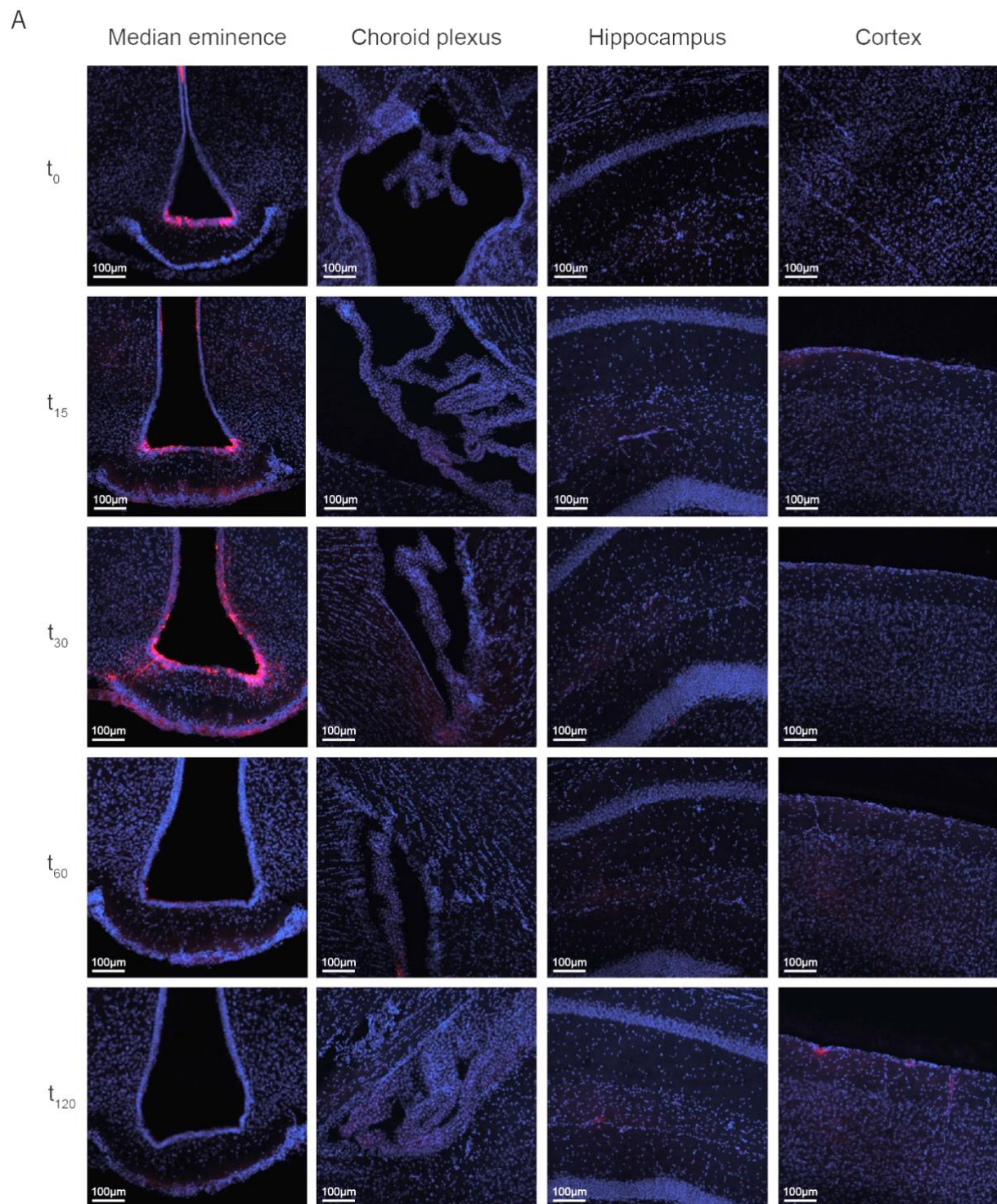


Figure 22: Kinetic of Tau-565 distribution in the wild-type mice.

Photomicrographs of the median eminence, choroid plexus, hippocampus and cortex of WT mice at different time points after Tau-565 (red) injection into the lateral ventricle. Tau-565 appears specifically in the median eminence as soon as the end of the injection time.

This Tau accumulation by tanyctic cell bodies and its intracellular transport could no longer be seen by 1-hour post-injection (Figure 22), reminiscent of its exocytosis over time by primary cultured tanyctes above. The distribution of Tau-565 along the third ventricle as a whole was also examined using tissue clearing and light-sheet imaging of Tau-565 injected brains 30 minutes after ICV Tau-565 injection. The Tau-565 signal was found to be concentrated along the ME, especially in ventral tanyctes (Figure 23A), further supporting a key role for these cells in trapping and clearing Tau from the brain. To verify the specificity of Tau uptake and secretion by tanyctes compared to other proteins, we performed ICV injections of fluorophore-coupled bovine serum albumin (BSA-565), which has a molecular weight of the same order of magnitude as Tau and bovine or human serum albumin have been used as a control for tau in previous studies^{248,333}; 30 minutes post-injection, the BSA-565 signal was detected along the lumen of the third ventricle, similar to Tau-565 in the rest of the brain, but not in tanyctic cell bodies or end-feet (Figure 23B). Next, we studied the route and kinetics of Tau-565 transport from the brain to the systemic blood circulation. The ME vasculature being part of the pituitary portal circulation, we could expect Tau exocytosed by tanyctes to follow a pituitary route. Indeed, we found Tau-565 fluorescence in end-feet contacting the capillaries of the median eminence and mouse pituitaries were positive for Tau-565 fluorescence 30 minutes after injection, further supporting a role for ME tanyctes as major Tau transporters, and the sequential release of Tau by tanyctic end-feet into the portal circulation and its transport to the pituitary (Figure 23C, D). In accordance with this observation, Tau-565 was detected in pituitary tissue by ELISA as soon as the injection ended and up to 1h, while it peaked in peripheral blood serum at 30 minutes post-injection, decreasing over time until the second hour post-injection (Figure 23E). To investigate any sexual dimorphism in the kinetic of Tau efflux from brain to blood, tail blood sampling was performed after Tau-565 ICV injections in male and females.

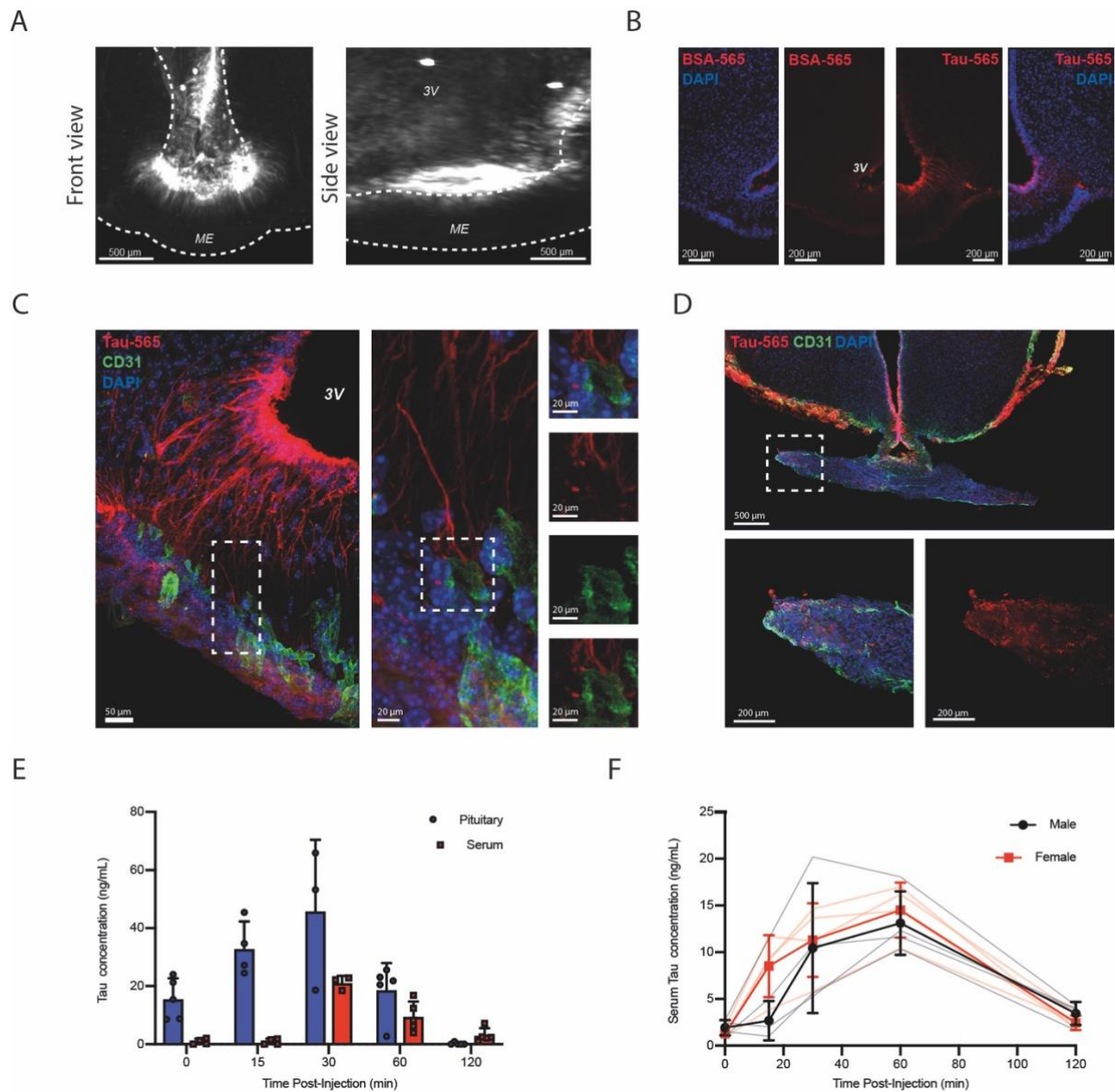


Figure 23: Tancytes transport tau from CSF to blood in male and female mice.

A. Coronal and sagittal projection of the ventral third ventricle (3V) of Tau-565 injected mice light-sheet 3D acquisition. Ventral tancytes of the median eminence (ME) are positive for Tau-565 (white). B. Photomicrograph of the third ventricle and median eminence of WT mice injected with BSA-565 (red) (left panels) or Tau-565 (red) (right panels). C. Representative photomicrograph of the median eminence of a Tau-565 (red)-injected wild-type (WT) mouse immunolabeled for CD31 (green) to visualize blood vessels. D. Photomicrograph of the median eminence and attached pituitary of a Tau-565 (red)-injected WT mouse immunolabeled for CD31 (green) to visualize blood vessels. E. ELISA measurement of human Tau in the pituitary and serum of Tau-565-injected WT mice (n=4, 3, 5 and 5 mice per time point). F. ELISA measurement of human Tau in tail-blood serum of Tau-565-injected WT male and female mice (n=4 per group).

No difference between male and females was found. Even if the serum tau concentration seems to rise faster in females in comparison to males, this difference was not significant (Figure 23F). This temporality of Tau detection in the brain, pituitary and blood also supports its transport through ME tanycytes to the portal circulation for delivery to the pituitary, and eventually to the systemic circulation.

Inhibition of tanycytic transport impairs CSF to blood transport of Tau

In order to investigate the specific role of tanycytes in Tau efflux from the brain to the blood, we used a murine model in which we arrested vesicular transport in tanycytes using the botulinum toxin light chain B (BoNT/B). BoNT/B prevents exocytosis in neurons and glial cells by cleaving vesicle-associated membrane proteins 1 and 2 (VAMPs), which mediate vesicular fusion and transport^{296,334}. Another BoNT/B target, VAMP3, is also implicated in endocytosis in platelets³³⁵. BoNT/B expression in tanycytes could thus be used to impair the uptake, transport and release of various substances transported by tanycytes, including Tau. Transgenic mice expressing a floxed BoNT/B, or iBot mice²⁹⁶, were infected with an AAV1/2-Dio2-iCre-GFP virus to induce Cre expression specifically in tanycytes (Figure 24 A, B). The infection rate of tanycytes was 71% for ventral tanycytes and 41% for dorsal tanycytes (Figure 24C). After ICV Tau-565 injection, iBot mice showed a dramatic reduction in the Tau-565 signal in tanycytic processes and endfeet as well as the underlying capillary bed compared to controls (Figure 24D), linked to reduced Tau-565 uptake by many infected tanycytic cell bodies at the ventricular wall (Figure 24E). A counting of GFP and Tau-565 positive tanycytes showed a consistent infection in control and iBot mice (n=5 and n=4, $60,8 \pm 7.2$ and $69,7 \pm 10.9$ cells per slide) accompanied by a reduction in Tau-565 positive tanycytes only in iBot mice (n=5 and n=4, $34,7 \pm 6.9$ and $3,4 \pm 4.8$ cells per slide, $p=1.12 \cdot 10^{-4}$).

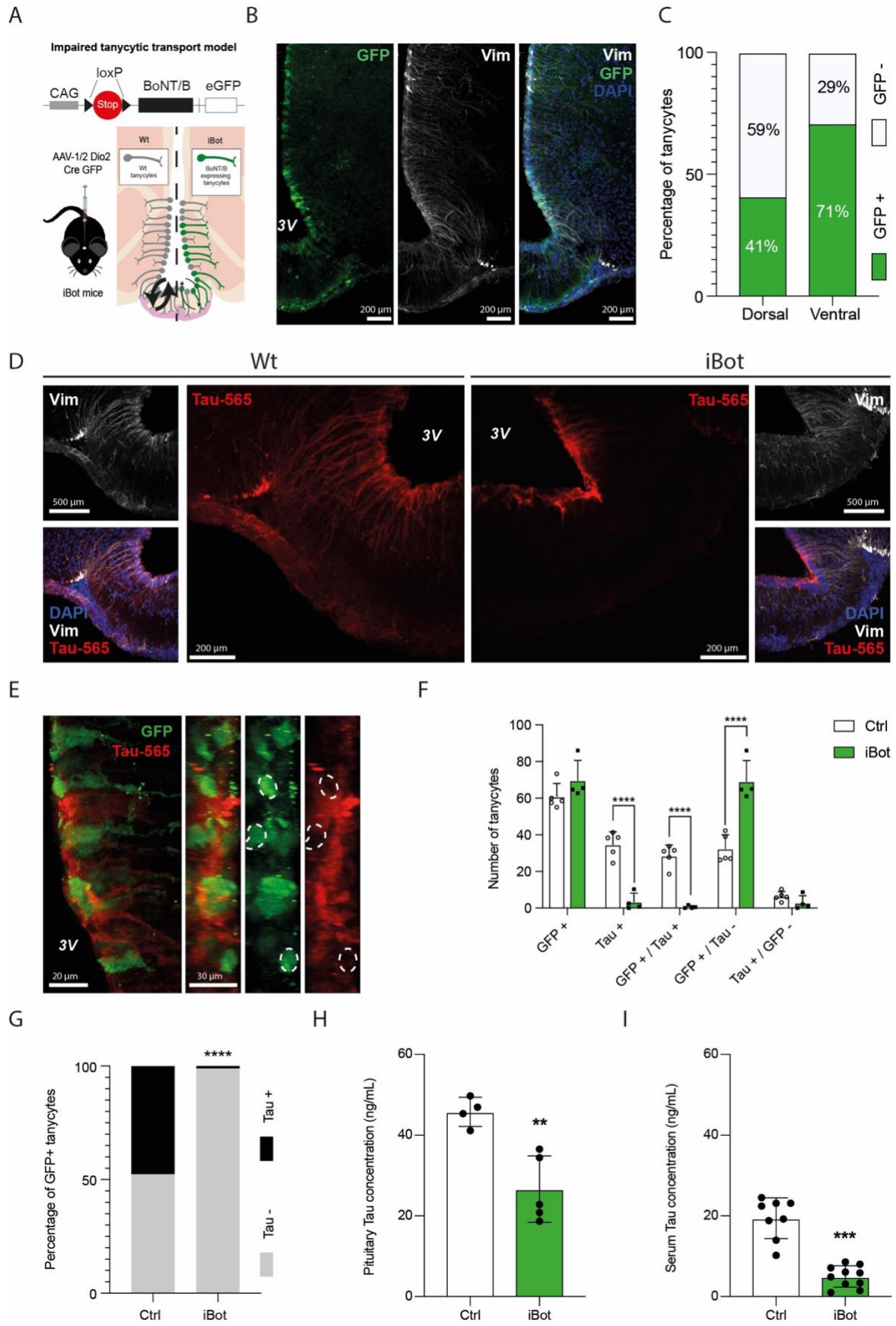


Figure 24: Inhibition of tanyctocyte's transcytosis blunts tau efflux from brain to blood.

A. Schematic of the iBot transgenic model. B. Photomicrograph of the median eminence of iBot mice injected with the AAV1/2-Dio2-Cre-A2-GFP virus, showing infected tanycytes (GFP, green) and immunolabeling for the tanycytic marker vimentin (white). C. Quantification of GFP-positive dorsal and ventral tanycytes in iBot mice injected with the AAV1/2-Dio2-Cre-A2-GFP virus (n=10 mice per group, 3-4 sections per mouse). D. Photomicrographs of Tau-565 (red) uptake in vimentin-immunopositive (white) tanycytes in the median eminence of Tau-565-injected WT mice (left panels) and iBot mice. E. Maximum intensity projection of the wall of the third ventricle of Tau-565 (red)-injected iBot mice, immunolabeled for GFP (green); z-stack acquisition (left panel) and z-axis reprojections (right panels) (right panels). F. Counting of GFP and Tau-565 positive tanycytes in control and iBot mice hypothalamus (n=5 and 4, 3 sections per mouse). Multiple t-test. Data are represented as means \pm S.D., ****, $p < 0,001$. G. Percentage of Tau-565 positive and negative infected tanycytes (GFP positive). Two-way ANOVA (mouse genotype, $F(1,14)=3.893.10-18$, $p > 0.99$; Tau uptake, $F(1,14)=182.8$, $p < 0.0001$; interaction, $F(1,14)=150.2$, $p < 0.0001$) followed by Sidak's multiple comparison post hoc test (Tau- Ctrl vs. iBot, $q(14)=8.666$, $p < 0,0001$; Tau+ Ctrl vs. iBot, $q(14)=8.666$, $p < 0,0001$). Data are presented as mean \pm S.D., ****, $p < 0,001$. H. ELISA measurement of human Tau in the pituitary of Tau-565-injected WT and iBot mice 30 minutes post-injection (n= 4 and 5 mice). Two-tailed unpaired t-test ($t(11)=4.293$, $p=0.004$). Data are presented as means \pm S.D., **, $p < 0.01$. I. ELISA measurement of human Tau in the serum of Tau-565-injected WT and iBot mice 30 minutes post-injection (n=8 and 10 mice). Two-tailed unpaired t-test ($t(16)=7.875$, $p < 0.001$). Data are presented as means \pm S.D., ***, $p < 0.001$.

Moreover, while GFP and Tau-565 positive tanycyte number was reduced in iBot compared to control mice, the number of Tau-565 positive but GFP negative tanycytes was identical (Figure 24F). When looking specifically at infected tanycytes, half was positive for Tau-565 in the control mice but only one percent was in iBot mice (Figure 24G). Next, ELISA dosage of pituitary extracts and serum from Tau-565 injected control and iBot mice were performed to confirm the interruption of the tanycytic shuttle of tau. Correspondingly, 30 minutes post-injection, pituitary concentrations of Tau were almost halved in iBot mice (n=5, 26.65 ± 8.22 ng/mL) compared to control mice (n=4, 47.53 ± 11.97 ng/mL, $p=0.004$, Figure 24H), whereas serum Tau concentrations underwent a 3.6-fold reduction, from 16.44 ± 6.66 ng/mL to 4.55 ± 2.85 ng/mL (n=8 and n=10, $p < 0.001$, Figure 24I), emphasizing the importance of tanycytic transport in Tau efflux from the brain to the blood.

Tau protein CSF to blood transport is altered in AD

Since CSF-to-blood ratios have been used in several studies to evaluate molecular transport into the brain across the BBB^{313,336}, we considered the ratio of plasma to CSF Tau in AD patients to be a proxy for its clearance in the opposite direction. Indeed, although Tau protein concentrations have been previously compared and found to be higher in the CSF and plasma of AD patients compared to normal subjects^{179,337}, the importance of the plasma-to-CSF Tau ratio as an indicator of Tau clearance from the brain has not been exploited so far. Plasma and CSF concentrations of total Tau protein for control and AD patients were extracted from the Alzheimer's Disease Neuroimaging Initiative (ADNI1) database³³⁸. After screening and data cleaning, 96 control patients and 88 AD patients, for whom plasma and CSF Tau concentrations were available at baseline, were selected. Mean plasma and CSF Tau levels were higher in AD patients (n=88, 3.128 ± 1.386 and 359 ± 131 pg/mL, respectively) than in control subjects (n=96, 2.503 ± 1.208 and 239 ± 85 pg/mL, $p=0.001$ and $p<0.0001$ respectively, (Figure 25A, B). Interestingly, however, the increase in Tau concentrations was not proportionate in the two compartments, and the plasma-to-CSF ratio of Tau was lower in AD patients (n=88, 0.01022 ± 0.005) than in controls (n=96, 0.01303 ± 0.007 , $p=0.005$), suggestive of a defect in brain-to-blood Tau efflux in these patients (Figure 25C). Remarkably, while the plasma-to-CSF Tau ratio was negatively correlated with age in control patients ($r= -0.3378$, $p=0.0008$, $R^2= 0.1141$), indicative of a mild age-related decline in clearance, this correlation was lost in AD patients ($r= -0.0008$, $p=0.99$, $R^2= 6.717 \cdot 10^{-7}$) (Figure 25D-F). However, when groups were stratified based on the median age of the cohort (75 years), the decrease in plasma-to-CSF Tau ratio values in AD patients compared to controls was evident in the younger but not in the older group, confirming the existence of an age-related decrease in clearance even in controls (Figure 25G).

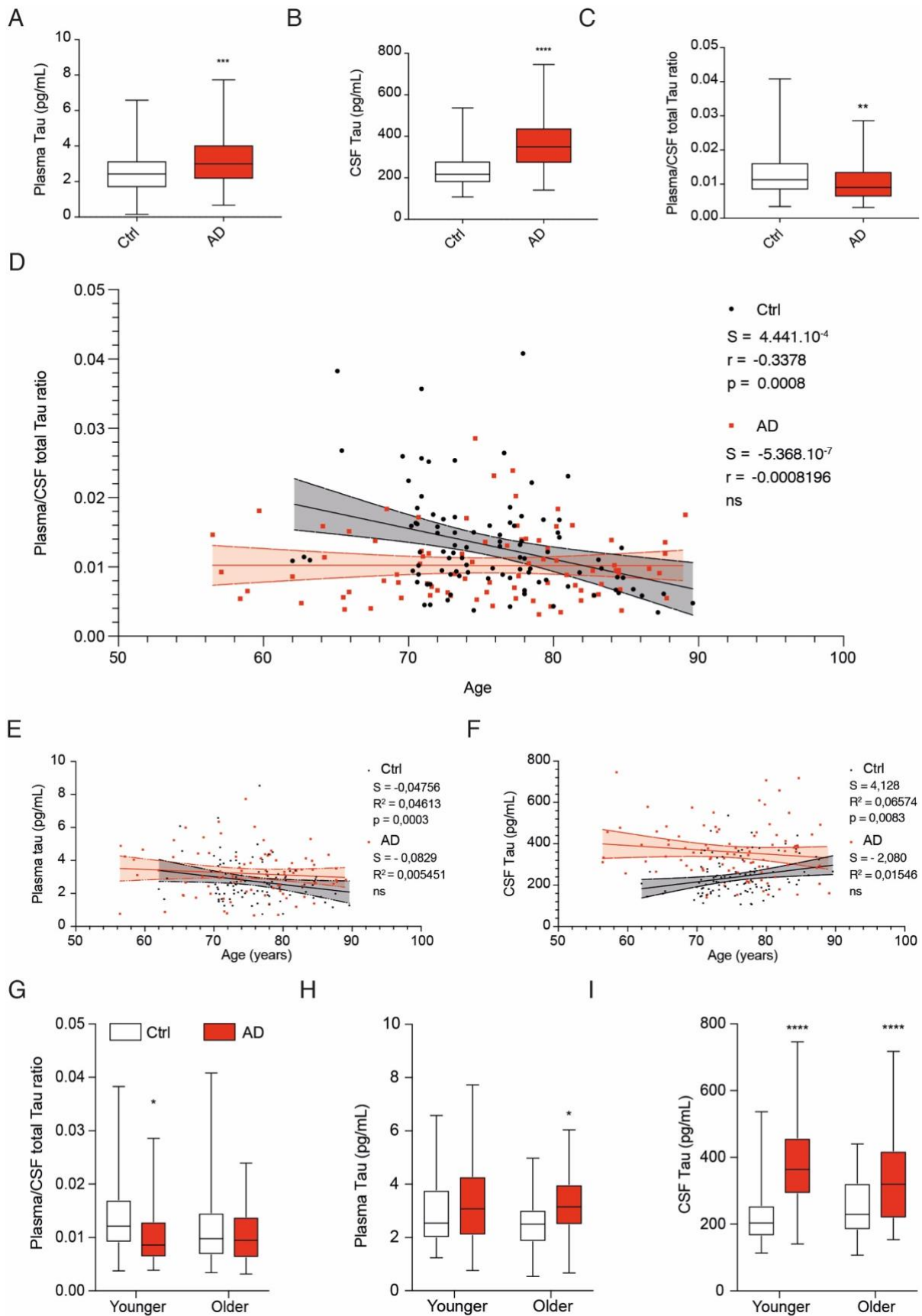


Figure 25 : Plasma-to-CSF Tau ratio is lower in AD patients.

A. Plasma Tau concentrations in control (white, n=96) and AD (red, n=88) patients. Two-tailed Mann-Whitney U test ($U=3443$, $p=0.001$). Data are presented as a box (median, lower and upper quartile) and whiskers (minimum and maximum); ***, $p<0.001$. B. CSF Tau concentrations in control (white, n=96) and AD (red, n=88) patients. Two-tailed Mann-Whitney U test ($U=2062$, $p<0.0001$). Data are presented as a box (median, lower and upper quartile) and whiskers (minimum and maximum); ****, $p<0.0001$. C. Plasma-to-CSF ratio of total Tau concentrations in control (white, n=96) and AD (red, n=88) patients. Two-tailed Mann-Whitney U test ($U=3176$, $p=0.005$). Data are presented as a box (median, lower and upper quartile) and whiskers (minimum and maximum); **, $p<0.01$. D. CSF Tau concentration distribution in function of age in control (black, n=96) and AD (red, n=88) patients. Linear regression model and 95% confidence interval for control (black, dashed-lines and black shadow) and AD patients (red dashed-lines and red shadow). E. Plasma Tau concentration distribution in function of age in control (black, n=96) and AD (red, n=88) patients. Linear regression model and 95% confidence interval for control (black dashed-lines and black shadow) and AD patients (red dashed-lines and red shadow). F. Plasma-to-CSF Tau ratio as a function of age in control (black) and AD (red) patients. Linear regression curve and 95% confidence interval for control (black dashed lines and grey shadow) and AD patients (red dashed lines and red shadow). G. Plasma-to-CSF Tau ratio stratified by age in control (younger: <75 years, n=49; older: >75 years, n=47) and AD (younger: <75 years, n=42; older: >75 years, n=46). Kruskal-Wallis test ($H(4)=11.03$, $p=0.0116$) followed by Dunn's multiple comparison post hoc test (Younger Ctrl vs. Younger AD, $Q(4)=2.995$, $p=0.0165$). F. Plasma Tau stratified by age in control (younger: <75 years, n=49; older: >75 years, n=47) and AD (younger: <75 years, n=42; older: >75 years, n=46). Kruskal-Wallis test ($H(4)=11.03$, $p=0.0103$) followed by Dunn's multiple comparison post hoc test (Older Ctrl vs. Older AD, $Q(4)=2.679$, $p=0.0443$). Data are presented as a box (median, lower and upper quartile) and whiskers (minimum and maximum); *, $p<0.05$. H. CSF Tau stratified by age in control (younger: <75 years, n=49; older: >75 years, n=47) and AD (younger: <75 years, n=42; older: >75 years, n=46). Kruskal-Wallis test ($H(4)=53.64$, $p<0.0001$) followed by Dunn's multiple comparison post hoc test (Younger Ctrl vs. Younger AD, $Q(4)=6.465$, $p<0.0001$; Older Ctrl vs. Older AD, $Q(4)=3.430$, $p<0.0001$). Data are presented as a box (median, lower and upper quartile) and whiskers (minimum and maximum); ****, $p<0.0001$.

Further analysis revealed that this age-related difference in the plasma-to-CSF Tau ratio was due to the fact that plasma Tau concentrations were not significantly lower in controls than in AD patients at younger ages, unlike older ones (Figure 25H), while the increase in CSF Tau concentrations in AD patients compared to controls was greater in the younger group than in the older one, although both increases were significant (Figure 25I).

Tanycytes show signs of Tau transport

Given our experiments above in rat primary tanycytes *in vitro* and mice *in vivo* and the finding that Tau efflux from the CSF to the blood is altered in AD patients, we used human post mortem brain tissues from six AD patients and five controls (Table 2) to further examine the hypothesis that tanycytes are Tau transporters. Using immunofluorescence labeling with the PHF1 antibody (anti-Tau pSer396/404), we noted no signal in the brain of control subjects (Figure 26A, B) but Tau-immunoreactive neurons with typical neurofibrillary tangles in the infundibulum of AD patients (Figure 26B). Interestingly, tanycytes displayed a pattern of Tau labeling that was quite different from neurofibrillary tangles, with Tau-positive puncta corresponding to vesicles both at the level of their cell bodies lining the third ventricle and along the proximal part of their vimentin-immunoreactive processes (Figure 26B).

Table 2: Patients' information.

	Sex	Group	Age	Braak stage	Thal stage	Post-mortem delay	Comorbidities	PHF1 signal Hypothalamus	Tanycytic degradation
Patient 1	M	Ctrl	50	0	0	16h	Ischemic cardiopathy, epilepsy, dyslipidemia	0	0
Patient 2	F	Ctrl	64	0	0	27h	Arterial hypertension, atrial fibrillation, aortic infectious endocarditis, strokes	0	0
Patient 3	M	Ctrl	36	0	0	80h	Atherosclerosis, obesity	0	0
Patient 4	M	Ctrl	62	0	0	19h	Stroke, arterial hypertension, dyslipidemia	0	0
Patient 5	M	Ctrl	69	I	0	21h	obliterative arteriopathy of the lower limbs, chronic glaucoma	0	0
Patient 6	F	AD	78	IV	IV	27h	Breast cancer, arterial hypertension	+++	+++
Patient 7	M	AD	52	VI	IV	32h	No history	+++	+++
Patient 8	M	AD	56	IV	V	14h	Smoking	+++	++
Patient 9	F	AD	56	V/VI	IV	36h	arterial hypertension, atrial fibrillation, infectious endocarditis Horton disease, arterial hypertension, dysthyroidism, osteoporosis, obstructive sleep apnea	0	+++
Patient 10	F	AD	88	III	III	24h	Arterial hypertension	0	+++
Patient 11	M	AD	69	V/VI	II	48h	Arterial hypertension	++	++
Patient 12	F	FTD Tau	58	NA	NA	40h	Asthma	++	0
Patient 13	M	FTD TDP-43	70	NA	NA	24h	No history	0	0
Patient 14	F	FTD TDP-43	67	IV	0	20h	AD associated Tau lesions but absence of amyloid beta	+	++
Patient 15	M	FTD TDP-43	70	NA	NA	12h	Presence of some Tau lesions in astrocytes, dyslipidemia	++	0

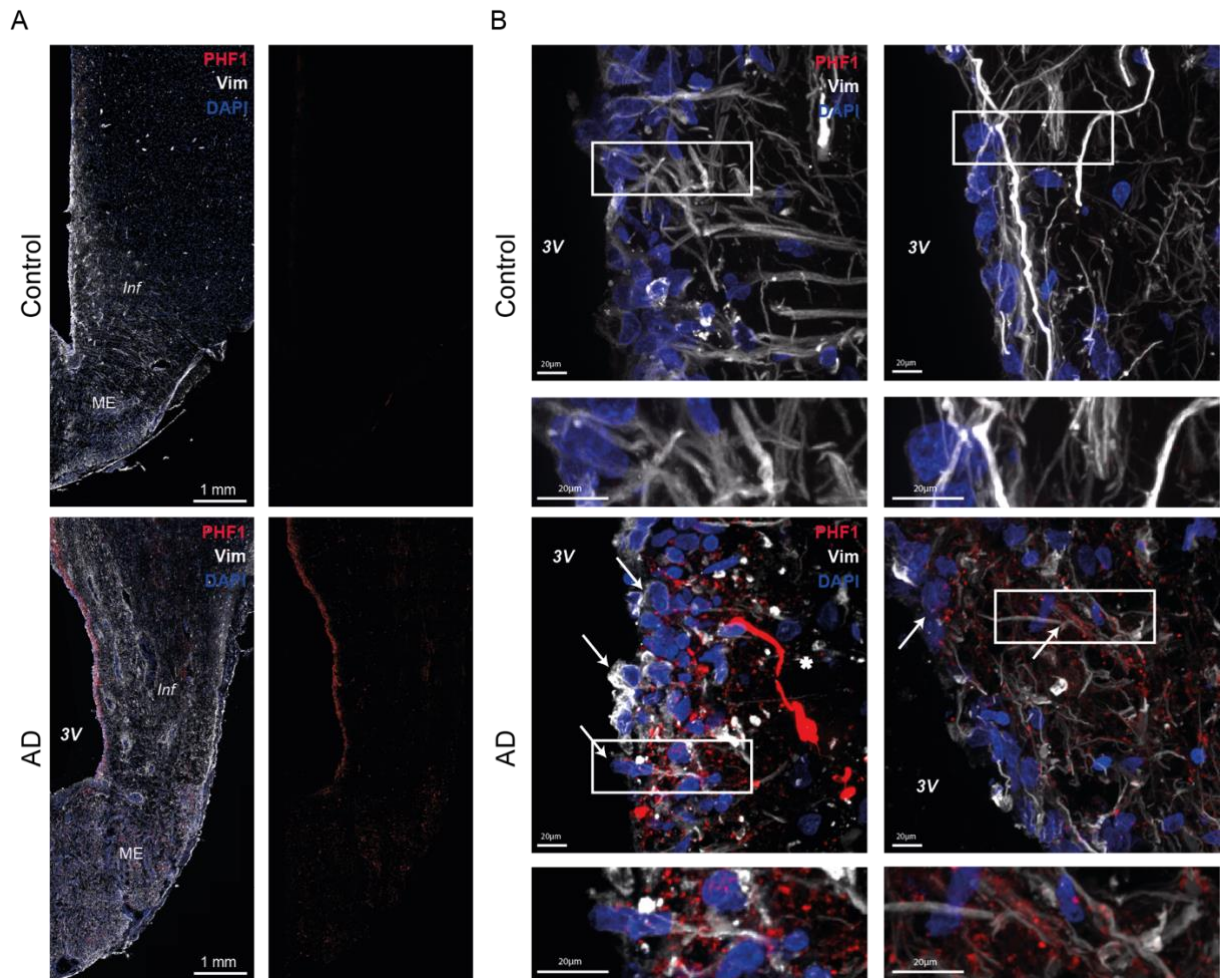


Figure 26: Tanycytes of AD patients contain Tau-positive vesicles.

A. Photomicrograph of tanycytes in the hypothalamus of control and AD patients immunolabeled for vimentin (white) and phosphorylated Tau (PHF1 antibody, Tau pSer396/404, red). **B.** Higher magnifications of tanycytic cell bodies and processes in the control and AD patients' brain, showing a typical neuron with a neurofibrillary tangle labeled by PHF1, and more punctate labeling corresponding to Tau-containing vesicles in tanycytes only in AD patients. White rectangle: higher magnification inset shown at right. White arrows: tanycytes containing PHF1-positive vesicles, white asterisk: PHF1-positive neurofibrillary tangle.

Tanycytes are specifically disorganized and degraded in AD

Strikingly, however, the morphology of tanycytes in AD patient brains was dramatically different from that in controls. Indeed, their vimentin cytoskeleton appeared fragmented, their processes seemed to be discontinuous and an accumulation of small vimentin-positive bodies could be observed (Figure 27A). To better understand the changes occurring in AD patient brains, we used the Ilastik segmentation toolkit to perform a machine-learning-aided analysis of vimentin immunolabeling³²⁹. After pixel classification, the detected objects were classified into two groups: “processes”, consisting of long, slim objects corresponding to tanycytic projections, and “fragments”, consisting of small rounded objects corresponding to putative tanycytic debris or truncated projections (Figure 27B). In agreement with this observation, the area covered by “processes” was lower in AD patients compared to controls, whereas the area covered by “fragments” was higher in AD patients than in controls (Figure 27C, D). Furthermore, in control subjects, 95% of the area covered by vimentin immunolabeling corresponded to tanycytic “processes”, whereas these represented only 57% of the vimentin signal in AD patients (n=5 for each group, $p < 0.001$, Figure 27E), highlighting a profound degradation of the structure of tanycytes in AD.

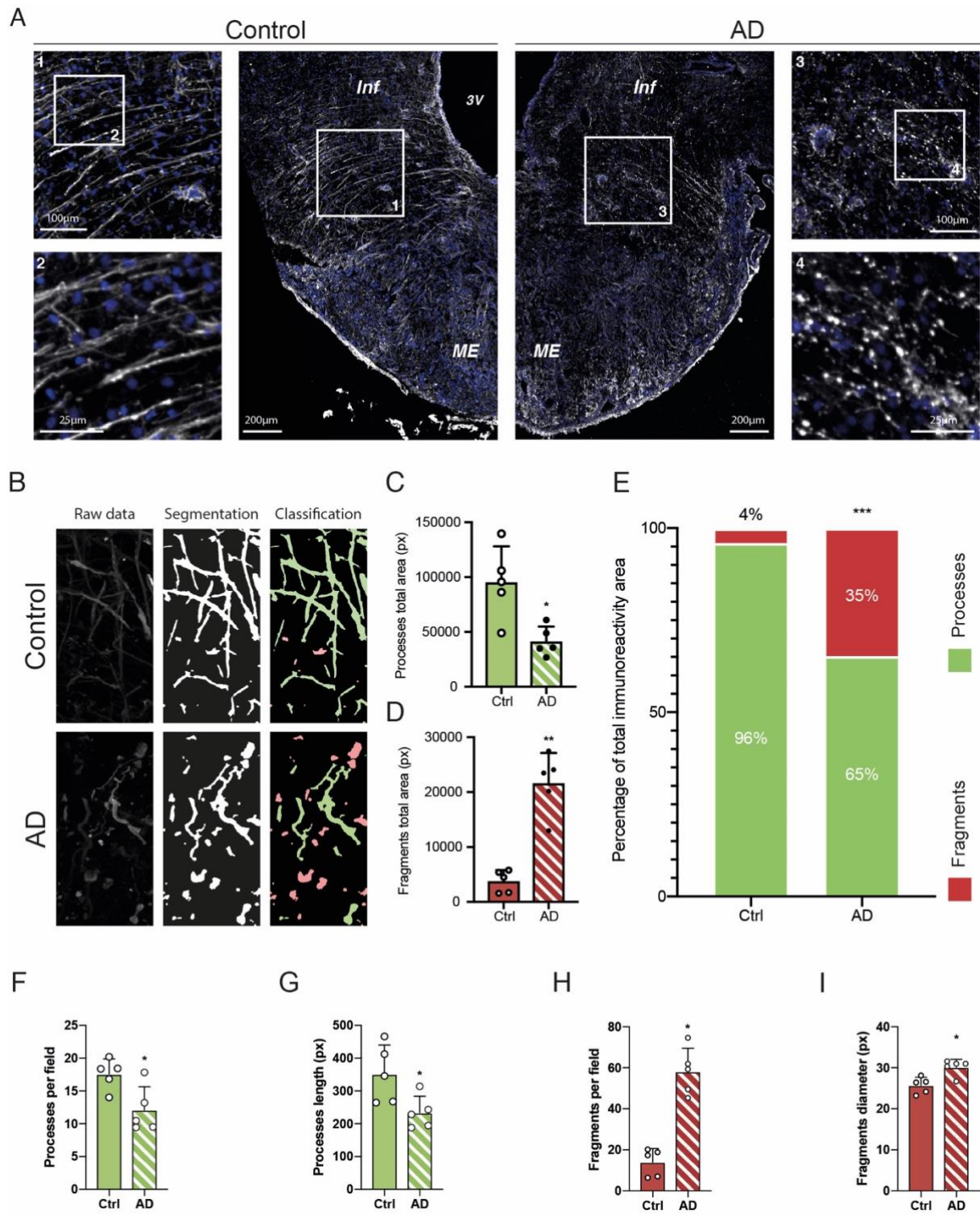


Figure 27: Tanyocytes in AD patients are degraded and disorganized

A. Photomicrographs of tanycytes in the median eminence and infundibulum of control (left panels) and AD patients (right panels) immunolabeled for vimentin (white). Insets: higher magnification images of tanycytic processes in control (left panels) and AD patients (right panels), showing fragmentation of vimentin-positive processes in the latter. **B.** Representation of the Ilastik analysis pipeline starting from raw data acquisition of vimentin immunolabeling (left panels) to segmentation of the vimentin signal (middle panels) to classification of tanycytic processes and fragments (green and red respectively, right panels). **C.** Graph representing the total area covered by processes in control (n=5) and AD patients (n=5). Two-tailed Mann-Whitney U test (U=1, p=0.02). Data are presented as means \pm S.D. *, p<0.05. **D.** Graph representing the total area covered by fragments in control (n=5) and AD patients (n=5). Two-tailed Mann-Whitney U test (U=0, p=0.008). Data are presented as means \pm S.D. **, p<0.01. **E.** Area covered by processes (green) vs. fragments (red) as a percentage of the total vimentin immunoreactive area in control (n=5) and AD patients (n=5). Two-way ANOVA (patient condition, F(1,16)=2.125.10-20, p>0.99; object class, F(1,16)=696.2, p<0.001; interaction, F(1,16)=173.1, p<0.001) followed by Sidak's multiple comparison post hoc test (Ctrl Processes vs. Ctrl Fragments, q(16)=27.96, p<0.001; AD Processes vs. AD Fragments, q(16)=9.355, p<0.001; Ctrl Fragments vs. AD Fragments, q(16)=9.302, p<0.001; Ctrl processes vs. AD processes, q(16)=9.302, p<0.001). Data are presented as means; ***, p<0.001. **F.** Graph of tanycytic processes per field in control (n=5) and AD patients (n=5). Two-tailed Mann-Whitney U test (U=1, p=0.0317). Data are presented as means \pm S.D. *, p<0.05. **G.** Graph of tanycytic process length in control (n=5) and AD patients (n=5). Two-tailed Mann-Whitney test (U=0, p=0.03). Data are presented as means \pm S.D. *, p<0.05. **H.** Graph of tanycytic fragments per field in control (n=5) and AD patients (n=5). Two-tailed Mann-Whitney U test (U=0, p=0.0079). Data are presented as means \pm S.D. *, p<0.05. **I.** Graph of tanycytic fragment diameter in control (n=5) and AD patients (n=5). Two-tailed Mann-Whitney U test (U=1, p=0.0159). Data are presented as means \pm S.D. *, p<0.05.

Intact tanycytic processes were much fewer in number and shorter in length in AD patient brains than in controls, and conversely, that fragmented or damaged tanycytic processes were more numerous and of larger diameter in AD patients supporting this view (Figure 27F-I). Next, to verify whether this degradation was limited to the vimentin cytoskeleton or whether the structural integrity of the entire cell was affected, we co-immunolabeled tissues for vimentin as well as GFAP, another cytoskeletal protein that interacts with vimentin in tanycytes to form the secondary cytoskeleton, or GPR50, a membrane receptor whose expression in the infundibulum is limited to tanycytes²⁷⁹. GFAP immunolabeling was seen in tanycytic structures in both control subjects and AD patients, most often colocalizing with vimentin, and reproduced the morphological alterations observed with the latter (Figure 28A). Similarly, GPR50, which was also expressed by tanycytes in both controls and AD patients, appeared to envelop vimentin-positive “fragments” rather than delineating intact processes in AD patients (Figure 28B). Interestingly, however, in some instances, fine vimentin-positive filaments could be seen linking the putative fragments of tanycytic process, giving rise to the appearance of a “string of pearls” (Figure 28C), indicating a condensation or aggregation of the tanycytic cytoskeleton or cytoplasmic contents to form bead-like structures rather than the disintegration of the cell or process as a whole. Strikingly, while tanycytic processes positive for both vimentin and GFAP presented a fragmented appearance, astrocytes expressing GFAP, but not vimentin, in the vicinity of these tanycytes did not display similar alterations in AD patients, suggesting that the degradation observed was specific to tanycytes (Figure 28D), and moreover, not an artifact caused by the plane of sectioning. As might be expected, this degradation of tanycytic processes also disrupted tanycyte-capillary interactions in AD patient brains, as seen using double immunolabeling for vimentin to identify tanycytic endfeet and caveolin 1 (Cav1) to label capillary walls (Figure 28E), implying functional consequences for blood-brain exchanges.

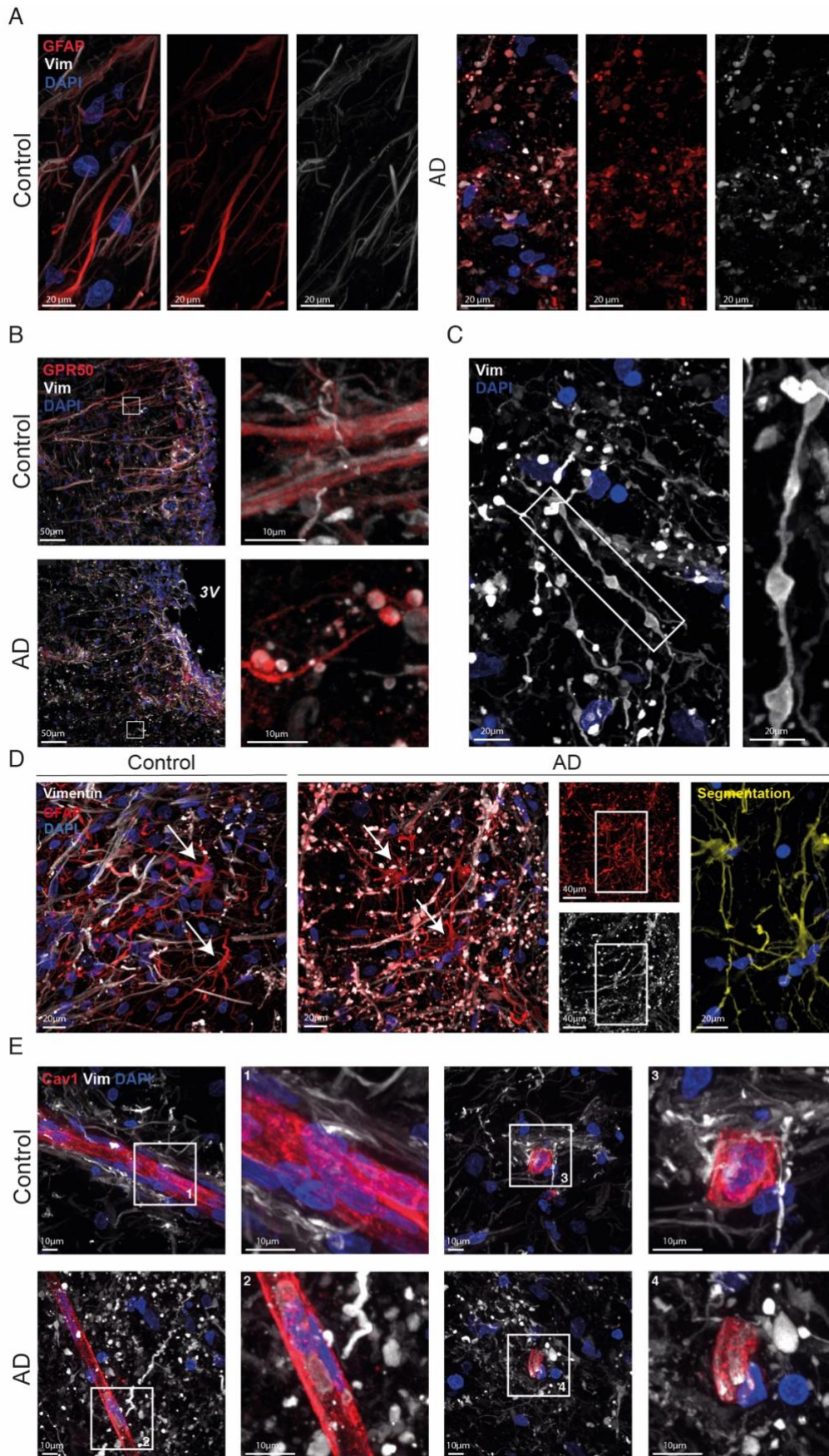


Figure 28: The cytoskeletal degradation is limited to tanyocytes and impairs their interaction with the vasculature.

A. Photomicrographs of tanycytes in the median eminence of control (top panels) and AD patients (bottom panels) immunolabeled for vimentin (white) and GPR50, a tanycytic membrane protein (red). Insets: high magnification photomicrographs of tanycytic processes in control (top panel) and AD patients (bottom panel) showing that the fragmentation in AD patients involves the entire tanycytic process and not just the vimentin cytoskeleton. **B.** Photomicrographs of tanycytes in the median eminence of an AD patient immunolabeled for vimentin (white). Inset: high magnification showing the “string of pearls” appearance of tanycytes in AD patients. **C.** Photomicrographs of tanycyte cytoskeleton immunolabeling (vimentin in white, GFAP in red) in control (left panels) and AD patients (right panels). **D.** Photomicrographs of the median eminence of control (left panel) and AD patients (right panels) immunolabeled for vimentin (white; tanycytes) and GFAP (red; tanycytes and astrocytes). The rightmost panel is a segmentation for astrocytes (GFAP not overlapping with vimentin in yellow, DAPI in blue). Arrows indicate astrocytic cell bodies. Inset: region subjected to segmentation at right. **E.** Photomicrograph of tanycyte-to-capillary contact in the infundibulum of control and AD patients immunolabeled for vimentin (white) to identify tanycytes and caveolin 1 (red) to identify capillaries. Capillaries parallel to the plane of the section are presented in the left panels and capillaries perpendicular to the plane of the section are presented in the right panels. Insets: higher magnification views of tanycyte-to-capillary contacts in control and AD patients.

Given the 3D distribution of Tau-transporting tanycytes in the mouse brain, we then wondered whether the degradation of tanycytes in the brain of AD patients was uniform or spatially differentiated. Interestingly, although an examination of vimentin immunolabeling in sagittal sections of the ME showed that these changes occurred all along the anteroposterior axis of the ME (Figure 29A), the putative fragmentation or beading of the tanycytic cytoskeleton in all patients was more pronounced in the infundibulum and the internal zone of the ME, close to the third ventricle, but was observed less frequently or not at all in the external part of the ME (Figure 29B). Finally, to determine whether this tanycytic degradation was specific to AD or could be more generalized, we compared vimentin immunolabeling in the brain of control subjects, AD patients and patients with frontotemporal dementia (FTD) of either the TDP-43 or Tau type. Intriguingly, regardless of FTD type, the tanycytic processes of FTD patients (n=4) were morphologically different from those in controls; however, except in one FTD patient brain that also revealed signs of AD post mortem (see Table 1), tanycytes did not display any beading (Figure 29C). Furthermore, Ilastik-based analysis of vimentin immunolabeling showed that FTD patients had a lower density of “processes” than control subjects, similar to AD

patients (Figure 29D). However, the reduced “process” area in FTD was not accompanied by an increase in the area covered by “fragments”, unlike in AD patients (Figure 29E). In addition, the proportion of “processes” to “fragments” was similar to that in controls, supporting a degradation of the tanyctic network without their disintegration (Figure 29F).

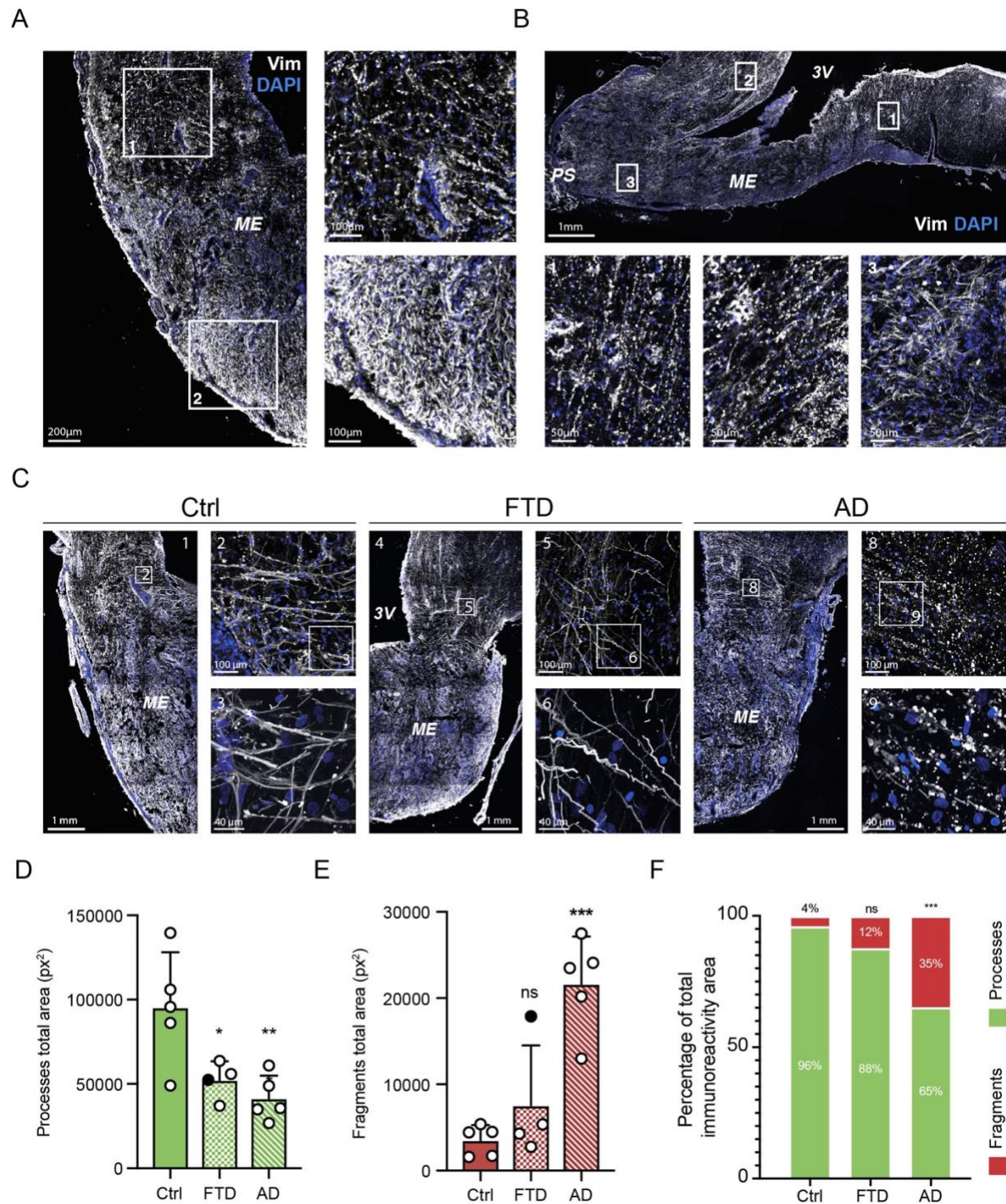


Figure 29: Tanyctic degradation occurs throughout the median eminence in AD but not in FTD

A. Photomicrographs of a median eminence in coronal section from an AD patient showing tanycytes immunolabeled for vimentin (white). Inset 1: higher magnification of the infundibular region. Inset 2: higher magnification of the external median eminence region. **B.** Photomicrograph of a median eminence in sagittal section from an AD patient showing tanycytes immunolabeled for vimentin (white). Inset 1: higher magnification of the posterior region of the median eminence. Inset 2: higher magnification of the median eminence adjoining the optic chiasma. Inset 3: higher magnification of the external median eminence close to the pituitary stalk. **C.** Photomicrographs of the median eminence and infundibulum of control (left panels), FTD (middle panels) and AD patients (right panels) showing tanycytes immunolabeled for vimentin (white). Numbered insets: localization of higher magnification photomicrographs showing the difference in tanycytic morphology between the three conditions. **D.** Total area covered by tanycytic processes in control (n=5), FTD (n=4) and AD patients (n=5). One-way ANOVA ($F(2,11)=8.136$, $p=0.0068$) followed by Tukey's multiple comparison post-hoc test (Ctrl vs. AD, $q(11)=5.433$, $p=0.0071$; Ctrl vs. FTD, $q(11)=4.096$, $p=0.0358$; AD vs. FTD, $q(11)=1.026$, $p=0.7538$). Data are presented as means \pm S.D. **, $p<0.01$; *, $p<0.05$. The FTD patient represented by a black dot also showed signs of AD in the brain post mortem. **E.** Total area covered by tanycytic fragments in control (n=5), FTD (n=4) and AD patients (n=5). One-way ANOVA ($F(2,11)=17.02$, $p=0.0004$) followed by Tukey's multiple comparison post-hoc test (Ctrl vs. AD, $q(11)=7.884$, $p=0.0004$; Ctrl vs. FTD, $q(11)=1.572$, $p=0.5269$; AD vs. FTD, $q(11)=5.861$, $p=0.0043$). Data are presented as means \pm S.D. ***, $p<0.001$; ns, non-significant. The FTD patient represented by a black dot also showed signs of AD in the brain post mortem. **F.** Area covered by tanycytic processes (green) and fragments (red) as a percentage of the total vimentin immunoreactive area in control (n=5), FTD (n=4) and AD patients (n=5). Two-way ANOVA (patient condition, $F(2,22)=3.280$, $p>0.99$; object class, $F(2,22)=687.2$, $p<0.001$; interaction, $F(2,22)=58.39$, $p<0.001$) followed by Sidak's multiple comparison post hoc test (for processes: Ctrl vs. FTD, $q(22)=1.791$, $p=0.2391$; Ctrl vs. AD, $q(22)=7.276$, $p<0.0001$; FTD vs. AD, $q(22)=5.069$, $p<0.001$; for fragments: Ctrl vs. FTD, $q(22)=1.791$, $p=0.2391$; Ctrl vs. AD, $q(22)=7.276$, $p<0.0001$; FTD vs. AD, $q(22)=5.069$, $p<0.001$). Data are presented as means; ***, $p<0.001$.

Together, these observations support the hypothesis that tanycytic pathology could be disease-specific, and the degradation of the tanycytic cytoskeleton in AD patients likely interferes with Tau efflux from the CSF, contributing to its accumulation in the brain.

Discussion

The accumulation and aggregation of both A β and Tau are hallmarks of AD and contribute to AD pathogenesis. A β clearance has been widely studied and involves both intra- and extracellular degradation, blood-brain barrier crossing, interstitial fluid clearance and cerebrospinal fluid (CSF) clearance^{339,340}. On the other hand, while Tau degradation is well documented (reviewed in³⁴¹), the mechanisms underlying its transport out of the brain and the exact paths that it follows to cross the BBB and reach the peripheral circulation are still poorly understood. Our findings above indicate that tanycytes are a significant contributor to Tau efflux from the CSF to the blood and that this clearance pathway might be impaired in the context of AD due to the morphological alteration of tanycytic processes, and presumably, the interruption of vesicular transport. Furthermore, our observations in FTD patient brains suggest that tanycytic degradation or dysfunction may be a more widespread feature of neurodegenerative disorders than currently imagined.

Tanycyte's contribution in tau clearance bigger picture

Several studies have used the injection of different Tau isoforms into the brain to highlight its ability to exit the parenchyma and/or cross the BBB^{239,240}, and have proposed the involvement of various brain structures such as the choroid plexus, arachnoid villi and a brain lymphatic system in this process^{233,342}. In our model of Tau ICV injection, the choroid plexus did not show any signs of Tau uptake. Additionally, while the contribution of the lymphatic system and arachnoid villi could not be assessed due to the destruction of the meninges during brain dissection, another study has revealed only a moderate effect of the disruption of the

brain lymphatic system on brain-to-blood Tau transfer ²⁴⁸. On the other hand, in our study, specifically disrupting vesicular transport in a significant proportion of tanyocytes, but not all of them, resulted in an incomplete but robust inhibition of Tau efflux to the periphery that lymphatic transport could not adequately compensate for. While the contribution of other players and processes such as BBB degradation and leakage cannot be ruled out, our experimental paradigm still reveals a major role for tanyocytes in Tau efflux.

Tanyocytes, a two-way conduit between CSF and blood

The directionality of tanyocyte's transport of Tau, from the CSF to the blood circulation, is itself striking, since these cells have until now been associated with the transcytotic shuttling of physiological blood-borne molecules into the CSF. In effect, this two-way secretory activity of tanyocytes – allowing meaningful metabolic hormones and signals to be captured from the circulation and released into the brain, while performing the reverse function for a molecule that needs to be eliminated, such as Tau, without themselves producing either of the two types of molecules released – corresponds to neither conventional secretion nor excretion. Exploring the molecules and mechanisms involved in this phenomenon and its involvement in normal physiology and pathological processes could represent a new avenue of research in the interaction of the brain and the periphery.

The chicken or the egg, is tanycytic alteration a cause or a consequence of Tau pathology?

While Tau accumulation in the brain in the context of AD has been observed in numerous studies, from mouse models to AD patients, studies describing circulating Tau levels in mice are rare ^{155,240,343,344}. The existence of an AD patient database that includes Tau

concentrations in the CSF and blood allowed us to indirectly evaluate Tau efflux by calculating the relative concentrations of Tau in the destination tissue, i.e., blood or plasma, vs. the compartment of origin, i.e., the CSF, as is often done in the reverse direction for other molecules. Although this value represents the balance of all influx/efflux mechanisms and is not specific to any single transport system, it is the only readout of Tau transport available in live patients. Interestingly, CSF concentrations of Tau in the AD group were already high at younger ages, whereas they gradually increased with age in control patients, catching up with the AD group. The resulting increase in Tau plasma-to-CSF ratio in younger AD patients sets this process apart from the physiological aging seen in control subjects. Age-related changes, including cell loss and impaired signaling cascades, have previously been observed in the tanycytes of both women and male rats^{319,322}. Although not previously noticed, our observation of tanycytic degradation across AD patients at different ages and stages of disease (our post mortem brains were obtained from patients ranging from 52-88 years old, but at Braak stages III-IV; Table 2), suggests that these changes could accompany or even contribute to increased Tau accumulation in the brain by disrupting its transport, rather than being secondary to Tau accumulation. On the other hand, in older AD patients, a compensatory efflux mechanism such as BBB leakage could explain why Tau does not continue to accumulate in the CSF, and why plasma Tau concentrations are also significantly higher than in age-matched controls.

Mechanisms of tanycytes degradation

The progressive “beading” of distal processes, a phenomenon known as clasmatodendrosis, has long been described to occur in astrocytes under a variety of pathological conditions³⁴⁵⁻³⁴⁷. In addition, amyloid plaques in animal models appear to trigger the phenomenon in surrounding astrocytes^{348,349}, and age-related astrocytic clasmatodendrosis is associated with an accumulation of A β in the hippocampus³⁵⁰. However, astrocytes in our patient brain sections displayed a perfectly normal morphology. In addition, there are few reports of the process in human AD brains, and tanycytic clasmatodendrosis, or

for that matter, any other morphological alteration in tanycytes, has not so far been described either in AD or in any other human disorder, and its causes, mechanisms and consequences deserve to be further explored. To do so, significant effort will have to be deployed in finding biological systems which would reproduce the tanycytic degradation observed in AD patients, starting with systematic observation of tanycytes in AD mice models.

Tanycytic alterations may be a cause of the metabolic and hormonal increased risks for AD onset

Regardless of the lack of prior evidence of tanycytic structural abnormalities, several disorders have been shown to be associated with their dysfunction. Notably, preclinical studies have revealed that impaired tanycytic function could underlie metabolic diseases such as type 2 diabetes and obesity, by interfering with the access of peripheral signals to hypothalamic circuits regulating metabolism and energy homeostasis ^{290–292,351}. Intriguingly, these conditions are also associated with an increased risk of developing AD, suggesting that tanycytes could be the long-sought missing link that is thought to exist between metabolic disorders and AD ^{264,352}. This link could partly reside in the recent description of the role of tanycytic insulin signaling. Insulin and insulin-like growth factor 1 have long been of particular interest in the field of AD. The hypothesis of AD being a type 3 diabetes is articulated around the development of a central insulin resistance and impaired brain glucose metabolism in AD patients ³⁵³. Since insulin signaling has been shown to be implicated in learning and memory, the central insulin resistance observed in AD is thought to participate in the progressive cognitive decline exhibited by the patients and to favor A β and tau pathology ^{354,355}. Yet, the role of insulin signaling in neurodegenerative processes is somewhat paradoxical as the genetic deletion of insulin signaling proteins have been shown to be protective in AD animal models ^{356–359}. Different origins to the central insulin resistance in AD have been proposed: the expression of several elements of the insulin signaling pathway are down-

regulated in the brain of AD patients, A β disrupt insulin receptor signal transduction and a controversial decrease of CSF insulin concentrations in AD patients ^{360–362}. Interestingly, this study describes more than a CSF insulin decrease as they also reported a decrease in CSF/plasma insulin ratio suggesting an impairment in insulin access to the brain ³⁶⁰. Tanycytes being recently described as a gateway for insulin to the brain, our observation of a disruption of the tanycytic processes is a plausible cause to this phenomenon and also participate in the deregulation of brain glucose metabolism. Moreover, as leptin transport is altered in mouse model of obesity, tau transport by tanycyte might also be disturbed and promote its accumulation in the brain.

The clinical manifestations of AD extend beyond cognitive and metabolic deficits, and include several features that could be attributed to neuroendocrine dysfunctions ³⁶³. In this context, ME tanycytic endfeet also interact with the terminals of neuroendocrine neurons to regulate the secretion of neurohormones of the hypothalamic-pituitary axes ²⁶⁴, suggesting that tanycytic pathology could also lie at the root of hormonal disturbances in AD, which themselves could also contribute to age- or disease-related cognitive and metabolic deficits ³⁶³.

Peripheral tau: a mere symbol of clearance or a real contributor to AD

The presence of tau in the plasma is thought to result from brain clearance and to have no pathological implications. However, few studies would suggest that plasma tau might have potential roles in AD. First, the intraperitoneal injection of tau seeds in an AD mouse model has been shown to promote the appearance of neuronal tau inclusions way earlier than in non-injected mice ³⁶⁴. Thus, it suggested that the tau seeds are able to reach the brain from the periphery. Second, tau aggregation is found in the pancreas of AD patients but also in patients with type 2 diabetes suggesting a link between tau aggregation and pancreatic dysfunction. Considering these data, tau in the plasma could have seeding properties and propagate either

from the periphery to the brain or from the brain to the periphery. This hypothesis is interesting as it echoes the recent hypothesis of a peripheral origin of Parkinson's Disease and the discovery of the potential transmission of A β pathology and Creutzfeldt-Jakob Disease after the administration of cadaveric growth hormone preparation contaminated with A β and tau³⁶⁵⁻³⁶⁷. But for now, data supporting the view of a peripheral tau seeding capacity are scarce. Plasma tau seeding potential has never been evaluated but the recent development of tau seeding biosensors could very well have the answer to this question^{368,369}. If tau in the plasma would be proven to have seeding properties, the pathway taken by tau seeds to enter the brain would be of particular interest. As we already demonstrated that tau can be transported by tanycytes from CSF to blood, it would be highly possible that they could transport tau seeds in the other direction.

New opportunities for tanycyte's role in AD

Setting the ground for follow-up studies, this work has established a clear role of tanycyte in tau clearance and their degradation in the course of AD. However, it raises numerous questions: (1) are all species of tau cleared by tanycytes, (2) what is the trigger and the mechanism of such degradation, (3) what is the pathological significance of tanycytic degradation.

While the use of the full-length tau isoform avoids any bias due to the lack of potentially interacting domains, it might not be the most relevant isoform in the context of AD. Full-length tau isn't the preponderant tau isoform in the brain or in the CSF or AD patients^{370,371}. Also, the truncation, phosphorylation or oligomerization of tau could impact its clearance by tanycytes. Supporting the view that all tau isoforms aren't equal in CSF to blood transfer, a study showed that a central fragment of tau, starting at the amino-acid 121 and ending at amino-acid 227 containing neither the microtubule-binding domains or N-terminal repeats, was slower to reach the blood circulation after its intracerebroventricular injection³⁷². Interestingly, a study of CSF tau by mass-spectrometry have shown that central fragments of Tau are enriched in the CSF

suggesting that they are either more secreted or less cleared³⁷⁰. The development of other fluorescently-labeled isoform and species of tau would allow to decipher the impact of the different tau domains and PTMs in its clearance from the brain to the periphery.

This study being the first description of a tancytic degradation in human diseases it raises substantial questions as what exactly occurs in tancytes and how. Post-mortem tissues are suitable for descriptive studies but do not enable the discrimination of mechanism leading the observed phenotype. However, several observations help us speculate the course of tancytic degradation and potential factors triggering such phenomenon. Tancytes are undergoing a cytoskeletal disruption which appears to be gradual. Indeed, we observed tancytes with vimentin-positive beadings along their processes and circular vimentin-positive aggregates in the infundibulum parenchyma which may be remnants of the beads after the fragmentation of the processes. Vimentin aggregation would then precede tancyte fragmentation. Vimentin aggregation has never been documented in tancytes but there are studies on giant axonal neuropathy (GAN) describing an intriguingly resembling event. perinuclear circular vimentin aggregation occurs in fibroblast derived from GAN patients involve the loss of function of the gigaxonin protein which targets vimentin filaments to the proteasome by ubiquitination³⁷³⁻³⁷⁶. Gigaxonin being a ubiquitously low expressed protein, it might represent a good candidate to explain vimentin aggregation in tancyte. The study of gigaxonin tancyte specific knock out mouse models would allow to determine its implication and the consequences of vimentin aggregates on tancytes. Indeed, vimentin aggregation could be detrimental for tancyte's functioning since several reports have highlighted the role of vimentin in several cellular function such as proteostasis or signaling pathways, among which ERK pathway³⁷⁷⁻³⁷⁹. Thus, its aggregation would possibly trigger a disruption in those functions.

Even if the observation of tancyte's processes degradation in AD strongly suggest an impaired tancytic tau shuttle and a possible promotion of tau accumulation and aggregation, we do not provide any direct proof of this statement. But, by taking advantage of the iBot mouse model, the creation of an AD mice model lacking tancytic tau transport is possible and would

directly address this issue. The evaluation of tau clearance in AD mouse models could also be considered in order to determine if tancyte-mediated clearance is impaired in those models. Lastly, in case of a successful mimicking of a tancytic vimentin aggregation in mouse models, the generation of a mouse line recapitulating both tau pathology and tancytic degradation would represent an elegant model for the study of tancytic degradation influence on AD.

Tancytes in other neurodegenerative diseases

Finally, the fact that tancytes are able to transport Tau and their very different alteration in FTD raises broader questions as to their role in the development of neurodegenerative diseases. The fact that they did not transport fluorescent BSA, which has a similar molecular weight, together with the observation of endogenous Tau in tancytic vesicles in human AD brains, is significant, as it suggests that there might be some selectivity in terms of their cargo, but could they also transport other pathological molecules such as A β or alpha-synuclein? How does the fact that they are morphologically different in FTD as compared to both controls and AD patients, as well as sparser or thinner in the former, affect their diverse functions?

Conclusion

In the present work, we tackled the question of a tau clearance by tanycyte both *in vitro* and *in vivo* as well its pertinence in post-mortem brain tissues of Alzheimer's disease patient. Collectively, our data support a significant role of tanycyte in the efflux of tau from the cerebrospinal fluid to the blood. This particular tau transfer was already described in the literature but was lacking a mechanistic explanation. By injecting fluorescently-labeled tau protein in wild-type mice and in a mouse model of impaired tanycytic transport we demonstrated the physiological contribution of tanycyte in this process. Furthermore, the presence of tau-positive puncta in tanycytes of Alzheimer's disease patients supported the possibility of tanycytic tau transport in humans. This transport is presumably impaired in the course of AD since a striking degradation of tanycyte's processes, along which molecules shuttles from the cerebrospinal fluid to the blood, was specifically observed in Alzheimer's disease patient's brains. These observations represent the first description of an alteration of tanycyte in a human disease and raise the question of their involvement in the development of neurodegenerative diseases.

Bibliography

1. den Dunnen, W. F. A., Brouwer, W. H., Bijlard, E., Kamphuis, J., van Linschoten, K., Eggens-Meijer, E. & Holstege, G. No disease in the brain of a 115-year-old woman. *Neurobiol Aging* **29**, 1127–1132 (2008).
2. World Alzheimer Report 2015, The Global Impact of Dementia: An analysis of prevalence, incidence, cost and trends. 87.
3. Bekris, L. M., Yu, C.-E., Bird, T. D. & Tsuang, D. W. Genetics of Alzheimer Disease. *J Geriatr Psychiatry Neurol* **23**, 213–227 (2010).
4. Gatz, M., Reynolds, C. A., Fratiglioni, L., Johansson, B., Mortimer, J. A., Berg, S., Fiske, A. & Pedersen, N. L. Role of genes and environments for explaining Alzheimer disease. *Arch Gen Psychiatry* **63**, 168–174 (2006).
5. Farrer, L. A., Cupples, L. A., Haines, J. L., Hyman, B., Kukull, W. A., Mayeux, R., Myers, R. H., Pericak-Vance, M. A., Risch, N. & van Duijn, C. M. Effects of age, sex, and ethnicity on the association between apolipoprotein E genotype and Alzheimer disease. A meta-analysis. APOE and Alzheimer Disease Meta Analysis Consortium. *JAMA* **278**, 1349–1356 (1997).
6. Verghese, P. B., Castellano, J. M., Garai, K., Wang, Y., Jiang, H., Shah, A., Bu, G., Frieden, C. & Holtzman, D. M. ApoE influences amyloid- β (A β) clearance despite minimal apoE/A β association in physiological conditions. *Proceedings of the National Academy of Sciences* **110**, E1807–E1816 (2013).
7. Di Maria, E., Cammarata, S., Parodi, M. I., Borghi, R., Benussi, L., Galli, M., Galimberti, D., Ghidoni, R., Gonella, D., Novello, C., Pollero, V., Perroni, L., Odetti, P., Scarpini, E., Binetti, G. & Tabaton, M. The H1 haplotype of the tau gene (MAPT) is associated with mild cognitive impairment. *J Alzheimers Dis* **19**, 909–914 (2010).
8. Allen, M., Kachadoorian, M., Quicksall, Z., Zou, F., Chai, H. S., Younkin, C., Crook, J. E., Pankratz, V. S., Carrasquillo, M. M., Krishnan, S., Nguyen, T., Ma, L., Malphrus, K., Lincoln, S., Bisceglia, G., Kolbert, C. P., Jen, J., Mukherjee, S., Kauwe, J. K., Crane, P. K., Haines, J. L., Mayeux, R., Pericak-Vance, M. A., Farrer, L. A., Schellenberg, G. D., Parisi, J. E., Petersen, R. C., Graff-Radford, N. R., Dickson, D. W., Younkin, S. G., Ertekin-Taner, N., & Alzheimer's Disease Genetics Consortium (ADGC). Association of MAPT haplotypes with Alzheimer's disease risk and MAPT brain gene expression levels. *Alzheimer's Research & Therapy* **6**, 39 (2014).
9. Sánchez-Juan, P., Moreno, S., de Rojas, I., Hernández, I., Valero, S., Alegret, M., Montreal, L., García González, P., Lage, C., López-García, S., Rodríguez-Rodríguez, E., Orellana, A., Tárraga, L., Boada, M. & Ruiz, A. The MAPT H1 Haplotype Is a Risk Factor for Alzheimer's Disease in APOE ϵ 4 Non-carriers. *Front Aging Neurosci* **11**, 327 (2019).
10. Grupe, A., Abraham, R., Li, Y., Rowland, C., Hollingworth, P., Morgan, A., Jehu, L., Segurado,

R., Stone, D., Schadt, E., Karnoub, M., Nowotny, P., Tacey, K., Catanese, J., Sninsky, J., Brayne, C., Rubinsztein, D., Gill, M., Lawlor, B., Lovestone, S., Holmans, P., O'Donovan, M., Morris, J. C., Thal, L., Goate, A., Owen, M. J. & Williams, J. Evidence for novel susceptibility genes for late-onset Alzheimer's disease from a genome-wide association study of putative functional variants. *Hum Mol Genet* **16**, 865–873 (2007).

11. Bertram, L. & Tanzi, R. E. Genome-wide association studies in Alzheimer's disease. *Hum Mol Genet* **18**, R137–R145 (2009).

12. Lambert, J.-C., Heath, S., Even, G., Campion, D., Sleegers, K., Hiltunen, M., Combarros, O., Zelenika, D., Bullido, M. J., Tavernier, B., Letenneur, L., Bettens, K., Berr, C., Pasquier, F., Fiévet, N., Barberger-Gateau, P., Engelborghs, S., De Deyn, P., Mateo, I., Franck, A., Helisalmi, S., Porcellini, E., Hanon, O., European Alzheimer's Disease Initiative Investigators, de Pancorbo, M. M., Lendon, C., Dufouil, C., Jaillard, C., Leveillard, T., Alvarez, V., Bosco, P., Mancuso, M., Panza, F., Nacmias, B., Bossù, P., Piccardi, P., Annoni, G., Seripa, D., Galimberti, D., Hannequin, D., Licastro, F., Soininen, H., Ritchie, K., Blanché, H., Dartigues, J.-F., Tzourio, C., Gut, I., Van Broeckhoven, C., Alperovitch, A., Lathrop, M. & Amouyel, P. Genome-wide association study identifies variants at CLU and CR1 associated with Alzheimer's disease. *Nat Genet* **41**, 1094–1099 (2009).

13. Wightman, D. P., Jansen, I. E., Savage, J. E., Shadrin, A. A., Bahrami, S., Holland, D., Rongve, A., Børte, S., Winsvold, B. S., Drange, O. K., Martinsen, A. E., Skogholt, A. H., Willer, C., Bråthen, G., Bosnes, I., Nielsen, J. B., Fritsche, L. G., Thomas, L. F., Pedersen, L. M., Gabrielsen, M. E., Johnsen, M. B., Meisingset, T. W., Zhou, W., Proitsi, P., Hodges, A., Dobson, R., Velayudhan, L., Heilbron, K., Auton, A., Sealock, J. M., Davis, L. K., Pedersen, N. L., Reynolds, C. A., Karlsson, I. K., Magnusson, S., Stefansson, H., Thordardottir, S., Jonsson, P. V., Snaedal, J., Zettergren, A., Skoog, I., Kern, S., Waern, M., Zetterberg, H., Blennow, K., Stordal, E., Hveem, K., Zwart, J.-A., Athanasiu, L., Selnes, P., Saltvedt, I., Sando, S. B., Ulstein, I., Djurovic, S., Fladby, T., Aarsland, D., Selbæk, G., Ripke, S., Stefansson, K., Andreassen, O. A. & Posthuma, D. A genome-wide association study with 1,126,563 individuals identifies new risk loci for Alzheimer's disease. *Nat Genet* **53**, 1276–1282 (2021).

14. Bellenguez, C., Küçükali, F., Jansen, I. E., Kleineidam, L., Moreno-Grau, S., Amin, N., Naj, A. C., Campos-Martin, R., Grenier-Boley, B., Andrade, V., Holmans, P. A., Boland, A., Damotte, V., van der Lee, S. J., Costa, M. R., Kuulasmaa, T., Yang, Q., de Rojas, I., Bis, J. C., Yaqub, A., Prokic, I., Chapuis, J., Ahmad, S., Giedraitis, V., Aarsland, D., Garcia-Gonzalez, P., Abdelnour, C., Alarcón-Martín, E., Alcolea, D., Alegret, M., Alvarez, I., Álvarez, V., Armstrong, N. J., Tsolaki, A., Antúnez, C., Appollonio, I., Arcaro, M., Archetti, S., Pastor, A. A., Arosio, B., Athanasiu, L., Bailly, H., Banaj, N., Baquero, M., Barral, S., Beiser, A., Pastor, A. B., Below, J. E., Benček, P., Benussi, L., Berr, C., Besse, C., Bessi, V., Binetti, G., Bizarro, A., Blesa, R., Boada, M., Boerwinkle, E., Borroni, B., Boschi, S., Bossù, P., Bråthen, G., Bressler, J., Bresner, C., Brodaty, H., Brookes, K. J., Brusco, L. I., Buiza-Rueda, D., Bürger, K., Burholt, V., Bush, W. S., Calero, M., Cantwell, L. B., Chene, G., Chung, J., Cuccaro, M. L., Carracedo, Á., Cecchetti, R., Cervera-Carles, L., Charbonnier, C., Chen, H.-H.,

Chillotti, C., Ciccone, S., Claassen, J. A. H. R., Clark, C., Conti, E., Corma-Gómez, A., Costantini, E., Custodero, C., Daian, D., Dalmasso, M. C., Daniele, A., Dardiotis, E., Dartigues, J.-F., de Deyn, P. P., de Paiva Lopes, K., de Witte, L. D., Debette, S., Deckert, J., del Ser, T., Denning, N., DeStefano, A., Dichgans, M., Diehl-Schmid, J., Diez-Fairen, M., Rossi, P. D., Djurovic, S., Duron, E., Düzel, E., Dufouil, C., Eiriksdottir, G., Engelborghs, S., Escott-Price, V., Espinosa, A., Ewers, M., Faber, K. M., Fabrizio, T., Nielsen, S. F., Fardo, D. W., Farotti, L., Fenoglio, C., Fernández-Fuertes, M., Ferrari, R., Ferreira, C. B., Ferri, E., Fin, B., Fischer, P., Fladby, T., Fließbach, K., Fongang, B., Fornage, M., Fortea, J., Foroud, T. M., Fostinelli, S., Fox, N. C., Franco-Macías, E., Bullido, M. J., Frank-García, A., Froelich, L., Fulton-Howard, B., Galimberti, D., García-Alberca, J. M., García-González, P., Garcia-Madrona, S., Garcia-Ribas, G., Ghidoni, R., Giegling, I., Giorgio, G., Goate, A. M., Goldhardt, O., Gomez-Fonseca, D., González-Pérez, A., Graff, C., Grande, G., Green, E., Grimmer, T., Grünblatt, E., Grunin, M., Gudnason, V., Guetta-Baranes, T., Haapasalo, A., Hadjigeorgiou, G., Haines, J. L., Hamilton-Nelson, K. L., Hampel, H., Hanon, O., Hardy, J., Hartmann, A. M., Hausner, L., Harwood, J., Heilmann-Heimbach, S., Helisalmi, S., Heneka, M. T., Hernández, I., Herrmann, M. J., Hoffmann, P., Holmes, C., Holstege, H., Vilas, R. H., Hulsman, M., Humphrey, J., Biessels, G. J., Jian, X., Johansson, C., Jun, G. R., Kastumata, Y., Kauwe, J., Kehoe, P. G., Kilander, L., Ståhlbom, A. K., Kivipelto, M., Koivisto, A., Kornhuber, J., Kosmidis, M. H., Kukull, W. A., Kuksa, P. P., Kunkle, B. W., Kuzma, A. B., Lage, C., Laukka, E. J., Launer, L., Lauria, A., Lee, C.-Y., Lehtisalo, J., Lerch, O., Lleó, A., Longstreth, W., Lopez, O., de Munain, A. L., Love, S., Löwemark, M., Luckcuck, L., Lunetta, K. L., Ma, Y., Macías, J., MacLeod, C. A., Maier, W., Mangialasche, F., Spallazzi, M., Marquié, M., Marshall, R., Martin, E. R., Montes, A. M., Rodríguez, C. M., Masullo, C., Mayeux, R., Mead, S., Mecocci, P., Medina, M., Meggy, A., Mehrabian, S., Mendoza, S., Menéndez-González, M., Mir, P., Moebus, S., Mol, M., Molina-Porcel, L., Montreal, L., Morelli, L., Moreno, F., Morgan, K., Mosley, T., Nöthen, M. M., Muchnik, C., Mukherjee, S., Nacmias, B., Ngandu, T., Nicolas, G., Nordestgaard, B. G., Olaso, R., Orellana, A., Orsini, M., Ortega, G., Padovani, A., Paolo, C., Papenberg, G., Parnetti, L., Pasquier, F., Pastor, P., Peloso, G., Pérez-Cordón, A., Pérez-Tur, J., Pericard, P., Peters, O., Pijnenburg, Y. A. L., Pineda, J. A., Piñol-Ripoll, G., Pisanu, C., Polak, T., Popp, J., Posthuma, D., Priller, J., Puerta, R., Quenez, O., Quintela, I., Thomassen, J. Q., Rábano, A., Rainero, I., Rajabli, F., Ramakers, I., Real, L. M., Reinders, M. J. T., Reitz, C., Reyes-Dumeyer, D., Ridge, P., Riedel-Heller, S., Riederer, P., Roberto, N., Rodriguez-Rodriguez, E., Rongve, A., Allende, I. R., Rosende-Roca, M., Royo, J. L., Rubino, E., Rujescu, D., Sáez, M. E., Sakka, P., Saltvedt, I., Sanabria, Á., Sánchez-Arjona, M. B., Sanchez-Garcia, F., Juan, P. S., Sánchez-Valle, R., Sando, S. B., Sarnowski, C., Satizabal, C. L., Scamosci, M., Scarmeas, N., Scarpini, E., Scheltens, P., Scherbaum, N., Scherer, M., Schmid, M., Schneider, A., Schott, J. M., Selbæk, G., Seripa, D., Serrano, M., Sha, J., Shadrin, A. A., Skrobot, O., Slifer, S., Snijders, G. J. L., Soininen, H., Solfrizzi, V., Solomon, A., Song, Y., Sorbi, S., Sotolongo-Grau, O., Spalletta, G., Spotke, A., Squassina, A., Stordal, E., Tartan, J. P., Tárraga, L., Tesí, N., Thalamuthu, A., Thomas, T., Tosto, G., Traykov, L., Tremolizzo, L., Tybjærg-Hansen, A., Uitterlinden, A., Ullgren, A., Ulstein, I., Valero,

- S., Valladares, O., Broeckhoven, C. V., Vance, J., Vardarajan, B. N., van der Lugt, A., Dongen, J. V., van Rooij, J., van Swieten, J., Vandenberghe, R., Verhey, F., Vidal, J.-S., Vogelgsang, J., Vyhnaek, M., Wagner, M., Wallon, D., Wang, L.-S., Wang, R., Weinhold, L., Wiltfang, J., Windle, G., Woods, B., Yannakouli, M., Zare, H., Zhao, Y., Zhang, X., Zhu, C., Zulaica, M., Farrer, L. A., Psaty, B. M., Ghanbari, M., Raj, T., Sachdev, P., Mather, K., Jessen, F., Ikram, M. A., de Mendonça, A., Hort, J., Tsolaki, M., Pericak-Vance, M. A., Amouyel, P., Williams, J., Frikke-Schmidt, R., Clarimon, J., Deleuze, J.-F., Rossi, G., Seshadri, S., Andreassen, O. A., Ingelsson, M., Hiltunen, M., Sleegers, K., Schellenberg, G. D., van Duijn, C. M., Sims, R., van der Flier, W. M., Ruiz, A., Ramirez, A. & Lambert, J.-C. New insights into the genetic etiology of Alzheimer's disease and related dementias. *Nat Genet* **54**, 412–436 (2022).
15. Livingston, G., Huntley, J., Sommerlad, A., Ames, D., Ballard, C., Banerjee, S., Brayne, C., Burns, A., Cohen-Mansfield, J., Cooper, C., Costafreda, S. G., Dias, A., Fox, N., Gitlin, L. N., Howard, R., Kales, H. C., Kivimäki, M., Larson, E. B., Ogunniyi, A., Orgeta, V., Ritchie, K., Rockwood, K., Sampson, E. L., Samus, Q., Schneider, L. S., Selbæk, G., Teri, L. & Mukadam, N. Dementia prevention, intervention, and care: 2020 report of the Lancet Commission. *Lancet* **396**, 413–446 (2020).
16. Johnson, D. K., Wilkins, C. H. & Morris, J. C. Accelerated Weight Loss May Precede Diagnosis in Alzheimer Disease. *Arch Neurol* **63**, 1312 (2006).
17. Vermunt, L., Sikkes, S. A. M., van den Hout, A., Handels, R., Bos, I., van der Flier, W. M., Kern, S., Ousset, P.-J., Maruff, P., Skoog, I., Verhey, F. R. J., Freund-Levi, Y., Tsolaki, M., Wallin, Å. K., Olde Rikkert, M., Soininen, H., Spuru, L., Zetterberg, H., Blennow, K., Scheltens, P., Muniz-Terrera, G., Visser, P. J., Alzheimer Disease Neuroimaging Initiative, AIBL Research Group, & ICTUS/DSA study groups. Duration of preclinical, prodromal, and dementia stages of Alzheimer's disease in relation to age, sex, and APOE genotype. *Alzheimers Dement* **15**, 888–898 (2019).
18. Prinz, P. N., Vitaliano, P. P., Vitiello, M. V., Bokan, J., Raskind, M., Peskind, E. & Gerber, C. Sleep, EEG and mental function changes in senile dementia of the Alzheimer's type. *Neurobiol Aging* **3**, 361–370 (1982).
19. Ju, Y.-E. S., McLeland, J. S., Toedebusch, C. D., Xiong, C., Fagan, A. M., Duntley, S. P., Morris, J. C. & Holtzman, D. M. Sleep quality and preclinical Alzheimer Disease. *JAMA Neurol* **70**, 587–593 (2013).
20. Spinedi, E. & Cardinali, D. P. Neuroendocrine-Metabolic Dysfunction and Sleep Disturbances in Neurodegenerative Disorders: Focus on Alzheimer's Disease and Melatonin. *NEN* **108**, 354–364 (2019).
21. Csernansky, J. G., Dong, H., Fagan, A. M., Wang, L., Xiong, C., Holtzman, D. M. & Morris, J. C. Plasma Cortisol and Progression of Dementia in DAT Subjects. *Am J Psychiatry* **163**, 2164–2169 (2006).
22. Prinz, P. N., Vitaliano, P. P., Vitiello, M. V., Bokan, J., Raskind, M., Peskind, E. & Gerber, C. Sleep, EEG and mental function changes in senile dementia of the Alzheimer's type. *Neurobiol Aging*

3, 361–370 (1982).

23. White, H., Pieper, C., Schmader, K. & Fillenbaum, G. Weight change in Alzheimer's disease. *J Am Geriatr Soc* **44**, 265–272 (1996).
24. Glenner, G. G. & Wong, C. W. Alzheimer's disease: Initial report of the purification and characterization of a novel cerebrovascular amyloid protein. *Biochemical and Biophysical Research Communications* **120**, 885–890 (1984).
25. Masters, C. L., Simms, G., Weinman, N. A., Multhaup, G., McDonald, B. L. & Beyreuther, K. Amyloid plaque core protein in Alzheimer disease and Down syndrome. *Proc Natl Acad Sci U S A* **82**, 4245–4249 (1985).
26. Grundke-Iqbal, I., Iqbal, K., Tung, Y. C., Quinlan, M., Wisniewski, H. M. & Binder, L. I. Abnormal phosphorylation of the microtubule-associated protein tau (tau) in Alzheimer cytoskeletal pathology. *Proceedings of the National Academy of Sciences* **83**, 4913–4917 (1986).
27. Kosik, K. S., Joachim, C. L. & Selkoe, D. J. Microtubule-associated protein tau (tau) is a major antigenic component of paired helical filaments in Alzheimer disease. *Proceedings of the National Academy of Sciences* **83**, 4044–4048 (1986).
28. Wood, J. G., Mirra, S. S., Pollock, N. J. & Binder, L. I. Neurofibrillary tangles of Alzheimer disease share antigenic determinants with the axonal microtubule-associated protein tau (tau). *Proc Natl Acad Sci U S A* **83**, 4040–4043 (1986).
29. Sinha, S., Anderson, J. P., Barbour, R., Basi, G. S., Caccavello, R., Davis, D., Doan, M., Dovey, H. F., Frigon, N., Hong, J., Jacobson-Croak, K., Jewett, N., Keim, P., Knops, J., Lieberburg, I., Power, M., Tan, H., Tatsuno, G., Tung, J., Schenk, D., Seubert, P., Suomensari, S. M., Wang, S., Walker, D., Zhao, J., McConlogue, L. & John, V. Purification and cloning of amyloid precursor protein beta-secretase from human brain. *Nature* **402**, 537–540 (1999).
30. Vassar, R., Bennett, B. D., Babu-Khan, S., Kahn, S., Mendiaz, E. A., Denis, P., Teplow, D. B., Ross, S., Amarante, P., Loeloff, R., Luo, Y., Fisher, S., Fuller, J., Edenson, S., Lile, J., Jarosinski, M. A., Biere, A. L., Curran, E., Burgess, T., Louis, J. C., Collins, F., Treanor, J., Rogers, G. & Citron, M. Beta-secretase cleavage of Alzheimer's amyloid precursor protein by the transmembrane aspartic protease BACE. *Science* **286**, 735–741 (1999).
31. Yan, R., Bienkowski, M. J., Shuck, M. E., Miao, H., Tory, M. C., Pauley, A. M., Brashier, J. R., Stratman, N. C., Mathews, W. R., Buhl, A. E., Carter, D. B., Tomasselli, A. G., Parodi, L. A., Heinrikson, R. L. & Gurney, M. E. Membrane-anchored aspartyl protease with Alzheimer's disease beta-secretase activity. *Nature* **402**, 533–537 (1999).
32. De Strooper, B., Saftig, P., Craessaerts, K., Vanderstichele, H., Guhde, G., Annaert, W., Von Figura, K. & Van Leuven, F. Deficiency of presenilin-1 inhibits the normal cleavage of amyloid precursor protein. *Nature* **391**, 387–390 (1998).
33. Wolfe, M. S., Xia, W., Ostaszewski, B. L., Diehl, T. S., Kimberly, W. T. & Selkoe, D. J. Two transmembrane aspartates in presenilin-1 required for presenilin endoproteolysis and gamma-secretase

activity. *Nature* **398**, 513–517 (1999).

34. Hussain, I., Powell, D., Howlett, D. R., Tew, D. G., Meek, T. D., Chapman, C., Gloger, I. S., Murphy, K. E., Southan, C. D., Ryan, D. M., Smith, T. S., Simmons, D. L., Walsh, F. S., Dingwall, C. & Christie, G. Identification of a novel aspartic protease (Asp 2) as beta-secretase. *Mol Cell Neurosci* **14**, 419–427 (1999).
35. Lin, X., Koelsch, G., Wu, S., Downs, D., Dashti, A. & Tang, J. Human aspartic protease memapsin 2 cleaves the beta-secretase site of beta-amyloid precursor protein. *Proc Natl Acad Sci U S A* **97**, 1456–1460 (2000).
36. Hortschansky, P., Schroeckh, V., Christopeit, T., Zandomenighi, G. & Fändrich, M. The aggregation kinetics of Alzheimer's β -amyloid peptide is controlled by stochastic nucleation. *Protein Sci* **14**, 1753–1759 (2005).
37. Takami, M., Nagashima, Y., Sano, Y., Ishihara, S., Morishima-Kawashima, M., Funamoto, S. & Ihara, Y. gamma-Secretase: successive tripeptide and tetrapeptide release from the transmembrane domain of beta-carboxyl terminal fragment. *J Neurosci* **29**, 13042–13052 (2009).
38. Wei, W., Nguyen, L. N., Kessels, H. W., Hagiwara, H., Sisodia, S. & Malinow, R. Amyloid beta from axons and dendrites reduces local spine number and plasticity. *Nat Neurosci* **13**, 190–196 (2010).
39. Ferreira, I. L., Bajouco, L. M., Mota, S. I., Auberson, Y. P., Oliveira, C. R. & Rego, A. C. Amyloid beta peptide 1–42 disturbs intracellular calcium homeostasis through activation of GluN2B-containing N-methyl-d-aspartate receptors in cortical cultures. *Cell Calcium* **51**, 95–106 (2012).
40. Scheuner, D., Eckman, C., Jensen, M., Song, X., Citron, M., Suzuki, N., Bird, T. D., Hardy, J., Hutton, M., Kukull, W., Larson, E., Levy-Lahad, E., Viitanen, M., Peskind, E., Poorkaj, P., Schellenberg, G., Tanzi, R., Wasco, W., Lannfelt, L., Selkoe, D. & Younkin, S. Secreted amyloid beta-protein similar to that in the senile plaques of Alzheimer's disease is increased in vivo by the presenilin 1 and 2 and APP mutations linked to familial Alzheimer's disease. *Nat Med* **2**, 864–870 (1996).
41. Holtzman, D. M., Bales, K. R., Tenkova, T., Fagan, A. M., Parsadanian, M., Sartorius, L. J., Mackey, B., Olney, J., McKeel, D., Wozniak, D. & Paul, S. M. Apolipoprotein E isoform-dependent amyloid deposition and neuritic degeneration in a mouse model of Alzheimer's disease. *Proc Natl Acad Sci U S A* **97**, 2892–2897 (2000).
42. Weingarten, M. D., Lockwood, A. H., Hwo, S. Y. & Kirschner, M. W. A protein factor essential for microtubule assembly. *Proc Natl Acad Sci U S A* **72**, 1858–1862 (1975).
43. Goedert, M., Spillantini, M. G., Jakes, R., Rutherford, D. & Crowther, R. A. Multiple isoforms of human microtubule-associated protein tau: sequences and localization in neurofibrillary tangles of Alzheimer's disease. *Neuron* **3**, 519–526 (1989).
44. Himmler, A., Drechsel, D., Kirschner, M. W. & Martin, D. W. Tau consists of a set of proteins with repeated C-terminal microtubule-binding domains and variable N-terminal domains. *Mol Cell Biol* **9**, 1381–1388 (1989).

45. Buée, L., Bussière, T., Buée-Scherrer, V., Delacourte, A. & Hof, P. R. Tau protein isoforms, phosphorylation and role in neurodegenerative disorders. *Brain Res Brain Res Rev* **33**, 95–130 (2000).
46. Goedert, M. & Jakes, R. Expression of separate isoforms of human tau protein: correlation with the tau pattern in brain and effects on tubulin polymerization. *The EMBO Journal* **9**, 4225–4230 (1990).
47. Dickson, D. W., Kouri, N., Murray, M. E. & Josephs, K. A. Neuropathology of Frontotemporal Lobar Degeneration–Tau (FTLD-Tau). *J Mol Neurosci* **45**, 384–389 (2011).
48. Mukrasch, M. D., Bibow, S., Korukottu, J., Jeganathan, S., Biernat, J., Griesinger, C., Mandelkow, E. & Zweckstetter, M. Structural polymorphism of 441-residue tau at single residue resolution. *PLoS Biol* **7**, e34 (2009).
49. Jeganathan, S., von Bergen, M., Brutlach, H., Steinhoff, H.-J. & Mandelkow, E. Global hairpin folding of tau in solution. *Biochemistry* **45**, 2283–2293 (2006).
50. Wang, Y. & Mandelkow, E. Tau in physiology and pathology. *Nat Rev Neurosci* **17**, 5–21 (2016).
51. Gu, Y., Oyama, F. & Ihara, Y. Tau is widely expressed in rat tissues. *J Neurochem* **67**, 1235–1244 (1996).
52. LoPresti, P., Szuchet, S., Papasozomenos, S. C., Zinkowski, R. P. & Binder, L. I. Functional implications for the microtubule-associated protein tau: localization in oligodendrocytes. *Proc Natl Acad Sci U S A* **92**, 10369–10373 (1995).
53. Ezerskiy, L. A., Schoch, K. M., Sato, C., Beltcheva, M., Horie, K., Rigo, F., Martynowicz, R., Karch, C. M., Bateman, R. J. & Miller, T. M. Astrocytic 4R tau expression drives astrocyte reactivity and dysfunction. *JCI Insight* **7**, (2022).
54. Guo, T., Noble, W. & Hanger, D. P. Roles of tau protein in health and disease. *Acta Neuropathol* **133**, 665–704 (2017).
55. Stamer, K., Vogel, R., Thies, E., Mandelkow, E. & Mandelkow, E.-M. Tau blocks traffic of organelles, neurofilaments, and APP vesicles in neurons and enhances oxidative stress. *J Cell Biol* **156**, 1051–1063 (2002).
56. Dixit, R., Ross, J. L., Goldman, Y. E. & Holzbaur, E. L. F. Differential Regulation of Dynein and Kinesin Motor Proteins by Tau. *Science* **319**, 1086–1089 (2008).
57. Frandemiche, M. L., De Seranno, S., Rush, T., Borel, E., Elie, A., Arnal, I., Lanté, F. & Buisson, A. Activity-Dependent Tau Protein Translocation to Excitatory Synapse Is Disrupted by Exposure to Amyloid-Beta Oligomers. *J Neurosci* **34**, 6084–6097 (2014).
58. Sultan, A., Nesslany, F., Violet, M., Bégard, S., Loyens, A., Talahari, S., Mansuroglu, Z., Marzin, D., Sergeant, N., Humez, S., Colin, M., Bonnefoy, E., Buée, L. & Galas, M.-C. Nuclear tau, a key player in neuronal DNA protection. *J Biol Chem* **286**, 4566–4575 (2011).
59. Violet, M., Delattre, L., Tardivel, M., Sultan, A., Chauderlier, A., Caillierez, R., Talahari, S., Nesslany, F., Lefebvre, B., Bonnefoy, E., Buée, L. & Galas, M.-C. A major role for Tau in neuronal DNA and RNA protection in vivo under physiological and hyperthermic conditions. *Front Cell Neurosci*

8, 84 (2014).

60. Rico, T., Gilles, M., Chauderlier, A., Comptdaer, T., Magnez, R., Chwastyniak, M., Drobecq, H., Pinet, F., Thuru, X., Buée, L., Galas, M.-C. & Lefebvre, B. Tau Stabilizes Chromatin Compaction. *Front Cell Dev Biol* **9**, 740550 (2021).
61. Alonso, A. del C., Grundke-Iqbal, I., Barra, H. S. & Iqbal, K. Abnormal phosphorylation of tau and the mechanism of Alzheimer neurofibrillary degeneration: Sequestration of microtubule-associated proteins 1 and 2 and the disassembly of microtubules by the abnormal tau. *Proc Natl Acad Sci U S A* **94**, 298–303 (1997).
62. Hanger, D. P., Byers, H. L., Wray, S., Leung, K.-Y., Saxton, M. J., Seereeram, A., Reynolds, C. H., Ward, M. A. & Anderton, B. H. Novel Phosphorylation Sites in Tau from Alzheimer Brain Support a Role for Casein Kinase 1 in Disease Pathogenesis *. *Journal of Biological Chemistry* **282**, 23645–23654 (2007).
63. Šimić, G., Babić Leko, M., Wray, S., Harrington, C., Delalle, I., Jovanov-Milošević, N., Bažadona, D., Buée, L., De Silva, R., Di Giovanni, G., Wischik, C. & Hof, P. R. Tau Protein Hyperphosphorylation and Aggregation in Alzheimer’s Disease and Other Tauopathies, and Possible Neuroprotective Strategies. *Biomolecules* **6**, 6 (2016).
64. Goedert, M., Jakes, R., Spillantini, M. G., Hasegawa, M., Smith, M. J. & Crowther, R. A. Assembly of microtubule-associated protein tau into Alzheimer-like filaments induced by sulphated glycosaminoglycans. *Nature* **383**, 550–553 (1996).
65. Arendt, T., Stieler, J., Strijkstra, A. M., Hut, R. A., Rüdiger, J., Van der Zee, E. A., Harkany, T., Holzer, M. & Härtig, W. Reversible paired helical filament-like phosphorylation of tau is an adaptive process associated with neuronal plasticity in hibernating animals. *J Neurosci* **23**, 6972–6981 (2003).
66. Planel, E., Richter, K. E. G., Nolan, C. E., Finley, J. E., Liu, L., Wen, Y., Krishnamurthy, P., Herman, M., Wang, L., Schachter, J. B., Nelson, R. B., Lau, L.-F. & Duff, K. E. Anesthesia leads to tau hyperphosphorylation through inhibition of phosphatase activity by hypothermia. *J Neurosci* **27**, 3090–3097 (2007).
67. Biernat, J., Gustke, N., Drewes, G., Mandelkow, E. M. & Mandelkow, E. Phosphorylation of Ser262 strongly reduces binding of tau to microtubules: distinction between PHF-like immunoreactivity and microtubule binding. *Neuron* **11**, 153–163 (1993).
68. Biernat, J. & Mandelkow, E. M. The development of cell processes induced by tau protein requires phosphorylation of serine 262 and 356 in the repeat domain and is inhibited by phosphorylation in the proline-rich domains. *Mol Biol Cell* **10**, 727–740 (1999).
69. Thies, E. & Mandelkow, E.-M. Missorting of tau in neurons causes degeneration of synapses that can be rescued by the kinase MARK2/Par-1. *J Neurosci* **27**, 2896–2907 (2007).
70. Hoover, B. R., Reed, M. N., Su, J., Penrod, R. D., Kotilinek, L. A., Grant, M. K., Pitstick, R., Carlson, G. A., Lanier, L. M., Yuan, L.-L., Ashe, K. H. & Liao, D. Tau mislocalization to dendritic spines mediates synaptic dysfunction independently of neurodegeneration. *Neuron* **68**, 1067–1081

(2010).

71. Guillozet-Bongaarts, A. L., Cahill, M. E., Cryns, V. L., Reynolds, M. R., Berry, R. W. & Binder, L. I. Pseudophosphorylation of tau at serine 422 inhibits caspase cleavage: in vitro evidence and implications for tangle formation in vivo. *J Neurochem* **97**, 1005–1014 (2006).
72. Dickey, C. A., Kamal, A., Lundgren, K., Klosak, N., Bailey, R. M., Dunmore, J., Ash, P., Shoraka, S., Zlatkovic, J., Eckman, C. B., Patterson, C., Dickson, D. W., Nahman, N. S., Hutton, M., Burrows, F. & Petrucelli, L. The high-affinity HSP90-CHIP complex recognizes and selectively degrades phosphorylated tau client proteins. *J Clin Invest* **117**, 648–658 (2007).
73. Min, S.-W., Cho, S.-H., Zhou, Y., Schroeder, S., Haroutunian, V., Seeley, W. W., Huang, E. J., Shen, Y., Masliah, E., Mukherjee, C., Meyers, D., Cole, P. A., Ott, M. & Gan, L. Acetylation of Tau Inhibits Its Degradation and Contributes to Tauopathy. *Neuron* **67**, 953–966 (2010).
74. Min, S.-W., Chen, X., Tracy, T. E., Li, Y., Zhou, Y., Wang, C., Shirakawa, K., Minami, S. S., Defensor, E., Mok, S. A., Sohn, P. D., Schilling, B., Cong, X., Ellerby, L., Gibson, B. W., Johnson, J., Krogan, N., Shamloo, M., Gestwicki, J., Masliah, E., Verdin, E. & Gan, L. Critical Role of Acetylation in Tau-Mediated Neurodegeneration and Cognitive Deficits. *Nat Med* **21**, 1154–1162 (2015).
75. Zilka, N., Filipcik, P., Koson, P., Fialova, L., Skrabana, R., Zilkova, M., Rolkova, G., Kontsekova, E. & Novak, M. Truncated tau from sporadic Alzheimer's disease suffices to drive neurofibrillary degeneration in vivo. *FEBS Lett* **580**, 3582–3588 (2006).
76. de Calignon, A., Fox, L. M., Pitstick, R., Carlson, G. A., Bacskai, B. J., Spires-Jones, T. L. & Hyman, B. T. Caspase activation precedes and leads to tangles. *Nature* **464**, 1201–1204 (2010).
77. Zhang, Z., Song, M., Liu, X., Kang, S. S., Kwon, I.-S., Duong, D. M., Seyfried, N. T., Hu, W. T., Liu, Z., Wang, J., Cheng, L., Sun, Y. E., Yu, S. P., Levey, A. I. & Ye, K. Cleavage of tau by asparagine endopeptidase mediates the neurofibrillary pathology in Alzheimer's disease. *Nat Med* **20**, 1254–1262 (2014).
78. Goedert, M., Wischik, C. M., Crowther, R. A., Walker, J. E. & Klug, A. Cloning and sequencing of the cDNA encoding a core protein of the paired helical filament of Alzheimer disease: identification as the microtubule-associated protein tau. *Proceedings of the National Academy of Sciences* **85**, 4051–4055 (1988).
79. Wischik, C. M., Novak, M., Edwards, P. C., Klug, A., Tichelaar, W. & Crowther, R. A. Structural characterization of the core of the paired helical filament of Alzheimer disease. *Proceedings of the National Academy of Sciences* **85**, 4884–4888 (1988).
80. Crowther, R. A. Straight and paired helical filaments in Alzheimer disease have a common structural unit. *Proc Natl Acad Sci U S A* **88**, 2288–2292 (1991).
81. von Bergen, M., Friedhoff, P., Biernat, J., Heberle, J., Mandelkow, E.-M. & Mandelkow, E. Assembly of τ protein into Alzheimer paired helical filaments depends on a local sequence motif (306VQIVYK311) forming β structure. *Proceedings of the National Academy of Sciences* **97**, 5129–5134 (2000).

82. von Bergen, M., Barghorn, S., Biernat, J., Mandelkow, E.-M. & Mandelkow, E. Tau aggregation is driven by a transition from random coil to beta sheet structure. *Biochimica et Biophysica Acta (BBA) - Molecular Basis of Disease* **1739**, 158–166 (2005).
83. Crowther, R. a., Olesen, O. f., Smith, M. j., Jakes, R. & Goedert, M. Assembly of Alzheimer-like filaments from full-length tau protein. *FEBS Letters* **337**, 135–138 (1994).
84. Friedhoff, P., Schneider, A., Mandelkow, E.-M. & Mandelkow, E. Rapid Assembly of Alzheimer-like Paired Helical Filaments from Microtubule-Associated Protein Tau Monitored by Fluorescence in Solution. *Biochemistry* **37**, 10223–10230 (1998).
85. GARCINI, E. M. de & AVILA, J. In Vitro Conditions for the Self-Polymerization of the Microtubule-Associated Protein, Tau Factor. *The Journal of Biochemistry* **102**, 1415–1421 (1987).
86. Kampers, T., Friedhoff, P., Biernat, J., Mandelkow, E.-M. & Mandelkow, E. RNA stimulates aggregation of microtubule-associated protein tau into Alzheimer-like paired helical filaments. *FEBS Letters* **399**, 344–349 (1996).
87. Wilson, D. M. & Binder, L. I. Free fatty acids stimulate the polymerization of tau and amyloid beta peptides. In vitro evidence for a common effector of pathogenesis in Alzheimer's disease. *Am J Pathol* **150**, 2181–2195 (1997).
88. Barghorn, S. & Mandelkow, E. Toward a Unified Scheme for the Aggregation of Tau into Alzheimer Paired Helical Filaments. *Biochemistry* **41**, 14885–14896 (2002).
89. SantaCruz, K., Lewis, J., Spires, T., Paulson, J., Kotilinek, L., Ingelsson, M., Guimaraes, A., DeTure, M., Ramsden, M., McGowan, E., Forster, C., Yue, M., Orne, J., Janus, C., Mariash, A., Kuskowski, M., Hyman, B., Hutton, M. & Ashe, K. H. Tau Suppression in a Neurodegenerative Mouse Model Improves Memory Function. *Science* **309**, 476–481 (2005).
90. Mocanu, M.-M., Nissen, A., Eckermann, K., Khlistunova, I., Biernat, J., Drexler, D., Petrova, O., Schönig, K., Bujard, H., Mandelkow, E., Zhou, L., Rune, G. & Mandelkow, E.-M. The potential for beta-structure in the repeat domain of tau protein determines aggregation, synaptic decay, neuronal loss, and coassembly with endogenous Tau in inducible mouse models of tauopathy. *J Neurosci* **28**, 737–748 (2008).
91. Alonso, A. del C., Li, B., Grundke-Iqbal, I. & Iqbal, K. Polymerization of hyperphosphorylated tau into filaments eliminates its inhibitory activity. *Proc Natl Acad Sci U S A* **103**, 8864–8869 (2006).
92. Lasagna-Reeves, C. A., Castillo-Carranza, D. L., Sengupta, U., Clos, A. L., Jackson, G. R. & Kaye, R. Tau oligomers impair memory and induce synaptic and mitochondrial dysfunction in wild-type mice. *Mol Neurodegener* **6**, 39 (2011).
93. Flach, K., Hilbrich, I., Schiffmann, A., Gärtner, U., Krüger, M., Leonhardt, M., Waschipky, H., Wick, L., Arendt, T. & Holzer, M. Tau Oligomers Impair Artificial Membrane Integrity and Cellular Viability. *J Biol Chem* **287**, 43223–43233 (2012).
94. Tian, H., Davidowitz, E., Lopez, P., Emadi, S., Moe, J. & Sierks, M. Trimeric Tau Is Toxic to Human Neuronal Cells at Low Nanomolar Concentrations. *Int J Cell Biol* **2013**, 260787 (2013).

95. Ghag, G., Bhatt, N., Cantu, D. V., Guerrero-Munoz, M. J., Ellsworth, A., Sengupta, U. & Kaye, R. Soluble tau aggregates, not large fibrils, are the toxic species that display seeding and cross-seeding behavior: Generation of tau aggregates via sonication. *Protein Science* **27**, 1901–1909 (2018).
96. Braak, H. & Braak, E. Neuropathological staging of Alzheimer-related changes. *Acta Neuropathol* **82**, 239–259 (1991).
97. Frost, B., Jacks, R. L. & Diamond, M. I. Propagation of tau misfolding from the outside to the inside of a cell. *J Biol Chem* **284**, 12845–12852 (2009).
98. Kfoury, N., Holmes, B. B., Jiang, H., Holtzman, D. M. & Diamond, M. I. Trans-cellular Propagation of Tau Aggregation by Fibrillar Species *. *Journal of Biological Chemistry* **287**, 19440–19451 (2012).
99. Wu, J. W., Herman, M., Liu, L., Simoes, S., Acker, C. M., Figueroa, H., Steinberg, J. I., Margittai, M., Kaye, R., Zurzolo, C., Di Paolo, G. & Duff, K. E. Small misfolded Tau species are internalized via bulk endocytosis and anterogradely and retrogradely transported in neurons. *J Biol Chem* **288**, 1856–1870 (2013).
100. Holmes, B. B., Furman, J. L., Mahan, T. E., Yamasaki, T. R., Mirbaha, H., Eades, W. C., Belaygorod, L., Cairns, N. J., Holtzman, D. M. & Diamond, M. I. Proteopathic tau seeding predicts tauopathy in vivo. *Proc Natl Acad Sci U S A* **111**, E4376–4385 (2014).
101. Clavaguera, F., Bolmont, T., Crowther, R. A., Abramowski, D., Frank, S., Probst, A., Fraser, G., Stalder, A. K., Beibel, M., Staufenbiel, M., Jucker, M., Goedert, M. & Tolnay, M. Transmission and spreading of tauopathy in transgenic mouse brain. *Nat Cell Biol* **11**, 909–913 (2009).
102. de Calignon, A., Polydoro, M., Suárez-Calvet, M., William, C., Adamowicz, D. H., Kopeikina, K. J., Pitstick, R., Sahara, N., Ashe, K. H., Carlson, G. A., Spires-Jones, T. L. & Hyman, B. T. Propagation of Tau Pathology in a Model of Early Alzheimer's Disease. *Neuron* **73**, 685–697 (2012).
103. Liu, L., Drouet, V., Wu, J. W., Witter, M. P., Small, S. A., Clelland, C. & Duff, K. Trans-synaptic spread of tau pathology in vivo. *PLoS One* **7**, e31302 (2012).
104. Clavaguera, F., Akatsu, H., Fraser, G., Crowther, R. A., Frank, S., Hench, J., Probst, A., Winkler, D. T., Reichwald, J., Staufenbiel, M., Ghetti, B., Goedert, M. & Tolnay, M. Brain homogenates from human tauopathies induce tau inclusions in mouse brain. *Proceedings of the National Academy of Sciences* **110**, 9535–9540 (2013).
105. Dujardin, S., Lécolle, K., Caillierez, R., Bégard, S., Zommer, N., Lachaud, C., Carrier, S., Dufour, N., Aurégan, G., Winderickx, J., Hantraye, P., Déglon, N., Colin, M. & Buée, L. Neuron-to-neuron wild-type Tau protein transfer through a trans-synaptic mechanism: relevance to sporadic tauopathies. *acta neuropathol commun* **2**, 1–14 (2014).
106. Narasimhan, S., Guo, J. L., Changolkar, L., Stieber, A., McBride, J. D., Silva, L. V., He, Z., Zhang, B., Gathagan, R. J., Trojanowski, J. Q. & Lee, V. M. Y. Pathological Tau Strains from Human Brains Recapitulate the Diversity of Tauopathies in Nontransgenic Mouse Brain. *J. Neurosci.* **37**, 11406–11423 (2017).

107. Furman, J. L., Vaquer-Alicea, J., White, C. L., Cairns, N. J., Nelson, P. T. & Diamond, M. I. Widespread Tau Seeding Activity at Early Braak Stages. *Acta Neuropathol* **133**, 91–100 (2017).
108. Seeley, W. W., Crawford, R. K., Zhou, J., Miller, B. L. & Greicius, M. D. Neurodegenerative Diseases Target Large-Scale Human Brain Networks. *Neuron* **62**, 42–52 (2009).
109. Franzmeier, N., Rubinski, A., Neitzel, J., Kim, Y., Damm, A., Na, D. L., Kim, H. J., Lyoo, C. H., Cho, H., Finsterwalder, S., Duering, M., Seo, S. W. & Ewers, M. Functional connectivity associated with tau levels in ageing, Alzheimer's, and small vessel disease. *Brain* **142**, 1093–1107 (2019).
110. Vogel, J. W., Iturria-Medina, Y., Strandberg, O. T., Smith, R., Levitis, E., Evans, A. C. & Hansson, O. Spread of pathological tau proteins through communicating neurons in human Alzheimer's disease. *Nat Commun* **11**, 2612 (2020).
111. Franzmeier, N., Dewenter, A., Frontzkowski, L., Dichgans, M., Rubinski, A., Neitzel, J., Smith, R., Strandberg, O., Ossenkoppele, R., Buerger, K., Duering, M., Hansson, O. & Ewers, M. Patient-centered connectivity-based prediction of tau pathology spread in Alzheimer's disease. *Science Advances* **6**, eabd1327 (2020).
112. Saman, S., Kim, W., Raya, M., Visnick, Y., Miro, S., Saman, S., Jackson, B., McKee, A. C., Alvarez, V. E., Lee, N. C. Y. & Hall, G. F. Exosome-associated Tau Is Secreted in Tauopathy Models and Is Selectively Phosphorylated in Cerebrospinal Fluid in Early Alzheimer Disease*. *Journal of Biological Chemistry* **287**, 3842–3849 (2012).
113. Skachokova, Z., Martinisi, A., Flach, M., Sprenger, F., Naegelin, Y., Steiner-Monard, V., Sollberger, M., Monsch, A. U., Goedert, M., Tolnay, M. & Winkler, D. T. Cerebrospinal fluid from Alzheimer's disease patients promotes tau aggregation in transgenic mice. *acta neuropathol commun* **7**, 1–9 (2019).
114. Shi, Y., Kirwan, P., Smith, J., MacLean, G., Orkin, S. H. & Livesey, F. J. A Human Stem Cell Model of Early Alzheimer's Disease Pathology in Down Syndrome. *Science Translational Medicine* **4**, 124ra29-124ra29 (2012).
115. Pooler, A. M., Phillips, E. C., Lau, D. H. W., Noble, W. & Hanger, D. P. Physiological release of endogenous tau is stimulated by neuronal activity. *EMBO Rep* **14**, 389–394 (2013).
116. Chai, X., Dage, J. L. & Citron, M. Constitutive secretion of tau protein by an unconventional mechanism. *Neurobiology of Disease* **48**, 356–366 (2012).
117. Karch, C. M., Jeng, A. T. & Goate, A. M. Extracellular Tau Levels Are Influenced by Variability in Tau That Is Associated with Tauopathies*. *Journal of Biological Chemistry* **287**, 42751–42762 (2012).
118. Plouffe, V., Mohamed, N.-V., Rivest-McGraw, J., Bertrand, J., Lauzon, M. & Leclerc, N. Hyperphosphorylation and Cleavage at D421 Enhance Tau Secretion. *PLOS ONE* **7**, e36873 (2012).
119. Tang, Z., Ioja, E., Bereczki, E., Hultenby, K., Li, C., Guan, Z., Winblad, B. & Pei, J.-J. mTor mediates tau localization and secretion: Implication for Alzheimer's disease. *Biochimica et Biophysica Acta (BBA) - Molecular Cell Research* **1853**, 1646–1657 (2015).

120. Fontaine, S. N., Zheng, D., Sabbagh, J. J., Martin, M. D., Chaput, D., Darling, A., Trotter, J. H., Stothert, A. R., Nordhues, B. A., Lussier, A., Baker, J., Shelton, L., Kahn, M., Blair, L. J., Stevens, S. M. & Dickey, C. A. DnaJ/Hsc70 chaperone complexes control the extracellular release of neurodegenerative-associated proteins. *EMBO J* **35**, 1537–1549 (2016).
121. Katsinelos, T., Zeitler, M., Dimou, E., Karakatsani, A., Müller, H.-M., Nachman, E., Steringer, J. P., Ruiz de Almodovar, C., Nickel, W. & Jahn, T. R. Unconventional Secretion Mediates the Trans-cellular Spreading of Tau. *Cell Reports* **23**, 2039–2055 (2018).
122. Merezhko, M., Brunello, C. A., Yan, X., Vihinen, H., Jokitalo, E., Uronen, R.-L. & Huttunen, H. J. Secretion of Tau via an Unconventional Non-vesicular Mechanism. *Cell Reports* **25**, 2027–2035.e4 (2018).
123. Xu, Y., Du, S., Marsh, J. A., Horie, K., Sato, C., Ballabio, A., Karch, C. M., Holtzman, D. M. & Zheng, H. TFEB regulates lysosomal exocytosis of tau and its loss of function exacerbates tau pathology and spreading. *Mol Psychiatry* **26**, 5925–5939 (2021).
124. Kim, W., Lee, S. & Hall, G. F. Secretion of human tau fragments resembling CSF-tau in Alzheimer's disease is modulated by the presence of the exon 2 insert. *FEBS Lett* **584**, 3085–3088 (2010).
125. Gómez-Ramos, A., Díaz-Hernández, M., Rubio, A., Miras-Portugal, M. T. & Avila, J. Extracellular tau promotes intracellular calcium increase through M1 and M3 muscarinic receptors in neuronal cells. *Molecular and Cellular Neuroscience* **37**, 673–681 (2008).
126. Díaz-Hernández, M., Gómez-Ramos, A., Rubio, A., Gómez-Villafuertes, R., Naranjo, J. R., Miras-Portugal, M. T. & Avila, J. Tissue-nonspecific Alkaline Phosphatase Promotes the Neurotoxicity Effect of Extracellular Tau*. *Journal of Biological Chemistry* **285**, 32539–32548 (2010).
127. Holmes, B. B., DeVos, S. L., Kfoury, N., Li, M., Jacks, R., Yanamandra, K., Ouidja, M. O., Brodsky, F. M., Marasa, J., Bagchi, D. P., Kotzbauer, P. T., Miller, T. M., Papy-Garcia, D. & Diamond, M. I. Heparan sulfate proteoglycans mediate internalization and propagation of specific proteopathic seeds. *Proceedings of the National Academy of Sciences* **110**, E3138–E3147 (2013).
128. Rauch, J. N., Luna, G., Guzman, E., Audouard, M., Challis, C., Sibih, Y. E., Leshuk, C., Hernandez, I., Wegmann, S., Hyman, B. T., Gradinaru, V., Kampmann, M. & Kosik, K. S. LRP1 is a master regulator of tau uptake and spread. *Nature* **580**, 381–385 (2020).
129. Mann, D. M. A. & Hardy, J. Amyloid or tau: the chicken or the egg? *Acta Neuropathol* **126**, 609–613 (2013).
130. Braak, H. & Del Tredici, K. Reply: the early pathological process in sporadic Alzheimer's disease. *Acta Neuropathol* **126**, 615–618 (2013).
131. Attems, J. & Jellinger, K. A. Amyloid and tau: neither chicken nor egg but two partners in crime! *Acta Neuropathol* **126**, 619–621 (2013).
132. Ossenkoppele, R., Schonhaut, D. R., Schöll, M., Lockhart, S. N., Ayakta, N., Baker, S. L., O'Neil, J. P., Janabi, M., Lazaris, A., Cantwell, A., Vogel, J., Santos, M., Miller, Z. A., Bettcher, B. M.,

- Vossel, K. A., Kramer, J. H., Gorno-Tempini, M. L., Miller, B. L., Jagust, W. J. & Rabinovici, G. D. Tau PET patterns mirror clinical and neuroanatomical variability in Alzheimer's disease. *Brain* **139**, 1551–1567 (2016).
133. Hardy, J. A. & Higgins, G. A. Alzheimer's Disease: The Amyloid Cascade Hypothesis. *Science* (1992) doi:10.1126/science.1566067.
134. McKhann, G., Drachman, D., Folstein, M., Katzman, R., Price, D. & Stadlan, E. M. Clinical diagnosis of Alzheimer's disease: Report of the NINCDS-ADRDA Work Group* under the auspices of Department of Health and Human Services Task Force on Alzheimer's Disease. *Neurology* **34**, 939–939 (1984).
135. Dubois, B., Feldman, H. H., Jacova, C., Hampel, H., Molinuevo, J. L., Blennow, K., DeKosky, S. T., Gauthier, S., Selkoe, D., Bateman, R., Cappa, S., Crutch, S., Engelborghs, S., Frisoni, G. B., Fox, N. C., Galasko, D., Habert, M.-O., Jicha, G. A., Nordberg, A., Pasquier, F., Rabinovici, G., Robert, P., Rowe, C., Salloway, S., Sarazin, M., Epelbaum, S., de Souza, L. C., Vellas, B., Visser, P. J., Schneider, L., Stern, Y., Scheltens, P. & Cummings, J. L. Advancing research diagnostic criteria for Alzheimer's disease: the IWG-2 criteria. *The Lancet Neurology* **13**, 614–629 (2014).
136. Albert, M. S., DeKosky, S. T., Dickson, D., Dubois, B., Feldman, H. H., Fox, N. C., Gamst, A., Holtzman, D. M., Jagust, W. J., Petersen, R. C., Snyder, P. J., Carrillo, M. C., Thies, B. & Phelps, C. H. The diagnosis of mild cognitive impairment due to Alzheimer's disease: Recommendations from the National Institute on Aging-Alzheimer's Association workgroups on diagnostic guidelines for Alzheimer's disease. *Alzheimers Dement* **7**, 270–279 (2011).
137. McKhann, G. M., Knopman, D. S., Chertkow, H., Hyman, B. T., Jack, C. R., Kawas, C. H., Klunk, W. E., Koroshetz, W. J., Manly, J. J., Mayeux, R., Mohs, R. C., Morris, J. C., Rossor, M. N., Scheltens, P., Carrillo, M. C., Thies, B., Weintraub, S. & Phelps, C. H. The diagnosis of dementia due to Alzheimer's disease: Recommendations from the National Institute on Aging-Alzheimer's Association workgroups on diagnostic guidelines for Alzheimer's disease. *Alzheimers Dement* **7**, 263–269 (2011).
138. Sperling, R. A., Aisen, P. S., Beckett, L. A., Bennett, D. A., Craft, S., Fagan, A. M., Iwatsubo, T., Jack, C. R., Kaye, J., Montine, T. J., Park, D. C., Reiman, E. M., Rowe, C. C., Siemers, E., Stern, Y., Yaffe, K., Carrillo, M. C., Thies, B., Morrison-Bogorad, M., Wagster, M. V. & Phelps, C. H. Toward defining the preclinical stages of Alzheimer's disease: Recommendations from the National Institute on Aging-Alzheimer's Association workgroups on diagnostic guidelines for Alzheimer's disease. *Alzheimers Dement* **7**, 280–292 (2011).
139. Linn, R. T., Wolf, P. A., Bachman, D. L., Knoefel, J. E., Cobb, J. L., Belanger, A. J., Kaplan, E. F. & D'Agostino, R. B. The 'Preclinical Phase' of Probable Alzheimer's Disease: A 13-Year Prospective Study of the Framingham Cohort. *Archives of Neurology* **52**, 485–490 (1995).
140. Jacobs, D. M., Sano, M., Dooneief, G., Marder, K., Bell, K. L. & Stern, Y. Neuropsychological detection and characterization of preclinical Alzheimer's disease. *Neurology* **45**, 957–962 (1995).

141. Bäckman, L., Small, B. J. & Fratiglioni, L. Stability of the preclinical episodic memory deficit in Alzheimer's disease. *Brain* **124**, 96–102 (2001).
142. Kawas, C. H., Corrada, M. M., Brookmeyer, R., Morrison, A., Resnick, S. M., Zonderman, A. B. & Arenberg, D. Visual memory predicts Alzheimer's disease more than a decade before diagnosis. *Neurology* **60**, 1089–1093 (2003).
143. Weintraub, S., Wicklund, A. H. & Salmon, D. P. The Neuropsychological Profile of Alzheimer Disease. *Cold Spring Harb Perspect Med* **2**, a006171 (2012).
144. Braak, H. & Braak, E. Neuropathological staging of Alzheimer-related changes. *Acta Neuropathol* **82**, 239–259 (1991).
145. Gold, G., Bouras, C., Kövari, E., Canuto, A., Glaría, B. G., Malky, A., Hof, P. R., Michel, J. P. & Giannakopoulos, P. Clinical validity of Braak neuropathological staging in the oldest-old. *Acta Neuropathol* **99**, 579–582; discussion 583–584 (2000).
146. Thal, D. R., Rüb, U., Orantes, M. & Braak, H. Phases of A beta-deposition in the human brain and its relevance for the development of AD. *Neurology* **58**, 1791–1800 (2002).
147. Serrano-Pozo, A., Qian, J., Muzikansky, A., Monsell, S. E., Montine, T. J., Frosch, M. P., Betensky, R. A. & Hyman, B. T. Thal Amyloid Stages Do Not Significantly Impact the Correlation Between Neuropathological Change and Cognition in the Alzheimer Disease Continuum. *J Neuropathol Exp Neurol* **75**, 516–526 (2016).
148. Seubert, P., Vigo-Pelfrey, C., Esch, F., Lee, M., Dovey, H., Davis, D., Sinha, S., Schiossmacher, M., Whaley, J., Swindlehurst, C., McCormack, R., Wolfert, R., Selkoe, D., Lieberburg, I. & Schenk, D. Isolation and quantification of soluble Alzheimer's β -peptide from biological fluids. *Nature* **359**, 325–327 (1992).
149. Motter, R., Vigo-Pelfrey, C., Kholodenko, D., Barbour, R., Johnson-Wood, K., Galasko, D., Chang, L., Miller, B., Clark, C. & Green, R. Reduction of beta-amyloid peptide₄₂ in the cerebrospinal fluid of patients with Alzheimer's disease. *Ann Neurol* **38**, 643–648 (1995).
150. Strozzyk, D., Blennow, K., White, L. R. & Launer, L. J. CSF A β 42 levels correlate with amyloid-neuropathology in a population-based autopsy study. *Neurology* **60**, 652–656 (2003).
151. Tapiola, T., Alafuzoff, I., Herukka, S.-K., Parkkinen, L., Hartikainen, P., Soininen, H. & Pirttilä, T. Cerebrospinal fluid {beta}-amyloid 42 and tau proteins as biomarkers of Alzheimer-type pathologic changes in the brain. *Arch Neurol* **66**, 382–389 (2009).
152. Dumurgier, J., Schraen, S., Gabelle, A., Vercauteren, O., Bombois, S., Laplanche, J.-L., Peoc'h, K., Sablonnière, B., Kastanenka, K. V., Delaby, C., Pasquier, F., Touchon, J., Hugon, J., Paquet, C. & Lehmann, S. Cerebrospinal fluid amyloid- β 42/40 ratio in clinical setting of memory centers: a multicentric study. *Alzheimers Res Ther* **7**, 30 (2015).
153. Wolozin, B. & Davies, P. Alzheimer-related neuronal protein A68: specificity and distribution. *Ann Neurol* **22**, 521–526 (1987).
154. Vandermeeren, M., Mercken, M., Vanmechelen, E., Six, J., van de Voorde, A., Martin, J. J. &

- Cras, P. Detection of tau proteins in normal and Alzheimer's disease cerebrospinal fluid with a sensitive sandwich enzyme-linked immunosorbent assay. *J Neurochem* **61**, 1828–1834 (1993).
155. Blennow, K., Wallin, A., Agren, H., Spenger, C., Siegfried, J. & Vanmechelen, E. Tau protein in cerebrospinal fluid: a biochemical marker for axonal degeneration in Alzheimer disease? *Mol Chem Neuropathol* **26**, 231–245 (1995).
156. Hesse, C., Rosengren, L., Andreasen, N., Davidsson, P., Vanderstichele, H., Vanmechelen, E. & Blennow, K. Transient increase in total tau but not phospho-tau in human cerebrospinal fluid after acute stroke. *Neurosci Lett* **297**, 187–190 (2001).
157. Riemenschneider, M., Wagenpfeil, S., Vanderstichele, H., Otto, M., Wiltfang, J., Kretschmar, H., Vanmechelen, E., Förstl, H. & Kurz, A. Phospho-tau/total tau ratio in cerebrospinal fluid discriminates Creutzfeldt-Jakob disease from other dementias. *Mol Psychiatry* **8**, 343–347 (2003).
158. Zetterberg, H., Hietala, M. A., Jonsson, M., Andreasen, N., Styrd, E., Karlsson, I., Edman, A., Popa, C., Rasulzada, A., Wahlund, L.-O., Mehta, P. D., Rosengren, L., Blennow, K. & Wallin, A. Neurochemical aftermath of amateur boxing. *Arch Neurol* **63**, 1277–1280 (2006).
159. Skillbäck, T., Rosén, C., Asztely, F., Mattsson, N., Blennow, K. & Zetterberg, H. Diagnostic performance of cerebrospinal fluid total tau and phosphorylated tau in Creutzfeldt-Jakob disease: results from the Swedish Mortality Registry. *JAMA Neurol* **71**, 476–483 (2014).
160. Ishiguro, K., Ohno, H., Arai, H., Yamaguchi, H., Urakami, K., Park, J. M., Sato, K., Kohno, H. & Imahori, K. Phosphorylated tau in human cerebrospinal fluid is a diagnostic marker for Alzheimer's disease. *Neurosci Lett* **270**, 91–94 (1999).
161. Kohnken, R., Buerger, K., Zinkowski, R., Miller, C., Kerkman, D., DeBernardis, J., Shen, J., Möller, H. J., Davies, P. & Hampel, H. Detection of tau phosphorylated at threonine 231 in cerebrospinal fluid of Alzheimer's disease patients. *Neurosci Lett* **287**, 187–190 (2000).
162. Vanmechelen, E., Vanderstichele, H., Davidsson, P., Van Kerschaver, E., Van Der Perre, B., Sjögren, M., Andreasen, N. & Blennow, K. Quantification of tau phosphorylated at threonine 181 in human cerebrospinal fluid: a sandwich ELISA with a synthetic phosphopeptide for standardization. *Neurosci Lett* **285**, 49–52 (2000).
163. Hu, Y. Y., He, S. S., Wang, X., Duan, Q. H., Grundke-Iqbal, I., Iqbal, K. & Wang, J. Levels of nonphosphorylated and phosphorylated tau in cerebrospinal fluid of Alzheimer's disease patients: an ultrasensitive bienzyme-substrate-recycle enzyme-linked immunosorbent assay. *Am J Pathol* **160**, 1269–1278 (2002).
164. Hampel, H., Buerger, K., Zinkowski, R., Teipel, S. J., Goernitz, A., Andreasen, N., Sjögren, M., DeBernardis, J., Kerkman, D., Ishiguro, K., Ohno, H., Vanmechelen, E., Vanderstichele, H., McCulloch, C., Moller, H.-J., Davies, P. & Blennow, K. Measurement of phosphorylated tau epitopes in the differential diagnosis of Alzheimer disease: a comparative cerebrospinal fluid study. *Arch Gen Psychiatry* **61**, 95–102 (2004).
165. Buerger, K., Ewers, M., Pirttilä, T., Zinkowski, R., Alafuzoff, I., Teipel, S. J., DeBernardis, J.,

- Kerkman, D., McCulloch, C., Soininen, H. & Hampel, H. CSF phosphorylated tau protein correlates with neocortical neurofibrillary pathology in Alzheimer's disease. *Brain* **129**, 3035–3041 (2006).
166. Janelidze, S., Stomrud, E., Palmqvist, S., Zetterberg, H., van Westen, D., Jeromin, A., Song, L., Hanlon, D., Tan Hehir, C. A., Baker, D., Blennow, K. & Hansson, O. Plasma β -amyloid in Alzheimer's disease and vascular disease. *Sci Rep* **6**, 26801 (2016).
167. Li, W.-W., Shen, Y.-Y., Tian, D.-Y., Bu, X.-L., Zeng, F., Liu, Y.-H., Chen, Y., Yao, X.-Q., Li, H.-Y., Chen, D.-W., Zhou, F.-Y., Yang, H., Li, Q.-M., Bao, W.-Q., Guan, Y.-H., Zhou, H.-D., Jin, R.-B. & Wang, Y.-J. Brain Amyloid- β Deposition and Blood Biomarkers in Patients with Clinically Diagnosed Alzheimer's Disease. *Journal of Alzheimer's Disease* **69**, 169–178 (2019).
168. Palmqvist, S., Janelidze, S., Stomrud, E., Zetterberg, H., Karl, J., Zink, K., Bittner, T., Mattsson, N., Eichenlaub, U., Blennow, K. & Hansson, O. Performance of Fully Automated Plasma Assays as Screening Tests for Alzheimer Disease-Related β -Amyloid Status. *JAMA Neurology* **76**, 1060–1069 (2019).
169. Keshavan, A., Pannee, J., Karikari, T. K., Rodriguez, J. L., Ashton, N. J., Nicholas, J. M., Cash, D. M., Coath, W., Lane, C. A., Parker, T. D., Lu, K., Buchanan, S. M., Keuss, S. E., James, S.-N., Murray-Smith, H., Wong, A., Barnes, A., Dickson, J. C., Heslegrave, A., Portelius, E., Richards, M., Fox, N. C., Zetterberg, H., Blennow, K. & Schott, J. M. Population-based blood screening for preclinical Alzheimer's disease in a British birth cohort at age 70. *Brain* **144**, 434–449 (2021).
170. Verberk, I. M. W., Slot, R. E., Verfaillie, S. C. J., Heijst, H., Prins, N. D., van Berckel, B. N. M., Scheltens, P., Teunissen, C. E. & van der Flier, W. M. Plasma Amyloid as Prescreener for the Earliest Alzheimer Pathological Changes. *Annals of Neurology* **84**, 648–658 (2018).
171. Zetterberg, H., Wilson, D., Andreasson, U., Minthon, L., Blennow, K., Randall, J. & Hansson, O. Plasma tau levels in Alzheimer's disease. *Alzheimers Res Ther* **5**, 9 (2013).
172. Mattsson, N., Zetterberg, H., Janelidze, S., Insel, P. S., Andreasson, U., Stomrud, E., Palmqvist, S., Baker, D., Hehir, C. A. T., Jeromin, A., Hanlon, D., Song, L., Shaw, L. M., Trojanowski, J. Q., Weiner, M. W., Hansson, O. & Blennow, K. Plasma tau in Alzheimer disease. *Neurology* **87**, 1827–1835 (2016).
173. Illán-Gala, I., Lleo, A., Karydas, A., Staffaroni, A. M., Zetterberg, H., Sivasankaran, R., Grinberg, L. T., Spina, S., Kramer, J. H., Ramos, E. M., Coppola, G., Joie, R. L., Rabinovici, G. D., Perry, D. C., Gorno-Tempini, M. L., Seeley, W. W., Miller, B. L., Rosen, H. J., Blennow, K., Boxer, A. L. & Rojas, J. C. Plasma Tau and Neurofilament Light in Frontotemporal Lobar Degeneration and Alzheimer Disease. *Neurology* **96**, e671–e683 (2021).
174. Mielke, M. M., Hagen, C. E., Xu, J., Chai, X., Vemuri, P., Lowe, V. J., Airey, D. C., Knopman, D. S., Roberts, R. O., Machulda, M. M., Jack Jr., C. R., Petersen, R. C. & Dage, J. L. Plasma phospho-tau₁₈₁ increases with Alzheimer's disease clinical severity and is associated with tau- and amyloid-positron emission tomography. *Alzheimer's & Dementia* **14**, 989–997 (2018).
175. Karikari, T. K., Pascoal, T. A., Ashton, N. J., Janelidze, S., Benedet, A. L., Rodriguez, J. L.,

Chamoun, M., Savard, M., Kang, M. S., Therriault, J., Schöll, M., Massarweh, G., Soucy, J.-P., Höglund, K., Brinkmalm, G., Mattsson, N., Palmqvist, S., Gauthier, S., Stomrud, E., Zetterberg, H., Hansson, O., Rosa-Neto, P. & Blennow, K. Blood phosphorylated tau 181 as a biomarker for Alzheimer's disease: a diagnostic performance and prediction modelling study using data from four prospective cohorts. *The Lancet Neurology* **19**, 422–433 (2020).

176. Thijssen, E. H., La Joie, R., Wolf, A., Strom, A., Wang, P., Iaccarino, L., Bourakova, V., Cobigo, Y., Heuer, H., Spina, S., VandeVrede, L., Chai, X., Proctor, N. K., Airey, D. C., Shcherbinin, S., Duggan Evans, C., Sims, J. R., Zetterberg, H., Blennow, K., Karydas, A. M., Teunissen, C. E., Kramer, J. H., Grinberg, L. T., Seeley, W. W., Rosen, H., Boeve, B. F., Miller, B. L., Rabinovici, G. D., Dage, J. L., Rojas, J. C. & Boxer, A. L. Diagnostic value of plasma phosphorylated tau181 in Alzheimer's disease and frontotemporal lobar degeneration. *Nat Med* **26**, 387–397 (2020).

177. Janelidze, S., Mattsson, N., Palmqvist, S., Smith, R., Beach, T. G., Serrano, G. E., Chai, X., Proctor, N. K., Eichenlaub, U., Zetterberg, H., Blennow, K., Reiman, E. M., Stomrud, E., Dage, J. L. & Hansson, O. Plasma P-tau181 in Alzheimer's disease: relationship to other biomarkers, differential diagnosis, neuropathology and longitudinal progression to Alzheimer's dementia. *Nat Med* **26**, 379–386 (2020).

178. Palmqvist, S., Janelidze, S., Quiroz, Y. T., Zetterberg, H., Lopera, F., Stomrud, E., Su, Y., Chen, Y., Serrano, G. E., Leuzy, A., Mattsson-Carlgrén, N., Strandberg, O., Smith, R., Villegas, A., Sepulveda-Falla, D., Chai, X., Proctor, N. K., Beach, T. G., Blennow, K., Dage, J. L., Reiman, E. M. & Hansson, O. Discriminative Accuracy of Plasma Phospho-tau217 for Alzheimer Disease vs Other Neurodegenerative Disorders. *JAMA* **324**, 772–781 (2020).

179. Barthélemy, N. R., Horie, K., Sato, C. & Bateman, R. J. Blood plasma phosphorylated-tau isoforms track CNS change in Alzheimer's disease. *Journal of Experimental Medicine* **217**, e20200861 (2020).

180. Karikari, T. K., Benedet, A. L., Ashton, N. J., Lantero Rodriguez, J., Snellman, A., Suárez-Calvet, M., Saha-Chaudhuri, P., Lussier, F., Kvartsberg, H., Rial, A. M., Pascoal, T. A., Andreasson, U., Schöll, M., Weiner, M. W., Rosa-Neto, P., Trojanowski, J. Q., Shaw, L. M., Blennow, K. & Zetterberg, H. Diagnostic performance and prediction of clinical progression of plasma phospho-tau181 in the Alzheimer's Disease Neuroimaging Initiative. *Mol Psychiatry* **26**, 429–442 (2021).

181. Chen, Z., Mengel, D., Keshavan, A., Rissman, R. A., Billinton, A., Perkinson, M., Percival-Alwyn, J., Schultz, A., Properzi, M., Johnson, K., Selkoe, D. J., Sperling, R. A., Patel, P., Zetterberg, H., Galasko, D., Schott, J. M. & Walsh, D. M. Learnings about the complexity of extracellular tau aid development of a blood-based screen for Alzheimer's disease. *Alzheimer's & Dementia* **15**, 487–496 (2019).

182. Chhatwal, J. P., Schultz, A. P., Dang, Y., Ostaszewski, B., Liu, L., Yang, H.-S., Johnson, K. A., Sperling, R. A. & Selkoe, D. J. Plasma N-terminal tau fragment levels predict future cognitive decline and neurodegeneration in healthy elderly individuals. *Nat Commun* **11**, 6024 (2020).

183. Leinonen, V., Alafuzoff, I., Aalto, S., Suotunen, T., Savolainen, S., Någren, K., Tapiola, T., Pirttilä, T., Rinne, J., Jääskeläinen, J. E., Soininen, H. & Rinne, J. O. Assessment of β -Amyloid in a Frontal Cortical Brain Biopsy Specimen and by Positron Emission Tomography With Carbon 11–Labeled Pittsburgh Compound B. *Archives of Neurology* **65**, 1304–1309 (2008).
184. Villemagne, V. L., Ataka, S., Mizuno, T., Brooks, W. S., Wada, Y., Kondo, M., Jones, G., Watanabe, Y., Mulligan, R., Nakagawa, M., Miki, T., Shimada, H., O’Keefe, G. J., Masters, C. L., Mori, H. & Rowe, C. C. High Striatal Amyloid β -Peptide Deposition Across Different Autosomal Alzheimer Disease Mutation Types. *Archives of Neurology* **66**, 1537–1544 (2009).
185. Burack, M. A., Hartlein, J., Flores, H. P., Taylor-Reinwald, L., Perlmutter, J. S. & Cairns, N. J. In vivo amyloid imaging in autopsy-confirmed Parkinson disease with dementia. *Neurology* **74**, 77–84 (2010).
186. Cho, H., Choi, J. Y., Hwang, M. S., Kim, Y. J., Lee, H. M., Lee, H. S., Lee, J. H., Ryu, Y. H., Lee, M. S. & Lyoo, C. H. In vivo cortical spreading pattern of tau and amyloid in the Alzheimer disease spectrum. *Ann Neurol* **80**, 247–258 (2016).
187. Cho, H., Choi, J. Y., Hwang, M. S., Lee, J. H., Kim, Y. J., Lee, H. M., Lyoo, C. H., Ryu, Y. H. & Lee, M. S. Tau PET in Alzheimer disease and mild cognitive impairment. *Neurology* **87**, 375–383 (2016).
188. Johnson, K. A., Schultz, A., Betensky, R. A., Becker, J. A., Sepulcre, J., Rentz, D., Mormino, E., Chhatwal, J., Amariglio, R., Papp, K., Marshall, G., Albers, M., Mauro, S., Pepin, L., Alverio, J., Judge, K., Philioussaint, M., Shoup, T., Yokell, D., Dickerson, B., Gomez-Isla, T., Hyman, B., Vasdev, N. & Sperling, R. Tau positron emission tomographic imaging in aging and early Alzheimer disease. *Ann Neurol* **79**, 110–119 (2016).
189. Schöll, M., Lockhart, S. N., Schonhaut, D. R., O’Neil, J. P., Janabi, M., Ossenkoppele, R., Baker, S. L., Vogel, J. W., Faria, J., Schwimmer, H. D., Rabinovici, G. D. & Jagust, W. J. PET Imaging of Tau Deposition in the Aging Human Brain. *Neuron* **89**, 971–982 (2016).
190. Lockhart, S. N., Baker, S. L., Okamura, N., Furukawa, K., Ishiki, A., Furumoto, S., Tashiro, M., Yanai, K., Arai, H., Kudo, Y., Harada, R., Tomita, N., Hiraoka, K., Watanuki, S. & Jagust, W. J. Dynamic PET Measures of Tau Accumulation in Cognitively Normal Older Adults and Alzheimer’s Disease Patients Measured Using [18F] THK-5351. *PLoS One* **11**, e0158460 (2016).
191. Duara, R., Grady, C., Haxby, J., Sundaram, M., Cutler, N. R., Heston, L., Moore, A., Schlageter, N., Larson, S. & Rapoport, S. I. Positron emission tomography in Alzheimer’s disease. *Neurology* **36**, 879–879 (1986).
192. Ibáñez, V., Pietrini, P., Alexander, G. E., Furey, M. L., Teichberg, D., Rajapakse, J. C., Rapoport, S. I., Schapiro, M. B. & Horwitz, B. Regional glucose metabolic abnormalities are not the result of atrophy in Alzheimer’s disease. *Neurology* **50**, 1585–1593 (1998).
193. Pietrini, P., Alexander, G. E., Furey, M. L., Hampel, H. & Guazzelli, M. The neurometabolic landscape of cognitive decline: in vivo studies with positron emission tomography in Alzheimer’s

disease. *International Journal of Psychophysiology* **37**, 87–98 (2000).

194. Alexander, G. E., Chen, K., Pietrini, P., Rapoport, S. I. & Reiman, E. M. Longitudinal PET Evaluation of Cerebral Metabolic Decline in Dementia: A Potential Outcome Measure in Alzheimer's Disease Treatment Studies. *AJP* **159**, 738–745 (2002).

195. Mosconi, L., Tsui, W. H., Herholz, K., Pupi, A., Drzezga, A., Lucignani, G., Reiman, E. M., Holthoff, V., Kalbe, E., Sorbi, S., Diehl-Schmid, J., Perneczky, R., Clerici, F., Caselli, R., Beuthien-Baumann, B., Kurz, A., Minoshima, S. & de Leon, M. J. Multicenter Standardized 18F-FDG PET Diagnosis of Mild Cognitive Impairment, Alzheimer's Disease, and Other Dementias. *J Nucl Med* **49**, 390–398 (2008).

196. Lamusuo, S., Jutila, L., Ylinen, A., Kälviäinen, R., Mervaala, E., Haaparanta, M., Jääskeläinen, S., Partanen, K., Vapalahti, M. & Rinne, J. [18F]FDG-PET Reveals Temporal Hypometabolism in Patients With Temporal Lobe Epilepsy Even When Quantitative MRI and Histopathological Analysis Show Only Mild Hippocampal Damage. *Archives of Neurology* **58**, 933–939 (2001).

197. Guedj, E., Champion, J. Y., Dudouet, P., Kaphan, E., Bregeon, F., Tissot-Dupont, H., Guis, S., Barthelemy, F., Habert, P., Ceccaldi, M., Million, M., Raoult, D., Cammilleri, S. & Eldin, C. 18F-FDG brain PET hypometabolism in patients with long COVID. *Eur J Nucl Med Mol Imaging* **48**, 2823–2833 (2021).

198. Probasco, J. C., Solnes, L., Nalluri, A., Cohen, J., Jones, K. M., Zan, E., Javadi, M. S. & Venkatesan, A. Abnormal brain metabolism on FDG-PET/CT is a common early finding in autoimmune encephalitis. *Neurol Neuroimmunol Neuroinflamm* **4**, e352 (2017).

199. Fox, N. C., Scahill, R. I., Crum, W. R. & Rossor, M. N. Correlation between rates of brain atrophy and cognitive decline in AD. *Neurology* **52**, 1687–1687 (1999).

200. Josephs, K. A., Whitwell, J. L., Ahmed, Z., Shiung, M. M., Weigand, S. D., Knopman, D. S., Boeve, B. F., Parisi, J. E., Petersen, R. C., Dickson, D. W. & Jack, C. R. Beta-amyloid burden is not associated with rates of brain atrophy. *Ann Neurol* **63**, 204–212 (2008).

201. Schott, J. M., Crutch, S. J., Frost, C., Warrington, E. K., Rossor, M. N. & Fox, N. C. Neuropsychological correlates of whole brain atrophy in Alzheimer's disease. *Neuropsychologia* **46**, 1732–1737 (2008).

202. Sluimer, J. D., van der Flier, W. M., Karas, G. B., Fox, N. C., Scheltens, P., Barkhof, F. & Vrenken, H. Whole-Brain Atrophy Rate and Cognitive Decline: Longitudinal MR Study of Memory Clinic Patients. *Radiology* **248**, 590–598 (2008).

203. Zetterberg, H. & Bendlin, B. B. Biomarkers for Alzheimer's disease—preparing for a new era of disease-modifying therapies. *Mol Psychiatry* **26**, 296–308 (2021).

204. Jeremic, D., Jiménez-Díaz, L. & Navarro-López, J. D. Past, present and future of therapeutic strategies against amyloid- β peptides in Alzheimer's disease: a systematic review. *Ageing Research Reviews* **72**, 101496 (2021).

205. Schneider, L. A resurrection of aducanumab for Alzheimer's disease. *The Lancet Neurology* **19**,

111–112 (2020).

206. Biogen. *A Phase 3 Multicenter, Randomized, Double-Blind, Placebo-Controlled, Parallel-Group Study to Evaluate the Efficacy and Safety of Aducanumab (BIIB037) in Subjects With Early Alzheimer's Disease*. <https://clinicaltrials.gov/ct2/show/NCT02477800> (2021).

207. Steinbrook, R. The Accelerated Approval of Aducanumab for Treatment of Patients With Alzheimer Disease. *JAMA Internal Medicine* **181**, 1281 (2021).

208. Chai, X., Wu, S., Murray, T. K., Kinley, R., Cella, C. V., Sims, H., Buckner, N., Hanmer, J., Davies, P., O'Neill, M. J., Hutton, M. L. & Citron, M. Passive Immunization with Anti-Tau Antibodies in Two Transgenic Models: REDUCTION OF TAU PATHOLOGY AND DELAY OF DISEASE PROGRESSION. *Journal of Biological Chemistry* **286**, 34457–34467 (2011).

209. Boutajangout, A., Ingadottir, J., Davies, P. & Singurdsson, E. M. Passive immunization targeting pathological phospho-tau protein in a mouse model reduces functional decline and clears tau aggregates from the brain. *J Neurochem* **118**, 658–667 (2011).

210. Castillo-Carranza, D. L., Sengupta, U., Guerrero-Muñoz, M. J., Lasagna-Reeves, C. A., Gerson, J. E., Singh, G., Estes, D. M., Barrett, A. D. T., Dineley, K. T., Jackson, G. R. & Kaye, R. Passive Immunization with Tau Oligomer Monoclonal Antibody Reverses Tauopathy Phenotypes without Affecting Hyperphosphorylated Neurofibrillary Tangles. *J Neurosci* **34**, 4260–4272 (2014).

211. Boimel, M., Grigoriadis, N., Loubopoulos, A., Haber, E., Abramsky, O. & Rosenmann, H. Efficacy and safety of immunization with phosphorylated tau against neurofibrillary tangles in mice. *Experimental Neurology* **224**, 472–485 (2010).

212. Theunis, C., Crespo-Biel, N., Gafner, V., Pihlgren, M., López-Deber, M. P., Reis, P., Hickman, D. T., Adolfsson, O., Chuard, N., Ndao, D. M., Borghgraef, P., Devijver, H., Leuven, F. V., Pfeifer, A. & Muhs, A. Efficacy and Safety of A Liposome-Based Vaccine against Protein Tau, Assessed in Tau.P301L Mice That Model Tauopathy. *PLOS ONE* **8**, e72301 (2013).

213. Kontsekova, E., Zilka, N., Kovacech, B., Novak, P. & Novak, M. First-in-man tau vaccine targeting structural determinants essential for pathological tau–tau interaction reduces tau oligomerisation and neurofibrillary degeneration in an Alzheimer's disease model. *Alzheimers Res Ther* **6**, 44 (2014).

214. Morishima-Kawashima, M., Hasegawa, M., Takio, K., Suzuki, M., Titani, K. & Ihara, Y. Ubiquitin is conjugated with amino-terminally processed tau in paired helical filaments. *Neuron* **10**, 1151–1160 (1993).

215. Abreha, M. H., Dammer, E. B., Ping, L., Zhang, T., Duong, D. M., Gearing, M., Lah, J. J., Levey, A. I. & Seyfried, N. T. Quantitative Analysis of the Brain Ubiquitylome in Alzheimer's Disease. *Proteomics* **18**, e1800108 (2018).

216. Arakhamia, T., Lee, C. E., Carlomagno, Y., Duong, D. M., Kunding, S. R., Wang, K., Williams, D., DeTure, M., Dickson, D. W., Cook, C. N., Seyfried, N. T., Petrucelli, L. & Fitzpatrick, A. W. P. Posttranslational modifications mediate the structural diversity of tauopathy strains. *Cell* **180**,

633-644.e12 (2020).

217. Cripps, D., Thomas, S. N., Jeng, Y., Yang, F., Davies, P. & Yang, A. J. Alzheimer disease-specific conformation of hyperphosphorylated paired helical filament-Tau is polyubiquitinated through Lys-48, Lys-11, and Lys-6 ubiquitin conjugation. *J Biol Chem* **281**, 10825–10838 (2006).
218. Lasagna-Reeves, C. A., Castillo-Carranza, D. L., Sengupta, U., Sarmiento, J., Troncoso, J., Jackson, G. R. & Kaye, R. Identification of oligomers at early stages of tau aggregation in Alzheimer's disease. *FASEB J* **26**, 1946–1959 (2012).
219. Keller, J. N., Hanni, K. B. & Markesbery, W. R. Impaired proteasome function in Alzheimer's disease. *J Neurochem* **75**, 436–439 (2000).
220. Ciechanover, A. & Kwon, Y. T. Degradation of misfolded proteins in neurodegenerative diseases: therapeutic targets and strategies. *Exp Mol Med* **47**, e147–e147 (2015).
221. Piras, A., Collin, L., Grüninger, F., Graff, C. & Rönnbäck, A. Autophagic and lysosomal defects in human tauopathies: analysis of post-mortem brain from patients with familial Alzheimer disease, corticobasal degeneration and progressive supranuclear palsy. *Acta Neuropathol Commun* **4**, 22 (2016).
222. Wang, Y., Martinez-Vicente, M., Krüger, U., Kaushik, S., Wong, E., Mandelkow, E.-M., Cuervo, A. M. & Mandelkow, E. Tau fragmentation, aggregation and clearance: the dual role of lysosomal processing. *Hum Mol Genet* **18**, 4153–4170 (2009).
223. Krüger, U., Wang, Y., Kumar, S. & Mandelkow, E.-M. Autophagic degradation of tau in primary neurons and its enhancement by trehalose. *Neurobiol Aging* **33**, 2291–2305 (2012).
224. Caballero, B., Wang, Y., Diaz, A., Tasset, I., Juste, Y. R., Stiller, B., Mandelkow, E.-M., Mandelkow, E. & Cuervo, A. M. Interplay of pathogenic forms of human tau with different autophagic pathways. *Aging Cell* **17**, e12692 (2018).
225. Li, L., Zhang, X. & Le, W. Autophagy Dysfunction in Alzheimer's Disease. *NDD* **7**, 265–271 (2010).
226. Vaz-Silva, J., Gomes, P., Jin, Q., Zhu, M., Zhuravleva, V., Quintremil, S., Meira, T., Silva, J., Dioli, C., Soares-Cunha, C., Daskalakis, N. P., Sousa, N., Sotiropoulos, I. & Waites, C. L. Endolysosomal degradation of Tau and its role in glucocorticoid-driven hippocampal malfunction. *EMBO J* **37**, e99084 (2018).
227. Ugbo, C., Fort-Aznar, L. & Sweeney, S. T. Leaky endosomes push tau over the seed limit. *Journal of Biological Chemistry* **294**, 18967–18968 (2019).
228. Martini-Stoica, H., Cole, A. L., Swartzlander, D. B., Chen, F., Wan, Y.-W., Bajaj, L., Bader, D. A., Lee, V. M. Y., Trojanowski, J. Q., Liu, Z., Sardiello, M. & Zheng, H. TFEB enhances astroglial uptake of extracellular tau species and reduces tau spreading. *J Exp Med* **215**, 2355–2377 (2018).
229. Rodriguez, L., Mohamed, N.-V., Desjardins, A., Lippé, R., Fon, E. A. & Leclerc, N. Rab7A regulates tau secretion. *Journal of Neurochemistry* **141**, 592–605 (2017).
230. Pilliod, J., Desjardins, A., Pernègre, C., Jamann, H., Larochelle, C., Fon, E. A. & Leclerc, N. Clearance of intracellular tau protein from neuronal cells via VAMP8-induced secretion. *J Biol Chem*

295, 17827–17841 (2020).

231. Yan, M. & Zheng, T. Role of the endolysosomal pathway and exosome release in tau propagation. *Neurochemistry International* **145**, 104988 (2021).

232. Iliff, J. J., Wang, M., Liao, Y., Plogg, B. A., Peng, W., Gundersen, G. A., Benveniste, H., Vates, G. E., Deane, R., Goldman, S. A., Nagelhus, E. A. & Nedergaard, M. A Paravascular Pathway Facilitates CSF Flow Through the Brain Parenchyma and the Clearance of Interstitial Solutes, Including Amyloid β . *Science translational medicine* **4**, 147ra111 (2012).

233. Tarasoff-Conway, J. M., Carare, R. O., Osorio, R. S., Glodzik, L., Butler, T., Fieremans, E., Axel, L., Rusinek, H., Nicholson, C., Zlokovic, B. V., Frangione, B., Blennow, K., Ménard, J., Zetterberg, H., Wisniewski, T. & de Leon, M. J. Clearance systems in the brain—implications for Alzheimer disease. *Nat Rev Neurol* **11**, 457–470 (2015).

234. van Veluw, S. J., Hou, S. S., Calvo-Rodriguez, M., Arbel-Ornath, M., Snyder, A. C., Frosch, M. P., Greenberg, S. M. & Bacskai, B. J. Vasomotion as a driving force for paravascular clearance in the awake mouse brain. *Neuron* **105**, 549-561.e5 (2020).

235. Xie, L., Kang, H., Xu, Q., Chen, M. J., Liao, Y., Thiyagarajan, M., O'Donnell, J., Christensen, D. J., Nicholson, C., Iliff, J. J., Takano, T., Deane, R. & Nedergaard, M. Sleep Drives Metabolite Clearance from the Adult Brain. *Science* **342**, 10.1126/science.1241224 (2013).

236. Iliff, J. J., Wang, M., Zeppenfeld, D. M., Venkataraman, A., Plog, B. A., Liao, Y., Deane, R. & Nedergaard, M. Cerebral Arterial Pulsation Drives Paravascular CSF–Interstitial Fluid Exchange in the Murine Brain. *J Neurosci* **33**, 18190–18199 (2013).

237. Plog, B. A., Dashnaw, M. L., Hitomi, E., Peng, W., Liao, Y., Lou, N., Deane, R. & Nedergaard, M. Biomarkers of Traumatic Injury Are Transported from Brain to Blood via the Glymphatic System. *J Neurosci* **35**, 518–526 (2015).

238. Iliff, J. J., Lee, H., Yu, M., Feng, T., Logan, J., Nedergaard, M. & Benveniste, H. Brain-wide pathway for waste clearance captured by contrast-enhanced MRI. *J Clin Invest* **123**, 1299–1309 (2013).

239. Iliff, J. J., Chen, M. J., Plog, B. A., Zeppenfeld, D. M., Soltero, M., Yang, L., Singh, I., Deane, R. & Nedergaard, M. Impairment of Glymphatic Pathway Function Promotes Tau Pathology after Traumatic Brain Injury. *The Journal of Neuroscience* **34**, 16180 (2014).

240. Harrison, I. F., Ismail, O., Machhada, A., Colgan, N., Ohene, Y., Nahavandi, P., Ahmed, Z., Fisher, A., Meftah, S., Murray, T. K., Ottersen, O. P., Nagelhus, E. A., O'Neill, M. J., Wells, J. A. & Lythgoe, M. F. Impaired glymphatic function and clearance of tau in an Alzheimer's disease model. *Brain* **143**, 2576–2593 (2020).

241. Ishida, K., Yamada, K., Nishiyama, R., Hashimoto, T., Nishida, I., Abe, Y., Yasui, M. & Iwatsubo, T. Glymphatic system clears extracellular tau and protects from tau aggregation and neurodegeneration. *J Exp Med* **219**, e20211275 (2022).

242. Kecheliev, V., Boss, L., Maheshwari, U., Konietzko, U., Keller, A., Razansky, D., Nitsch, R. M., Klohs, J. & Ni, R. Aquaporin 4 is differentially increased and depolarized in association with tau

and amyloid-beta. 2022.04.26.489273 Preprint at <https://doi.org/10.1101/2022.04.26.489273> (2022).

243. Aspelund, A., Antila, S., Proulx, S. T., Karlsen, T. V., Karaman, S., Detmar, M., Wiig, H. & Alitalo, K. A dural lymphatic vascular system that drains brain interstitial fluid and macromolecules. *J Exp Med* **212**, 991–999 (2015).
244. Louveau, A., Smirnov, I., Keyes, T. J., Eccles, J. D., Rouhani, S. J., Peske, J. D., Derecki, N. C., Castle, D., Mandell, J. W., Lee, K. S., Harris, T. H. & Kipnis, J. Structural and functional features of central nervous system lymphatic vessels. *Nature* **523**, 337–341 (2015).
245. Absinta, M., Ha, S.-K., Nair, G., Sati, P., Luciano, N. J., Palisoc, M., Louveau, A., Zghloul, K. A., Pittaluga, S., Kipnis, J. & Reich, D. S. Human and nonhuman primate meninges harbor lymphatic vessels that can be visualized noninvasively by MRI. *eLife* **6**, e29738 (2017).
246. Johnston, M., Zakharov, A., Papaiconomou, C., Salmasi, G. & Armstrong, D. Evidence of connections between cerebrospinal fluid and nasal lymphatic vessels in humans, non-human primates and other mammalian species. *Cerebrospinal Fluid Res* **1**, 2 (2004).
247. Albayram, M. S., Smith, G., Tufan, F., Tuna, I. S., Bostancıklıoğlu, M., Zile, M. & Albayram, O. Non-invasive MR imaging of human brain lymphatic networks with connections to cervical lymph nodes. *Nat Commun* **13**, 203 (2022).
248. Patel, T. K., Habimana-Griffin, L., Gao, X., Xu, B., Achilefu, S., Alitalo, K., McKee, C. A., Sheehan, P. W., Musiek, E. S., Xiong, C., Coble, D. & Holtzman, D. M. Dural lymphatics regulate clearance of extracellular tau from the CNS. *Mol Neurodegener* **14**, 11 (2019).
249. Weed, L. H. The absorption of cerebrospinal fluid into the venous system. *American Journal of Anatomy* **31**, 191–221 (1923).
250. Banks, W. A., Kovac, A., Majerova, P., Bullock, K. M., Shi, M. & Zhang, J. Tau Proteins Cross the Blood-Brain Barrier. *Journal of Alzheimer's Disease* **55**, 411–419 (2017).
251. Wang, J., Jin, W.-S., Bu, X.-L., Zeng, F., Huang, Z.-L., Li, W.-W., Shen, L.-L., Zhuang, Z.-Q., Fang, Y., Sun, B.-L., Zhu, J., Yao, X.-Q., Zeng, G.-H., Dong, Z.-F., Yu, J.-T., Hu, Z., Song, W., Zhou, H.-D., Jiang, J.-X., Liu, Y.-H. & Wang, Y.-J. Physiological clearance of tau in the periphery and its therapeutic potential for tauopathies. *Acta Neuropathol* **136**, 525–536 (2018).
252. van Deurs, B. & Koehler, J. K. Tight junctions in the choroid plexus epithelium. A freeze-fracture study including complementary replicas. *Journal of Cell Biology* **80**, 662–673 (1979).
253. Mullier, A., Bouret, S. G., Prevot, V. & Dehouck, B. Differential distribution of tight junction proteins suggests a role for tanycytes in blood-hypothalamus barrier regulation in the adult mouse brain. *J Comp Neurol* **518**, 943–962 (2010).
254. Langlet, F., Mullier, A., Bouret, S. G., Prevot, V. & Dehouck, B. Tanycyte-Like Cells Form a Blood–Cerebrospinal Fluid Barrier in the Circumventricular Organs of the Mouse Brain. *J Comp Neurol* **521**, 3389–3405 (2013).
255. Zhang, Y. & Pardridge, W. M. Mediated efflux of IgG molecules from brain to blood across the blood-brain barrier. *J Neuroimmunol* **114**, 168–172 (2001).

256. Bell, R. D., Sagare, A. P., Friedman, A. E., Bedi, G. S., Holtzman, D. M., Deane, R. & Zlokovic, B. V. Transport pathways for clearance of human Alzheimer's amyloid beta-peptide and apolipoproteins E and J in the mouse central nervous system. *J Cereb Blood Flow Metab* **27**, 909–918 (2007).
257. Benarroch, E. E. Circumventricular organs: Receptive and homeostatic functions and clinical implications. *Neurology* **77**, 1198–1204 (2011).
258. Balland, E., Dam, J., Langlet, F., Caron, E., Steculorum, S., Messina, A., Rasika, S., Falluel-Morel, A., Anouar, Y., Dehouck, B., Trinquet, E., Jockers, R., Bouret, S. G. & Prévot, V. Hypothalamic tanycytes are an ERK-gated conduit for leptin into the brain. *Cell Metab* **19**, 293–301 (2014).
259. Wagner, H.-J. & Pilgrim, Ch. Extracellular and transcellular transport of horseradish peroxidase (HRP) through the hypothalamic tanycyte ependyma. *Cell Tissue Res.* **152**, (1974).
260. Zheng, Q., Huang, T., Zhang, L., Zhou, Y., Luo, H., Xu, H. & Wang, X. Dysregulation of Ubiquitin-Proteasome System in Neurodegenerative Diseases. *Frontiers in Aging Neuroscience* **8**, (2016).
261. Ramón y Cajal, S. *Histologie du système nerveux de l'homme & des vertébrés*. 1–1012 (Maloine, 1909). doi:10.5962/bhl.title.48637.
262. Horstmann, E. [The fiber glia of selacean brain]. *Z Zellforsch Mikrosk Anat* **39**, 588–617 (1954).
263. Akmayev, I. G., Fidelina, O. V., Kabolova, Z. A., Popov, A. P. & Schitkova, T. A. Morphological aspects of the hypothalamic-hypophyseal system. IV. Medial basal hypothalamus. An experimental morphological study. *Z Zellforsch Mikrosk Anat* **137**, 493–512 (1973).
264. Prevot, V., Dehouck, B., Sharif, A., Ciofi, P., Giacobini, P. & Clasadonte, J. The Versatile Tanycyte: A Hypothalamic Integrator of Reproduction and Energy Metabolism. *Endocrine Reviews* **39**, 333–368 (2018).
265. J. Everitt, B., Meister, B., Hökfelt, T., Melander, T., Terenius, L., Rökaeus, Å., Theodorsson-Norheim, E., Dockray, G., Edwardson, J., Cuello, C., Elde, R., Goldstein, M., Hemmings, H., Ouimet, C., Walaas, I., Greengard, P., Vale, W., Weber, E., Wu, J.-Y. & Chang, K.-J. The hypothalamic arcuate nucleus-median eminence complex: Immunohistochemistry of transmitters, peptides and DARPP-32 with special reference to coexistence in dopamine neurons. *Brain Research Reviews* **11**, 97–155 (1986).
266. Meister, B., Hökfelt, T., Tsuruo, Y., Hemmings, H., Ouimet, C., Greengard, P. & Goldstein, M. DARPP-32, a dopamine- and cyclic AMP-regulated phosphoprotein in tanycytes of the mediobasal hypothalamus: distribution and relation to dopamine and luteinizing hormone-releasing hormone neurons and other glial elements. *Neuroscience* **27**, 607–622 (1988).
267. Ouimet, C. C., LaMantia, A. S., Goldman-Rakic, P., Rakic, P. & Greengard, P. Immunocytochemical localization of DARPP-32, a dopamine and cyclic-AMP-regulated phosphoprotein, in the primate brain. *J Comp Neurol* **323**, 209–218 (1992).
268. Pixley, S. K. R., Kobayashi, Y. & de Vellis, J. A monoclonal antibody against vimentin: Characterization. *Developmental Brain Research* **15**, 185–199 (1984).
269. Fekete, C., Gereben, B., Doleschall, M., Harney, J. W., Dora, J. M., Bianco, A. C., Sarkar, S.,

- Liposits, Z., Rand, W., Emerson, C., Kacs Kovics, I., Larsen, P. R. & Lechan, R. M. Lipopolysaccharide induces type 2 iodothyronine deiodinase in the mediobasal hypothalamus: implications for the nonthyroidal illness syndrome. *Endocrinology* **145**, 1649–1655 (2004).
270. Milesi, S., Simonneaux, V. & Klosen, P. Downregulation of Deiodinase 3 is the earliest event in photoperiodic and photorefractory activation of the gonadotropic axis in seasonal hamsters. *Sci Rep* **7**, 17739 (2017).
271. Müller-Fielitz, H., Stahr, M., Bernau, M., Richter, M., Abele, S., Krajka, V., Benzin, A., Wenzel, J., Kalies, K., Mittag, J., Heuer, H., Offermanns, S. & Schwaninger, M. Tanycytes control the hormonal output of the hypothalamic-pituitary-thyroid axis. *Nat Commun* **8**, 484 (2017).
272. Chouaf-Lakhdar, L., Fèvre-Montange, M., Brisson, C., Strazielle, N., Gamrani, H. & Didier-Bazès, M. Proliferative activity and nestin expression in periventricular cells of the adult rat brain. *NeuroReport* **14**, 633–636 (2003).
273. Xu, Y., Tamamaki, N., Noda, T., Kimura, K., Itokazu, Y., Matsumoto, N., Dezawa, M. & Ide, C. Neurogenesis in the ependymal layer of the adult rat 3rd ventricle. *Experimental Neurology* **192**, 251–264 (2005).
274. Lee, D. A., Bedont, J. L., Pak, T., Wang, H., Song, J., Miranda-Angulo, A., Takiar, V., Charubhumi, V., Balordi, F., Takebayashi, H., Aja, S., Ford, E., Fishell, G. & Blackshaw, S. Tanycytes of the hypothalamic median eminence form a diet-responsive neurogenic niche. *Nat Neurosci* **15**, 700–702 (2012).
275. Miranda-Angulo, A. L., Byerly, M. S., Mesa, J., Wang, H. & Blackshaw, S. Rax regulates hypothalamic tanycyte differentiation and barrier function in mice. *J Comp Neurol* **522**, 876–899 (2014).
276. Robins, S. C., Stewart, I., McNay, D. E., Taylor, V., Giachino, C., Goetz, M., Ninkovic, J., Briancon, N., Maratos-Flier, E., Flier, J. S., Kokoeva, M. V. & Placzek, M. α -Tanycytes of the adult hypothalamic third ventricle include distinct populations of FGF-responsive neural progenitors. *Nat Commun* **4**, 2049 (2013).
277. Chaker, Z., George, C., Petrovska, M., Caron, J.-B., Lacube, P., Caillé, I. & Holzenberger, M. Hypothalamic neurogenesis persists in the aging brain and is controlled by energy-sensing IGF-I pathway. *Neurobiol Aging* **41**, 64–72 (2016).
278. Mu, W., Li, S., Xu, J., Guo, X., Wu, H., Chen, Z., Qiao, L., Helfer, G., Lu, F., Liu, C. & Wu, Q.-F. Hypothalamic Rax⁺ tanycytes contribute to tissue repair and tumorigenesis upon oncogene activation in mice. *Nat Commun* **12**, 2288 (2021).
279. Sidibe, A., Mullier, A., Chen, P., Baroncini, M., Boutin, J. A., Delagrangé, P., Prevot, V. & Jockers, R. Expression of the orphan GPR50 protein in rodent and human dorsomedial hypothalamus, tanycytes and median eminence. *Journal of Pineal Research* **48**, 263–269 (2010).
280. Chen, R., Wu, X., Jiang, L. & Zhang, Y. Single-Cell RNA-Seq Reveals Hypothalamic Cell Diversity. *Cell Reports* **18**, 3227–3241 (2017).
281. Campbell, J. N., Macosko, E. Z., Fenselau, H., Pers, T. H., Lyubetskaya, A., Tenen, D.,

- Goldman, M., Verstegen, A. M. J., Resch, J. M., McCarroll, S. A., Rosen, E. D., Lowell, B. B. & Tsai, L. A Molecular Census of Arcuate Hypothalamus and Median Eminence Cell Types. *Nat Neurosci* **20**, 484–496 (2017).
282. Feder, M. E. & Walser, J.-C. The biological limitations of transcriptomics in elucidating stress and stress responses. *J Evol Biol* **18**, 901–910 (2005).
283. Haan, N., Goodman, T., Najdi-Samiei, A., Stratford, C. M., Rice, R., El Agha, E., Bellusci, S. & Hajihosseini, M. K. Fgf10-expressing tanycytes add new neurons to the appetite/energy-balance regulating centers of the postnatal and adult hypothalamus. *J Neurosci* **33**, 6170–6180 (2013).
284. Pérez-Martín, M., Cifuentes, M., Grondona, J. M., López-Ávalos, M. D., Gómez-Pinedo, U., García-Verdugo, J. M. & Fernández-Llebrez, P. IGF-I stimulates neurogenesis in the hypothalamus of adult rats. *European Journal of Neuroscience* **31**, 1533–1548 (2010).
285. Ciofi, P., Garret, M., Lapirot, O., Lafon, P., Loyens, A., Prévot, V. & Levine, J. E. Brain-Endocrine Interactions: A Microvascular Route in the Mediobasal Hypothalamus. *Endocrinology* **150**, 5509–5519 (2009).
286. Morita, S. & Miyata, S. Different vascular permeability between the sensory and secretory circumventricular organs of adult mouse brain. *Cell Tissue Res* **349**, 589–603 (2012).
287. Langlet, F., Levin, B. E., Luquet, S., Mazzone, M., Messina, A., Dunn-Meynell, A. A., Balland, E., Lacombe, A., Mazur, D., Carmeliet, P., Bouret, S. G., Prevot, V. & Dehouck, B. Tanycytic VEGF-A Boosts Blood-Hypothalamus Barrier Plasticity and Access of Metabolic Signals to the Arcuate Nucleus in Response to Fasting. *Cell Metab* **17**, 607–617 (2013).
288. Kobayashi, H., Wada, M., Uemura, H. & Ueck, M. Uptake of peroxidase from the third ventricle by ependymal cells of the median eminence. *Z.Zellforsch* **127**, 545–551 (1972).
289. Nozaki, M. Absorption of Intraventricularly Injected Peroxidase by Tanycytes of the Median Eminence of the Neonatal Rat. *Anatom Histol Embryol* **6**, 351–354 (1977).
290. Duquenne, M., Fogueira, C., Bourouh, C., Millet, M., Silva, A., Clasadonte, J., Imbernon, M., Fernandois, D., Martinez-Corral, I., Kusumakshi, S., Caron, E., Rasika, S., Deliglia, E., Jouy, N., Oishi, A., Mazzone, M., Trinquet, E., Tavernier, J., Kim, Y.-B., Ory, S., Jockers, R., Schwaninger, M., Boehm, U., Nogueiras, R., Annicotte, J.-S., Gasman, S., Dam, J. & Prévot, V. Leptin brain entry via a tanycytic LepR–EGFR shuttle controls lipid metabolism and pancreas function. *Nat Metab* **3**, 1071–1090 (2021).
291. Collden, G., Balland, E., Parkash, J., Caron, E., Langlet, F., Prevot, V. & Bouret, S. G. Neonatal overnutrition causes early alterations in the central response to peripheral ghrelin. *Mol Metab* **4**, 15–24 (2015).
292. Porniece Kumar, M., Cremer, A. L., Klemm, P., Steuernagel, L., Sundaram, S., Jais, A., Hausen, A. C., Tao, J., Secher, A., Pedersen, T. Å., Schwaninger, M., Wunderlich, F. T., Lowell, B. B., Backes, H. & Brüning, J. C. Insulin signalling in tanycytes gates hypothalamic insulin uptake and regulation of AgRP neuron activity. *Nat Metab* **3**, 1662–1679 (2021).
293. Gabery, S., Salinas, C. G., Paulsen, S. J., Ahnfelt-Rønne, J., Alanentalo, T., Baquero, A. F.,

- Buckley, S. T., Farkas, E., Fekete, C., Frederiksen, K. S., Hogendorf, W. F. J., Helms, H. C. C., Jeppesen, J. F., John, L. M., Pyke, C., Nøhr, J., Lu, T. T., Poley-Wolf, J., Prevot, V., Raun, K., Simonsen, L., Sun, G., Szilvásy-Szabó, A., Willenbrock, H., Secher, A. & Knudsen, L. B. Semaglutide lowers body weight in rodents via distributed neural pathways. *JCI Insight* **5**, (2020).
294. Imbernon, M., Saponaro, C., Helms, H. C. C., Duquenne, M., Fernandois, D., Deligia, E., Denis, R. G. P., Chao, D. H. M., Rasika, S., Staels, B., Pattou, F., Pfrieger, F. W., Brodin, B., Luquet, S., Bonner, C. & Prevot, V. Tanycytes control hypothalamic liraglutide uptake and its anti-obesity actions. *Cell Metabolism* **34**, 1054-1063.e7 (2022).
295. Pena-Leon, V., Folgueira, C., Barja-Fernández, S., Pérez-Lois, R., Da Silva Lima, N., Martin, M., Heras, V., Martinez-Martinez, S., Valero, P., Iglesias, C., Duquenne, M., Al-Massadi, O., Beiroa, D., Souto, Y., Fidalgo, M., Sowmyalakshmi, R., Guallar, D., Cunarro, J., Castelao, C., Senra, A., González-Saenz, P., Vázquez-Cobela, R., Leis, R., Sabio, G., Mueller-Fielitz, H., Schwaninger, M., López, M., Tovar, S., Casanueva, F. F., Valjent, E., Diéguez, C., Prevot, V., Nogueiras, R. & Seoane, L. M. Prolonged breastfeeding protects from obesity by hypothalamic action of hepatic FGF21. *Nat Metab* **4**, 901–917 (2022).
296. Slezak, M., Grosche, A., Niemiec, A., Tanimoto, N., Pannicke, T., Münch, T. A., Crocker, B., Isope, P., Härtig, W., Beck, S. C., Huber, G., Ferracci, G., Perraut, M., Reber, M., Miehe, M., Demais, V., Lévêque, C., Metzger, D., Szklarczyk, K., Przewlocki, R., Seeliger, M. W., Sage-Ciocca, D., Hirrlinger, J., Reichenbach, A., Reibel, S. & Pfrieger, F. W. Relevance of Exocytotic Glutamate Release from Retinal Glia. *Neuron* **74**, 504–516 (2012).
297. Herbison, A. E. Control of puberty onset and fertility by gonadotropin-releasing hormone neurons. *Nat Rev Endocrinol* **12**, 452–466 (2016).
298. Prevot, V., Croix, D., Rialas, C. M., Poulain, P., Fricchione, G. L., Stefano, G. B. & Beauvillain, J. C. Estradiol coupling to endothelial nitric oxide stimulates gonadotropin-releasing hormone release from rat median eminence via a membrane receptor. *Endocrinology* **140**, 652–659 (1999).
299. Prevot, V., Cornea, A., Mungenast, A., Smiley, G. & Ojeda, S. R. Activation of erbB-1 signaling in tanycytes of the median eminence stimulates transforming growth factor beta1 release via prostaglandin E2 production and induces cell plasticity. *J Neurosci* **23**, 10622–10632 (2003).
300. de Seranno, S., d'Anglemont de Tassigny, X., Estrella, C., Loyens, A., Kasparov, S., Leroy, D., Ojeda, S. R., Beauvillain, J.-C. & Prevot, V. Role of estradiol in the dynamic control of tanycyte plasticity mediated by vascular endothelial cells in the median eminence. *Endocrinology* **151**, 1760–1772 (2010).
301. Fekete, C. & Lechan, R. M. Central regulation of hypothalamic-pituitary-thyroid axis under physiological and pathophysiological conditions. *Endocr Rev* **35**, 159–194 (2014).
302. Sánchez, E., Vargas, M. A., Singru, P. S., Pascual, I., Romero, F., Fekete, C., Charli, J.-L. & Lechan, R. M. Tanycyte pyroglutamyl peptidase II contributes to regulation of the hypothalamic-pituitary-thyroid axis through glial-axonal associations in the median eminence. *Endocrinology* **150**,

2283–2291 (2009).

303. Farkas, E., Varga, E., Kovács, B., Szilvássy-Szabó, A., Cote-Vélez, A., Péterfi, Z., Matziari, M., Tóth, M., Zelena, D., Mezriczky, Z., Kádár, A., Kővári, D., Watanabe, M., Kano, M., Mackie, K., Rózsa, B., Ruska, Y., Tóth, B., Máté, Z., Erdélyi, F., Szabó, G., Gereben, B., Lechan, R. M., Charli, J.-L., Joseph-Bravo, P. & Fekete, C. A Glial-Neuronal Circuit in the Median Eminence Regulates Thyrotropin-Releasing Hormone-Release via the Endocannabinoid System. *iScience* **23**, 100921 (2020).
304. Navarro, M., Rodriguez de Fonseca, F., Alvarez, E., Chowen, J. A., Zueco, J. A., Gomez, R., Eng, J. & Blázquez, E. Colocalization of glucagon-like peptide-1 (GLP-1) receptors, glucose transporter GLUT-2, and glucokinase mRNAs in rat hypothalamic cells: evidence for a role of GLP-1 receptor agonists as an inhibitory signal for food and water intake. *J Neurochem* **67**, 1982–1991 (1996).
305. García, M. A., Millán, C., Balmaceda-Aguilera, C., Castro, T., Pastor, P., Montecinos, H., Reinicke, K., Zúñiga, F., Vera, J. C., Oñate, S. A. & Nualart, F. Hypothalamic ependymal-glia cells express the glucose transporter GLUT2, a protein involved in glucose sensing. *J Neurochem* **86**, 709–724 (2003).
306. Millán, C., Martínez, F., Cortés-Campos, C., Lizama, I., Yañez, M. J., Llanos, P., Reinicke, K., Rodríguez, F., Peruzzo, B., Nualart, F. & García, M. A. Glial glucokinase expression in adult and post-natal development of the hypothalamic region. *ASN Neuro* **2**, e00035 (2010).
307. Orellana, J. A., Sáez, P. J., Cortés-Campos, C., Elizondo, R. J., Shoji, K. F., Contreras-Duarte, S., Figueroa, V., Velarde, V., Jiang, J. X., Nualart, F., Sáez, J. C. & García, M. A. Glucose increases intracellular free Ca²⁺ in tanycytes via ATP released through connexin 43 hemichannels. *Glia* **60**, 53–68 (2012).
308. Bolborea, M., Pollatzek, E., Benford, H., Sotelo-Hitschfeld, T. & Dale, N. Hypothalamic tanycytes generate acute hyperphagia through activation of the arcuate neuronal network. *Proc Natl Acad Sci U S A* **117**, 14473–14481 (2020).
309. Frayling, C., Britton, R. & Dale, N. ATP-mediated glucosensing by hypothalamic tanycytes. *J Physiol* **589**, 2275–2286 (2011).
310. Benford, H., Bolborea, M., Pollatzek, E., Lossow, K., Hermans-Borgmeyer, I., Liu, B., Meyerhof, W., Kasparov, S. & Dale, N. A sweet taste receptor-dependent mechanism of glucosensing in hypothalamic tanycytes. *Glia* **65**, 773–789 (2017).
311. Pellerin, L. & Magistretti, P. J. Glutamate uptake into astrocytes stimulates aerobic glycolysis: a mechanism coupling neuronal activity to glucose utilization. *Proc Natl Acad Sci U S A* **91**, 10625–10629 (1994).
312. Lhomme, T., Clasadonte, J., Imbernon, M., Fernandois, D., Sauve, F., Caron, E., da Silva Lima, N., Heras, V., Martinez-Corral, I., Mueller-Fielitz, H., Rasika, S., Schwaninger, M., Nogueiras, R. & Prevot, V. Tanycytic networks mediate energy balance by feeding lactate to glucose-insensitive POMC neurons. *J Clin Invest* **131**, e140521.
313. Caro, J. F., Kolaczynski, J. W., Nyce, M. R., Ohannesian, J. P., Opentanova, I., Goldman, W.

- H., Lynn, R. B., Zhang, P.-L., Sinha, M. K. & Considine, R. V. Decreased cerebrospinal-fluid/serum leptin ratio in obesity: a possible mechanism for leptin resistance. *The Lancet* **348**, 159–161 (1996).
314. Wallum, B. J., Taborsky, G. J., Porte, D., Figlewicz, D. P., Jacobson, L., Beard, J. C., Ward, W. K. & Dorsa, D. Cerebrospinal fluid insulin levels increase during intravenous insulin infusions in man. *J Clin Endocrinol Metab* **64**, 190–194 (1987).
315. Kern, W., Benedict, C., Schultes, B., Plohr, F., Moser, A., Born, J., Fehm, H. L. & Hallschmid, M. Low cerebrospinal fluid insulin levels in obese humans. *Diabetologia* **49**, 2790–2792 (2006).
316. Severi, I., Fosca, M., Colleluori, G., Marini, F., Imperatori, L., Senzacqua, M., Di Vincenzo, A., Barbatelli, G., Fiori, F., Rau, J. V. & Giordano, A. High-Fat Diet Impairs Mouse Median Eminence: A Study by Transmission and Scanning Electron Microscopy Coupled with Raman Spectroscopy. *International Journal of Molecular Sciences* **22**, 8049 (2021).
317. Pataky, M. W., Young, W. F. & Nair, K. S. Hormonal and Metabolic Changes of Aging and the Influence of Lifestyle Modifications. *Mayo Clin Proc* **96**, 788–814 (2021).
318. Scott, D. E. & Sladek, J. R. Age related changes in the endocrine hypothalamus: I. Tanycytes and the blood-brain-cerebrospinal fluid barrier. *Neurobiology of Aging* **2**, 89–94 (1981).
319. Zoli, M., Ferraguti, F., Frasoldati, A., Biagini, G. & Agnati, L. F. Age-related alterations in tanycytes of the mediobasal hypothalamus of the male rat. *Neurobiology of Aging* **16**, 77–83 (1995).
320. Yin, W., Wu, D., Noel, M. L. & Gore, A. C. Gonadotropin-Releasing Hormone Neuroterminals and Their Microenvironment in the Median Eminence: Effects of Aging and Estradiol Treatment. *Endocrinology* **150**, 5498–5508 (2009).
321. Yin, W. & Gore, A. C. The Hypothalamic Median Eminence and its Role in Reproductive Aging. *Ann N Y Acad Sci* **1204**, 113–122 (2010).
322. Koopman, A. C. M., Taziaux, M. & Bakker, J. Age-related changes in the morphology of tanycytes in the human female infundibular nucleus/median eminence. *J Neuroendocrinol* **29**, (2017).
323. Zhang, Y., Kim, M. S., Jia, B., Yan, J., Zuniga-Hertz, J. P., Han, C. & Cai, D. Hypothalamic stem cells control ageing speed partly through exosomal miRNAs. *Nature* **548**, 52–57 (2017).
324. Zussy, C., Brureau, A., Delair, B., Marchal, S., Keller, E., Ixart, G., Naert, G., Meunier, J., Chevallier, N., Maurice, T. & Givalois, L. Time-Course and Regional Analyses of the Physiopathological Changes Induced after Cerebral Injection of an Amyloid β Fragment in Rats. *Am J Pathol* **179**, 315–334 (2011).
325. Pelletier, G., Dupont, A. & Puviani, R. Ultrastructural study of the uptake of peroxidase by the rat median eminence. *Cell Tissue Res* **156**, 521–532 (1975).
326. Jp, B., M, D., Am, C. & J, F.-D. Transmission and scanning electron-microscopic observations on tanycytes in the mediobasal hypothalamus and the median eminence of adrenalectomized rats. *Cell and tissue research* **221**, (1982).
327. Peruzzo, B., Pastor, F., Blázquez, J., Amat, P. & Rodríguez, E. Polarized endocytosis and transcytosis in the hypothalamic tanycytes of the rat. *Cell Tissue Res* **317**, (2004).

328. Okamoto, A., Fujii, R., Yoshimura, R. & Miyata, S. Transcytosis of tanycytes in the circumventricular organs of adult mouse brain. *Neuroscience Letters* **779**, 136633 (2022).
329. Berg, S., Kutra, D., Kroeger, T., Straehle, C. N., Kausler, B. X., Haubold, C., Schiegg, M., Ales, J., Beier, T., Rudy, M., Eren, K., Cervantes, J. I., Xu, B., Beuttenmueller, F., Wolny, A., Zhang, C., Koethe, U., Hamprecht, F. A. & Kreshuk, A. ilastik: interactive machine learning for (bio)image analysis. *Nat Methods* **16**, 1226–1232 (2019).
330. Danis, C., Despres, C., Bessa, L. M., Malki, I., Merzougui, H., Huvent, I., Qi, H., Lippens, G., Cantrelle, F.-X., Schneider, R., Hanouille, X., Smet-Nocca, C. & Landrieu, I. Nuclear Magnetic Resonance Spectroscopy for the Identification of Multiple Phosphorylations of Intrinsically Disordered Proteins. *Journal of Visualized Experiments : JoVE* (2016) doi:10.3791/55001.
331. Belle, M., Godefroy, D., Couly, G., Malone, S. A., Collier, F., Giacobini, P. & Chédotal, A. Tridimensional Visualization and Analysis of Early Human Development. *Cell* **169**, 161-173.e12 (2017).
332. Prevot, V., Cornea, A., Mungenast, A., Smiley, G. & Ojeda, S. R. Activation of erbB-1 Signaling in Tanycytes of the Median Eminence Stimulates Transforming Growth Factor α 1 Release via Prostaglandin E2 Production and Induces Cell Plasticity. 11.
333. Veys, L., Van houcke, J., Aerts, J., Van Pottelberge, S., Mahieu, M., Coens, A., Melki, R., Moechars, D., De Muynck, L. & De Groef, L. Absence of Uptake and Prion-Like Spreading of Alpha-Synuclein and Tau After Intravitreal Injection of Preformed Fibrils. *Front Aging Neurosci* **12**, 614587 (2021).
334. Schiavo, G. G., Benfenati, F., Poulain, B., Rossetto, O., de Laureto, P. P., DasGupta, B. R. & Montecucco, C. Tetanus and botulinum-B neurotoxins block neurotransmitter release by proteolytic cleavage of synaptobrevin. *Nature* **359**, 832–835 (1992).
335. Banerjee, M., Joshi, S., Zhang, J., Moncman, C. L., Yadav, S., Bouchard, B. A., Storrie, B. & Whiteheart, S. W. Cellubrevin/vesicle-associated membrane protein-3-mediated endocytosis and trafficking regulate platelet functions. *Blood* **130**, 2872–2883 (2017).
336. Skillbäck, T., Delsing, L., Synnergren, J., Mattsson, N., Janelidze, S., Nägga, K., Kilander, L., Hicks, R., Wimo, A., Winblad, B., Hansson, O., Blennow, K., Eriksdotter, M. & Zetterberg, H. CSF/serum albumin ratio in dementias: a cross-sectional study on 1861 patients. *Neurobiology of Aging* **59**, 1–9 (2017).
337. Guo, Y., Huang, Y.-Y., Shen, X.-N., Chen, S.-D., Hu, H., Wang, Z.-T., Tan, L., Yu, J.-T., & the Alzheimer's Disease Neuroimaging Initiative. Characterization of Alzheimer's tau biomarker discordance using plasma, CSF, and PET. *Alzheimer's Research & Therapy* **13**, 93 (2021).
338. Weiner, M. W., Veitch, D. P., Aisen, P. S., Beckett, L. A., Cairns, N. J., Green, R. C., Harvey, D., Jack, C. R., Jagust, W., Liu, E., Morris, J. C., Petersen, R. C., Saykin, A. J., Schmidt, M. E., Shaw, L., Siuciak, J. A., Soares, H., Toga, A. W., Trojanowski, J. Q., & Alzheimer's Disease Neuroimaging Initiative. The Alzheimer's Disease Neuroimaging Initiative: A review of papers published since its

- inception. *Alzheimer's & Dementia* **8**, (2012).
339. Yoon, S.-S. & Jo, S. A. Mechanisms of Amyloid- β Peptide Clearance: Potential Therapeutic Targets for Alzheimer's Disease. *Biomolecules & Therapeutics* **20**, 245 (2012).
340. Bates, K. A., Verdile, G., Li, Q.-X., Ames, D., Hudson, P., Masters, C. L. & Martins, R. N. Clearance mechanisms of Alzheimer's amyloid- β peptide: implications for therapeutic design and diagnostic tests. *Mol Psychiatry* **14**, 469–486 (2009).
341. Chesser, A. S., Pritchard, S. M. & Johnson, G. V. W. Tau Clearance Mechanisms and Their Possible Role in the Pathogenesis of Alzheimer Disease. *Frontiers in Neurology* **4**, (2013).
342. Xin, S.-H., Tan, L., Cao, X., Yu, J.-T. & Tan, L. Clearance of Amyloid Beta and Tau in Alzheimer's Disease: from Mechanisms to Therapy. *Neurotox Res* **34**, 733–748 (2018).
343. Mattsson, N., Zetterberg, H., Janelidze, S., Insel, P. S., Andreasson, U., Stomrud, E., Palmqvist, S., Baker, D., Hehir, C. A. T., Jeromin, A., Hanlon, D., Song, L., Shaw, L. M., Trojanowski, J. Q., Weiner, M. W., Hansson, O. & Blennow, K. Plasma tau in Alzheimer disease. *Neurology* **87**, 1827 (2016).
344. Barten, D. M., Cadelina, G. W., Hoque, N., DeCarr, L. B., Guss, V. L., Yang, L., Sankaranarayanan, S., Wes, P. D., Flynn, M. E., Meredith, J. E., Ahlijanian, M. K. & Albright, C. F. Tau transgenic mice as models for cerebrospinal fluid tau biomarkers. *J Alzheimers Dis* **24 Suppl 2**, 127–141 (2011).
345. Chen, A., Akinyemi, R. O., Hase, Y., Firbank, M. J., Ndung'u, M. N., Foster, V., Craggs, L. J. L., Washida, K., Okamoto, Y., Thomas, A. J., Polvikoski, T. M., Allan, L. M., Oakley, A. E., O'Brien, J. T., Horsburgh, K., Ihara, M. & Kalara, R. N. Frontal white matter hyperintensities, clasmatodendrosis and gliovascular abnormalities in ageing and post-stroke dementia. *Brain* **139**, 242–258 (2016).
346. Tomimoto, H., Akiguchi, I., Wakita, H., Suenaga, T., Nakamura, S. & Kimura, J. Regressive changes of astroglia in white matter lesions in cerebrovascular disease and Alzheimer's disease patients. *Acta Neuropathol* **94**, 146–152 (1997).
347. Hase, Y., Horsburgh, K., Ihara, M. & Kalara, R. N. White matter degeneration in vascular and other ageing-related dementias. *J Neurochem* **144**, 617–633 (2018).
348. Daschil, N. & Humpel, C. Green-Fluorescent Protein+ Astrocytes Attach to Beta-Amyloid Plaques in an Alzheimer Mouse Model and Are Sensitive for Clasmatodendrosis. *Frontiers in Aging Neuroscience* **8**, (2016).
349. Lana, D., Ugolini, F. & Giovannini, M. G. Space-Dependent Glia–Neuron Interplay in the Hippocampus of Transgenic Models of β -Amyloid Deposition. *International Journal of Molecular Sciences* **21**, (2020).
350. Lana, D., Iovino, L., Nosi, D., Wenk, G. L. & Giovannini, M. G. The neuron-astrocyte-microglia triad involvement in neuroinflammation mechanisms in the CA3 hippocampus of memory-impaired aged rats. *Experimental Gerontology* **83**, 71–88 (2016).
351. Balland, E., Dam, J., Langlet, F., Caron, E., Steculorum, S., Messina, A., Rasika, S., Falluel-

- Morel, A., Anouar, Y., Dehouck, B., Trinquet, E., Jockers, R., Bouret, S. G. & Prévot, V. Hypothalamic tanycytes are an ERK-gated conduit for leptin into the brain. *Cell Metab* **19**, 293–301 (2014).
352. Raikwar, S. P., Bhagavan, S. M., Ramaswamy, S. B., Thangavel, R., Dubova, I., Selvakumar, G. P., Ahmed, M. E., Kempuraj, D., Zaheer, S., Iyer, S. & Zaheer, A. Are Tanycytes the Missing Link Between Type 2 Diabetes and Alzheimer's Disease? *Mol Neurobiol* **56**, 833–843 (2019).
353. Kandimalla, R., Thirumala, V. & Reddy, P. H. Is Alzheimer's disease a Type 3 Diabetes? A critical appraisal. *Biochimica et Biophysica Acta (BBA) - Molecular Basis of Disease* **1863**, 1078–1089 (2017).
354. Bedse, G., Di Domenico, F., Serviddio, G. & Cassano, T. Aberrant insulin signaling in Alzheimer's disease: current knowledge. *Frontiers in Neuroscience* **9**, (2015).
355. Nguyen, T. T., Ta, Q. T. H., Nguyen, T. K. O., Nguyen, T. T. D. & Van Giau, V. Type 3 Diabetes and Its Role Implications in Alzheimer's Disease. *Int J Mol Sci* **21**, 3165 (2020).
356. Freude, S., Hettich, M. M., Schumann, C., Stöhr, O., Koch, L., Köhler, C., Udelhoven, M., Leeser, U., Müller, M., Kubota, N., Kadowaki, T., Krone, W., Schröder, H., Brüning, J. C. & Schubert, M. Neuronal IGF-1 resistance reduces Aβ accumulation and protects against premature death in a model of Alzheimer's disease. *FASEB J* **23**, 3315–3324 (2009).
357. Killick, R., Scales, G., Leroy, K., Causevic, M., Hooper, C., Irvine, E. E., Choudhury, A. I., Drinkwater, L., Kerr, F., Al-Qassab, H., Stephenson, J., Yilmaz, Z., Giese, K. P., Brion, J.-P., Withers, D. J. & Lovestone, S. Deletion of *Irs2* reduces amyloid deposition and rescues behavioural deficits in APP transgenic mice. *Biochem Biophys Res Commun* **386**, 257–262 (2009).
358. Cohen, E., Paulsson, J. F., Blinder, P., Burstyn-Cohen, T., Du, D., Estepa, G., Adame, A., Pham, H. M., Holzenberger, M., Kelly, J. W., Masliah, E. & Dillin, A. Reduced IGF-1 signaling delays age-associated proteotoxicity in mice. *Cell* **139**, 1157–1169 (2009).
359. Steculorum, S. M., Solas, M. & Brüning, J. C. The paradox of neuronal insulin action and resistance in the development of aging-associated diseases. *Alzheimer's & Dementia* **10**, S3–S11 (2014).
360. Craft, S., Peskind, E., Schwartz, M. W., Schellenberg, G. D., Raskind, M. & Porte, D. Cerebrospinal fluid and plasma insulin levels in Alzheimer's disease: relationship to severity of dementia and apolipoprotein E genotype. *Neurology* **50**, 164–168 (1998).
361. Steen, E., Terry, B. M., Rivera, E. J., Cannon, J. L., Neely, T. R., Tavares, R., Xu, X. J., Wands, J. R. & de la Monte, S. M. Impaired insulin and insulin-like growth factor expression and signaling mechanisms in Alzheimer's disease--is this type 3 diabetes? *J Alzheimers Dis* **7**, 63–80 (2005).
362. Zhao, W.-Q., De Felice, F. G., Fernandez, S., Chen, H., Lambert, M. P., Quon, M. J., Krafft, G. A. & Klein, W. L. Amyloid beta oligomers induce impairment of neuronal insulin receptors. *FASEB J* **22**, 246–260 (2008).
363. Ishii, M. & Iadecola, C. Metabolic and Non-Cognitive Manifestations of Alzheimer's Disease: The Hypothalamus as Both Culprit and Target of Pathology. *Cell Metab* **22**, 761–776 (2015).
364. Clavaguera, F., Hench, J., Lavenir, I., Schweighauser, G., Frank, S., Goedert, M. & Tolnay, M.

Peripheral administration of tau aggregates triggers intracerebral tauopathy in transgenic mice. *Acta Neuropathol* **127**, 299–301 (2014).

365. Santos, S. F., de Oliveira, H. L., Yamada, E. S., Neves, B. C. & Pereira, A. The Gut and Parkinson's Disease—A Bidirectional Pathway. *Frontiers in Neurology* **10**, (2019).

366. Jaunmuktane, Z., Mead, S., Ellis, M., Wadsworth, J. D. F., Nicoll, A. J., Kenny, J., Launchbury, F., Linehan, J., Richard-Loendt, A., Walker, A. S., Rudge, P., Collinge, J. & Brandner, S. Evidence for human transmission of amyloid- β pathology and cerebral amyloid angiopathy. *Nature* **525**, 247–250 (2015).

367. Purro, S. A., Farrow, M. A., Linehan, J., Nazari, T., Thomas, D. X., Chen, Z., Mengel, D., Saito, T., Saido, T., Rudge, P., Brandner, S., Walsh, D. M. & Collinge, J. Transmission of amyloid- β protein pathology from cadaveric pituitary growth hormone. *Nature* **564**, 415–419 (2018).

368. Lathuiliere, A. & Hyman, B. T. Quantitative Methods for the Detection of Tau Seeding Activity in Human Biofluids. *Front Neurosci* **15**, 654176 (2021).

369. Cecon, E., Oishi, A., Luka, M., Ndiaye-Lobry, D., François, A., Panayi, F., Dam, J., Machado, P. & Jockers, R. Novel repertoire of tau biosensors to monitor pathological tau transformation and seeding activity in living cells. 2022.03.18.484918 Preprint at <https://doi.org/10.1101/2022.03.18.484918> (2022).

370. Barthélemy, N. R., Fenaille, F., Hirtz, C., Sergeant, N., Schraen-Maschke, S., Vialaret, J., Buée, L., Gabelle, A., Junot, C., Lehmann, S. & Becher, F. Tau Protein Quantification in Human Cerebrospinal Fluid by Targeted Mass Spectrometry at High Sequence Coverage Provides Insights into Its Primary Structure Heterogeneity. *J. Proteome Res.* **15**, 667–676 (2016).

371. Trabzuni, D., Wray, S., Vandrovcova, J., Ramasamy, A., Walker, R., Smith, C., Luk, C., Gibbs, J. R., Dillman, A., Hernandez, D. G., Arepalli, S., Singleton, A. B., Cookson, M. R., Pittman, A. M., de Silva, R., Weale, M. E., Hardy, J. & Ryten, M. MAPT expression and splicing is differentially regulated by brain region: relation to genotype and implication for tauopathies. *Hum Mol Genet* **21**, 4094–4103 (2012).

372. Banks, W. A., Kovac, A., Majerova, P., Bullock, K. M., Shi, M. & Zhang, J. Tau Proteins Cross the Blood-Brain Barrier. *Journal of Alzheimer's Disease* **55**, 411–419 (2017).

373. Bomont, P. Intermediate filament aggregation in fibroblasts of giant axonal neuropathy patients is aggravated in non dividing cells and by microtubule destabilization. *Human Molecular Genetics* **12**, 813–822 (2003).

374. Cleveland, D. W., Yamanaka, K. & Bomont, P. Gigaxonin controls vimentin organization through a tubulin chaperone-independent pathway. *Hum Mol Genet* **18**, 1384–1394 (2009).

375. Boizot, A., Talmat-Amar, Y., Morrogh, D., Kuntz, N. L., Halbert, C., Chabrol, B., Houlden, H., Stojkovic, T., Schulman, B. A., Rautenstrauss, B. & Bomont, P. The instability of the BTB-KELCH protein Gigaxonin causes Giant Axonal Neuropathy and constitutes a new penetrant and specific diagnostic test. *Acta Neuropathol Commun* **2**, 47 (2014).

376. Chen, P.-H., Hu, J., Wu, J., Huynh, D. T., Smith, T. J., Pan, S., Bisnett, B. J., Smith, A. B., Lu, A., Condon, B. M., Chi, J.-T. & Boyce, M. Gigaxonin glycosylation regulates intermediate filament turnover and may impact giant axonal neuropathy etiology or treatment. *JCI Insight* **5**, (2020).
377. Perlson, E., Hanz, S., Ben-Yaakov, K., Segal-Ruder, Y., Seger, R. & Fainzilber, M. Vimentin-Dependent Spatial Translocation of an Activated MAP Kinase in Injured Nerve. *Neuron* **45**, 715–726 (2005).
378. Pattabiraman, S., Azad, G. K., Amen, T., Brielle, S., Park, J. E., Sze, S. K., Meshorer, E. & Kaganovich, D. Vimentin protects differentiating stem cells from stress. *Sci Rep* **10**, 19525 (2020).
379. Morrow, C. S., Porter, T. J., Xu, N., Arndt, Z. P., Ako-Asare, K., Heo, H. J., Thompson, E. A. N. & Moore, D. L. Vimentin coordinates protein turnover at the aggresome during neural stem cell quiescence exit. *Cell Stem Cell* **26**, 558-568.e9 (2020).

Role of tanycytes in Tau clearance and their relevance in Alzheimer's Disease

Alzheimer's disease is characterized by an accumulation of both A β and tau in the brain causing neurodegeneration. Currently described clearance mechanisms for tau involve the brain glymphatic and lymphatic system from which tau can slowly egress to the blood. However, studies have shown that tau can rapidly reach the blood circulation after intracerebroventricular injections, suggesting the existence of a direct CSF to blood transport, but the path taken by tau to reach the circulation within minutes is still unknown. Tau being described as incapable of crossing the blood-brain barrier, a plausible path for tau brain exit is through the blood-CSF barriers (BCSFB). A particular BCSFB is located at the median eminence where hypothalamic tanycytes, whose cell bodies form the floor of the third ventricle and send long processes to the underlying pituitary portal capillary bed, form a bridge between the CSF and the blood. In this work, we show that tanycyte are able to take up and transport tau *in vitro* using tanycyte primary cultures. The production of a fluorescently-labeled tau allowed us to track tau path from the CSF to the blood and to confirm the implication of tanycyte in its transport. Using a novel model of tanycytic shuttle interruption, we demonstrated the major contribution of tanycytes in tau egress from the brain. Lastly, the study of human hypothalamic and median eminence post-mortem tissue showed a sign of tau transport in tanycyte of AD patients and a dramatic alteration of their cytoskeleton which was not observed in another neurodegenerative disease. Altogether, our results demonstrate the role of tanycytes in tau clearance and their implication in the pathophysiology of Alzheimer's disease. Such data raise the questions of tanycytes as actors of the CSF clearance and their potential implications in other neurodegenerative diseases.